THESIS FOR THE DEGREE OF DOCTOR OF PHILOSOPHY (PHD)

COMPARATIVE ANALYSIS OF CHONDROGENIC MODELS AND INVESTIGATION OF CALCIUM HOMEOSTASIS IN DIFFERENTIATING CHONDROCYTES

Roland Ádám Takács

Supervisor: Dr. Róza Zákány, MD, PhD

UNIVERSITY OF DEBRECEN
DOCTORAL SCHOOL OF MOLECULAR MEDICINE

DEBRECEN, 2020

Table of Contents

List of Abbreviations and Acronyms

AP: alkaline phosphatase

ADAMTS: a disintegrin and metalloproteinase with thrombospondin motifs

Ala-Gln: alanyl-glutamine

AM: acetoxymethyl ester

ARC: arachidonate-regulated Ca^{2+} channel

ATP: adenosine-5'-triphosphate

b-C3H10T1/2: BMP-2 overexpressing C3H10T1/2 cell

BMP: bone morphogenic protein

BMPR1A and BMPR1B: bone morphogenetic protein receptor, type 1A and 1B

CAD: CRAC Activation Domain

CaMKII: Ca^{2+}-calmodulin dependent protein kinase II

cAMP: cyclic adenosine monophosphate

CC: coiled coil

c-C3H10T1/2: control C3H10T1/2 cell

CDK: cyclin D-dependent kinase

cDNA: complementary DNA

CKO: conditional knockout

CMF-PBS: calcium and magnesium-free phosphate buffered saline

cMyc: cellular Myc

COL10A1: type X collagen, alpha 1 chain

COL1A1: type I collagen, alpha 1 chain

COL2A1: type II collagen, alpha 1 chain

COMP: cartilage oligomeric matrix protein

compound H-7: [1-(5-isoquinolinesulfonyl)-2-methylpiperazine]

CPA: cyclopiazonic acid

CRAC: Ca^{2+} release-activated Ca^{2+} channel

CREB: cAMP-responsive element binding protein

Ct value: PCR cycle number at which the sample's reaction curve intersects the threshold line

CsA: cyclosporine A

DAG: diacylglycerol

Dax1: dosage-sensitive sex reversal, adrenal hypoplasia critical region, on chromosome X, gene 1

DMEM: Dulbecco's modified Eagle's medium

DMMB: dimethylmethylene blue

DMSO: dimethyl sulfoxide

dNTP: deoxynucleoside-5'-triphosphate

dORAI: drosophila ORAI

dseptin: drosophila septin

dSTIM: drosophila STIM

DTT: dithiothreitol

ECM: extracellular matrix

EDTA: ethylenediaminetetraacetic acid

EFh: EF-hand, a helix-loop-helix structural domain

EGF: epidermal growth factor

EGTA: ethylene glycol-bis(β-aminoethyl ether)-N,N,N',N'-tetraacetic acid

ENaCs: epithelial sodium channels

ER: endoplasmic reticulum

ERK: extracellular signal-regulated kinase, a class of mitogen-activated protein kinases

ESC: embryonic stem cell

FABP4: fatty acid binding protein 4

FCF: forchlorfenuron

FCS: fetal calf serum

FGF: fibroblast growth factor

FTHM: full time at half maximum

G interface: GTP-binding domain

GAG: glycosaminoglycan

GAPDH: glyceraldehyde-3-phosphate dehydrogenase

GDF5: growth and differentiation factor-5

GDP: guanosine-5'-diphosphate

GTP: guanosine-5'-triphosphate

H-89: N-[2-[[(E)-3-(4-bromophenyl)prop-2-enyl]amino]ethyl]isoquinoline-5-sulfonamide

HA: hyaluronic acid

Hapln1: hyaluronan and proteoglycan link protein 1

Has: hyaluronan synthase

hASC: human adipose tissue-derived stem cell

HCl: hydrogen chloride

HD: high cellular density

HDC: high density cultures

HEPES: 4-(2-Hydroxyethyl)-1-piperazineethanesulfonic acid

hESC: human embryonic stem cell

hMSC: human mesenchymal stem cell

HRP: horseradish peroxidase

HVA: high voltage-activated channels

IGF: insulin-like growth factor

IM: interterritorial matrix

InsP3: inositol-1,4,5-trisphosphate

InsP3Rs: inositol-1,4,5-trisphosphate receptors

iPSC: induced pluripotent stem cell

JNK: c-Jun N-terminal kinase, a class of mitogen-activated protein kinases

kDa: kilodalton

Klf: Krüppel-like factor

$LaCl_3$: lanthanum trichloride

LTR: long terminal repeat

LVA: low voltage-activated channels

MAPKKKs: mitogen-activated protein kinase kinase kinases

MAPKKs: mitogen-activated protein kinase kinases

MAPKs: mitogen-activated protein kinases

mbMSC: mouse bone marrow mesenchymal stem cell

mCU: mitochondrial uniporter

MEF2: myocyte enhancer factor-2

mESC: mouse embryonic stem cell

MMPs: matrix metalloproteinases

MPSV: myeloproliferative sarcoma virus

mRNA: messenger ribonucleic acid

MSC: mesenchymal stem cell

MTT: 3-(4,5-dimethylthiazol-2-yl)-2,5-diphenyltetrazolium bromide

Myc: transcription factor family named after the avian myelocytomatosis virus

NANOG: a pluripotency farctor named after Tir na nÓg – Land of Youth

NC interface: N□terminal and C□terminal regions

N-cadherin: neural calcium-dependent adhesion molecule

N-CAM: neural cell adhesion molecule

NCX: Na^+/Ca^{2+}-exchanger

NFAT: nuclear factor of activated T cells

NF-κB: nuclear factor kappa-light-chain-enhancer of activated B cells

NIH: National Institutes of Health

NMDA: N-methyl-D-aspartate

NTP: nucleoside-5'-triphosphate

OA: osteoarthritits

OC: osteocalcin

Oct: octamer-binding transcription factor

OD: optical density

OP: osteopontin

ORAI: calcium release-activated calcium channel protein

OSX: osterix

P2X: ATP-gated P2X receptor cation channel family

P2Y: family of purinergic G protein-coupled receptors

p38: a class of mitogen-activated protein kinases

PBS: phosphate buffered saline

PCM: pericellular matrix

PCR: polymerase chain reaction

PDBU: phorbol 12,13-dibutyrate

PG: proteoglycan

PIP_2: phosphatidylinositol 4,5-bisphosphate

PKA: protein kinase A

PKC: protein kinase C

PLC: phosphoinositide phospholipase C

P-loop: phosphate-binding loop

PM: plasma membrane

PMCA: plasma membrane Ca^{2+} ATPase

PouV: POU domain, class 5

PP: protein phosphatase

PPARγ: peroxisome proliferator-activated receptor gamma

PPIA: peptidyl-prolyl isomerase A

PPP: phosphoprotein phosphatase

Prg4: proteoglycan 4 or lubricin

P-SOX9: phospho-SOX9

PTHrP: parathyroid hormone-related protein

qPCR: quantitative polymerase chain reaction

RAS: a family of small GTPases

ROI: region of interest

RPLP0: 60S acidic ribosomal protein P0

RT: reverse transcriptase

RT-PCR: reverse transcription polymerase chain reaction

RT-qPCR: reverse transcription quantitative polymerase chain reaction

RUNX2: runt related transcription factor 2

RyRs: ryanodine receptors

Sall4: spalt-like transcription factor 4

SAM: sterile alpha motif

SB: SOCE blockers (LaCl3 and YM-58483) combined with CPA

SC: stem cell

SD: standard deviation

SDS: sodium dodecyl sulfate

SDS-PAGE: sodium dodecyl sulfate polyacrylamide gel electrophoresis

SEM: standard error of the mean

Ser: L-serine

SERCA: sarco/endoplasmic reticulum Ca^{2+} ATPase

SHH: sonic hedgehog

shRNA: short hairpin RNA

siRNA: small interfering RNA

SMAD: downstream effectors of TGF-beta signals, portmanteau for Sma and Mad

Snorc: Small NOvel Rich in Cartilage

SOAR: STIM1 ORAI activating region

SOCE: store-operated Ca^{2+} entry

Sox: sex-determining region Y-related high mobility group-box gene

Stat3: signal transducer and activator of transcription 3

STIM: stromal interaction molecule

SUE: septin unique element

SV40: simian vacuolating virus 40

Tcf3: transcription factor 3

TGF-beta: transforming growth factor beta

Thr: L-threonine

TIRF: total internal reflection fluorescence microscopy

TM: territorial matrix

Tris: 2-Amino-2-(hydroxymethyl)propane-1,3-diol

TRP: transient receptor potential channel

TRPC: canonical transient receptor potential channels

TRPV: transient receptor potential vanilloid

Tyr: L-tyrosine

VDCC: voltage-dependent Ca^{2+} channel

Wnt: a portmanteau for the names Wingless and Int-1

YM-58483: 4-methyl-4'-(3,5-bis(trifluoromethyl)-1H-pyrazol-1-yl)-1,2,3-thiadiazole-5-carboxanilide

Zfp281: Krüppel-like zinc finger transcription factor 281

1. Introduction, Aims and Objectives

Musculoskeletal disorders comprise a set of diseases that affect a major portion of the population at various stages throughout their life. Typically, these conditions include alterations that cause a significant deterioration in one's quality of living, particularly in the case of osteoarthritis or discopathy; with the latter one also attributed as a nervous system disease. Severe forms of the above musculoskeletal diseases are strongly age- and weight-related, which – in the light of current tendencies in the relevant composition of modern Western societies – is something that makes them an even more critical issue for the future. The World Health Organization of the United Nations recognized the stake of this matter and launched an independent global non-profit organization, the Bone and Joint Decade [1] for the period between 2000 and 2010 to reduce the burden and cost of musculoskeletal conditions to individuals, careers and society worldwide. The organization has been remandated in 2010 as the Global Alliance for Musculoskeletal Health owing to the importance of their job and the long-continued nature of the crisis. A vital pillar of reaching these dignified goals is carrying out cutting-edge research aimed at understanding basic biological processes of the involved tissues, such as pathways and genetic factors that govern various functions of developing and mature articular cartilage.

Our research group at the Department of Anatomy, Histology and Embryology has several decades of experience in studying *in vitro* chondrogenesis. As it is reflected in the following work, we are putting effort into expanding the range of our experiments to multiple chondrogenic models, including chick and mouse embryonic primary micromass cultures, C3H10T1/2 cell line-based colonies and even bone marrow-derived human mesenchymal stem cells (hMSCs), which are not represented here. Moreover, we are also working on gathering data on the role of certain genes in cartilage development from *in vivo* experiments with conditional knockout (CKO) mice. Although there are examples where chondrogenic differentiation of the C3H10T1/2 cell line and primary limb bud-derived micromass cultures has been analyzed, we concluded that an exhaustive comparison under well-standardized conditions, which takes into account mRNA expression profiles of numerous genes that are characteristic for differentiation towards selected mesenchymal (i.e. chondro-, osteo- and adipogenic) lineages in an array of models would fill an important gap in our knowledge; enabling simultaneous comparison of mouse and chicken, plus primary and cell line-based chondrogenic models. Accordingly, **our aims and objectives** were partly to find answers for the following questions:

1. How will mRNA-levels change throughout an extended culturing period during an expression analysis of a well-selected pool of marker genes in control and *BMP-2*

overexpressing C3H10T1/2 micromass cultures, as well as mouse and chick embryonic limb bud-derived micromass cultures?

2. What will differentiation potentials in osteo- and chondrogenic directions reflect in the above models based on marker gene mRNA levels? Are there cells undergoing adipogenic differentiation in the colonies?
3. Will morphological observations following histological staining procedures that are suitable for determining cellular morphology, chondrogenic differentiation, matrix mineralization and lipid accumulation in high density cultures (HDC) determine any difference in the examined models? If yes, what are these differences? Are these results coherent with those obtained from investigating marker gene expression levels?
4. Are there cells that maintain a pluripotent state in HDC? If so, is there a difference in the expression of pluripotency markers among the models?
5. Finally, which model(s) are the most suitable for conducting research on chondrogenesis (if there is an unequivocally superior one at all)? What are some of the main practical considerations?

After exploring the above questions, we have decided to move on to further issues regarding Ca^{2+} signaling during cartilage development using the chicken HDC model. So far, Ca^{2+} homeostasis has been described in many cell and tissue types including cartilage. However, most of the available information on Ca^{2+} homeostasis is collected from studying mature and/or hypertrophic chondrocytes of clinically relevant territories. In the recent years, our laboratory has successfully enriched the available literature on chondrogenesis, with special regards to intracellular Ca^{2+} events, related signaling molecules and pathways. In our opinion, this is the most important, as future cartilage-healing approaches will surely need to be based on a detailed knowledge of signaling events of how a mesenchymal cell differentiates into a mature chondrocyte, in which – with contribution of works from our laboratory – Ca^{2+} is already known as a prominent secondary messenger of chondrogenic intracellular events. To this end, we were also interested in addressing the ensuing issues:

1. Do the differentiating chondrocytes of our model possess voltage-dependent Ca^{2+} channels (VDCCs) or the molecules that are required for store-operated Ca^{2+} entry (SOCE)?
2. What is the input of internal Ca^{2+} stores and the involvement of Ca^{2+} release-activated Ca^{2+} channels (CRACs) and VDCCs in generating and maintaining high-frequency repetitive Ca^{2+} transients to modulate cellular functions such as differentiation, metabolic activity and proliferation?
3. What kind of dynamics can be characterized at high spatial and temporal resolution by analyzing intracellular Ca^{2+} transients of individual chondrifying cells using LIVE confocal

Ca^{2+} imaging microscopy? Can the observed dynamics be modified by adjusting the extracellular ionic milieu or by the application of SOCE and/or VDCC blockers?

4. Will we be able to observe altered parameters in store depletion-induced SOCE following application of SOCE blockers in single cell Ca^{2+} measurements?
5. What kinds of alterations, if any, can we notice on such cellular parameters as differentiation, metabolic activity and proliferation of chondrogenic chick HDC following the application of an inhibitor of septin rearrangement, which – according to recent research [2] – is of key importance in the activation of CRACs?
6. In conclusion, the final aim of this work is to provide a refined model of Ca^{2+} signaling events including Ca^{2+} influx and release functions with the inclusion of a recently uncovered regulator of SOCE in the well-established chicken chondrifying HDC during *in vitro* chondrogenesis.

Accordingly, this PhD thesis is an attempt to synthesize our results gathered in a hard-to-define field that simultaneously draws merit from embryology, biochemistry and physiology into a work that will hopefully contribute to the advancement towards the Holy Grail of cartilage research, an ideal cure for chondropathies. Following an overview of the latest literature that summarizes essential information on articular cartilage biology and pathology with a special emphasis on *in vitro* chondrogenic models, genetic factors and signaling pathways that regulate chondrogenesis, a comparative analysis of notable chondrogenic models, as well as novel developments and factors in the relationship of intracellular Ca^{2+} concentration changes and chondrogenesis will be provided.

2. Literature Review

2.1. Histology of Cartilage

Cartilage is one of the main connective and supporting tissues, thus it is an essential component of the vertebrate body, including humans. As such, it plays a versatile role in both the phase of development and maturity. The early embryonic skeleton mostly consists of hyaline cartilage tissue, the role of which, in addition to providing structural support, is to contribute a template to long bones that form by means of endochondral ossification. The entire template is not converted to bone tissue during this process, certain parts of it are maintained as cartilage: the epiphyseal (or growth) plate is responsible for longitudinal growth of said bones until it completely ossifies in early adulthood, while the parts covering the articular surfaces – that are responsible for providing wear-resistance and shock-absorbance – ideally remain intact for the entire life of the organism. Further cartilaginous structures can be found in joints in addition to articular cartilage (e.g. discs and menisci), moreover, multiple structures that require some degree of flexibility are also composed of cartilage in the head, neck and thorax region (such as nose, ear, larynx. trachea, bronchi) [3] *(Fig. 2.1.)*.

Cartilage is not a uniform tissue type in multiple respects; most importantly, different groups can be characterized both developmentally and structurally. Although cartilage arises from mesenchyme during chondrogenesis, it can arise as a derivative of two main germ layers during early development: most cartilage of the head and neck region spawns from the neural crest (ectoderm), while in the remaining parts of the body it is the derivative of the mesoderm (either paraxial or lateral plate) [4] *(Fig. 2.1.)*. Furthermore, there are three main types of mature cartilage, which are dissimilar in their appearance and mechanical properties due to their extracellular matrix (ECM) characteristics: hyaline cartilage, elastic cartilage and fibrocartilage. Since this work is focused on articular cartilage composed of hyaline cartilage, the ensuing segments will provide the detailed discussion of this tissue type alone.

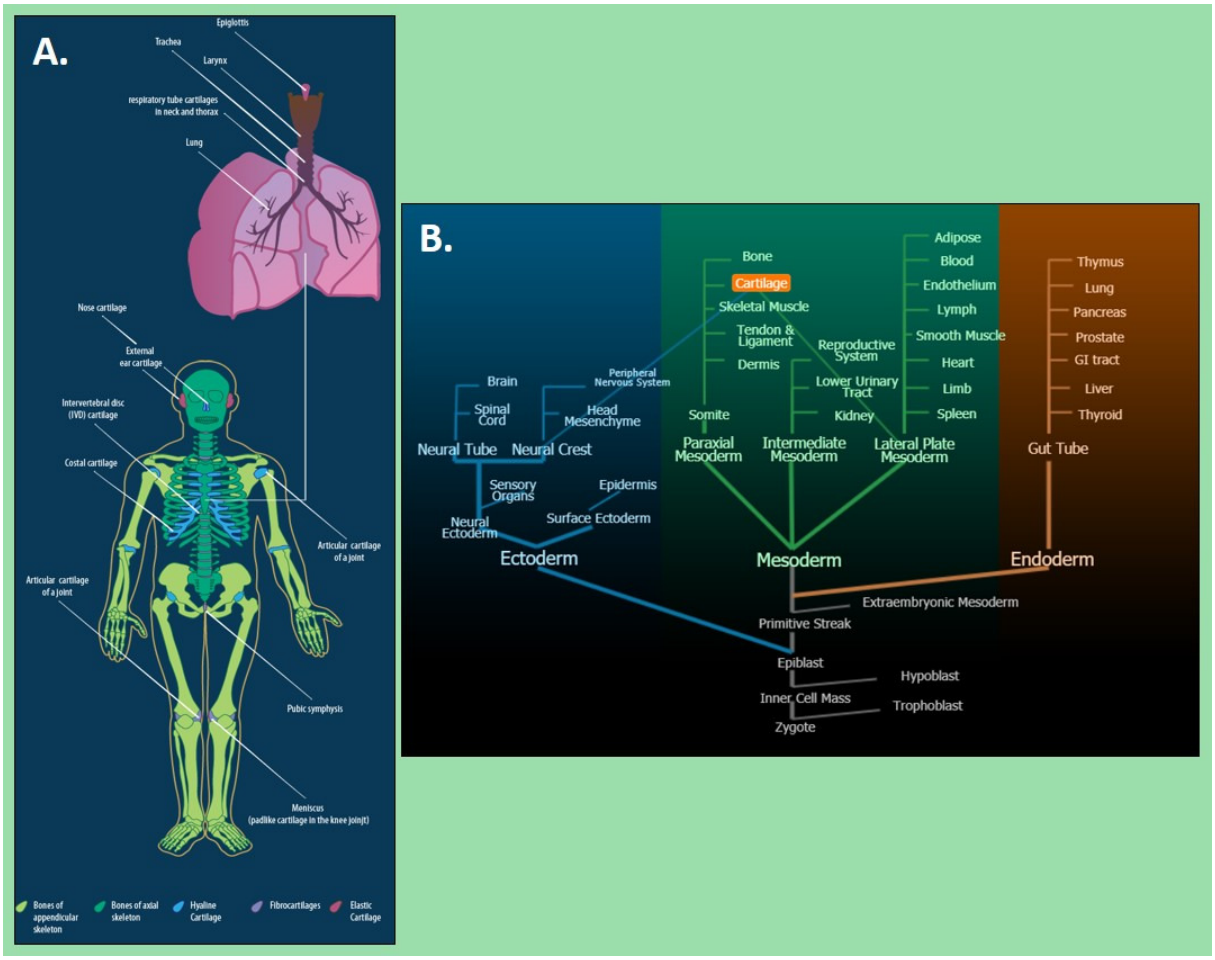

Fig. 2.1. (A) Various types of cartilage tissue can be found in different organs and organ systems of the human body with the musculoskeletal and the respiratory systems being the main locations for cartilage to appear. (B) Forming cartilage is provided by three different embryonic cell populations. Cranial neural crest cells contribute to most of the cartilaginous structures in the head region while cartilage of the appendix region of the limbs and of the axial skeleton is contributed by the lateral plate mesoderm and the sclerotomes derived from the paraxial mesoderm, respectively [5].

2.1.1. Hyaline Cartilage

This tissue type appears in three, functionally distinct forms throughout the human body: as **permanent cartilage** being present in the respiratory tract, forming costal cartilages and nasal cartilages. At these places, it is surrounded by a special connective tissue capsule termed as perichondrium. Articular cartilage is a unique variant of permanent cartilage, where perichondrium lacks from the surface of the tissue. Hyaline cartilage can also serve a template to bones that form by endochondral ossification; this is the so called **transient subtype** of the tissue. A mutual characteristic of all three forms is the relatively low volume of cells that contribute about 5% of the wet weight of the tissue in mature articular cartilage [6]. The remaining portion of the tissue, the abundant organic ECM consists of a complex structure of cartilage-specific molecules that can be classified into three main categories [7].

Collagens represent the most abundant and thus the most important structural macromolecules of the ECM in articular cartilage accounting for 10 to 20% of the wet weight of the tissue [6]. Numerous types of collagen are present in the articular cartilage, however the vast majority collagens is represented by **type II** [8, 9]. However, other collagen types, present in a lesser ratio, also play important roles: type IX links other matrix components to the collagen network, type X organizes the fibrils into an ordinate network, type XI regulates the length of the collagen fibers, whereas type VI fibrils form the majority of the capsular matrix [10, 11] and bind to integrin receptors on the cell surface, thus interconnecting chondrocytes with the ECM.

Proteoglycans (PGs) form another essential and expansive group of ECM macromolecules, making up 10 to 15% of the wet weight of articular cartilage [12]. Proteoglycans are large protein-polysaccharide molecules forming either monomers or aggregates [13]. **Aggrecan** is the most prominent PG type in articular cartilage. Each aggrecan monomer consists of a core protein to which around 150 glycosaminoglycan polysaccharides (GAG) are attached covalently. The individual GAG sidechains are separated from one another by charge repulsion. The name of this PG is derived from the fact that in cartilage tissue, aggrecan monomers usually associate with **hyaluronic acid** (HA) to form aggregates *(Fig. 2.2.)*. These aggregates are composed of approximately 150 PGs, which attach non-covalently to a central HA by small glycoproteins called **hyaluronan and proteoglycan link protein 1 (Hapln1)** [13]. PGs provide articular cartilage a resistance against compressive forces and deformations by attracting water and thus causing its hydration. Other small PG types (such as biglycan, fibromodulin and decorin) that are also present in various connective tissue types, are also notable as hyaline cartilage ECM components. These are mainly responsible for maintaining the matrix structure.

The third major group of ECM macromolecules is comprised of **multiadhesive glycoproteins** (e.g. chondronectin, tenascin and fibronectin). Their leading role is to link chondrocytes and PGs to the structure formed by collagen fibrils. The group also includes Hapln1 that stabilizes aggregates of aggrecan and HA [14]. Further members of the group are perifibrillar adapter proteins, the main ones (in addition to the above-mentioned collagen IX) being decorin, cartilage oligomeric matrix protein (COMP) and matrilin-3 [15].

Mature chondrocytes are spherical cells and the sole resident cell type of hyaline cartilage. These cells are located in lacunae within the ECM and a few neighboring cells form isogenous groups called chondrons *(Fig. 2.2.)*. Macromolecules in the **cartilage matrix** are not distributed evenly, thus, the ECM can be divided into three different regions based on staining properties, fiber arrangement and PG distribution. The chondrocyte links its surface to a transparent pericellular glycocalyx which in

turn is enclosed by a pericellular capsule forming the so called *pericellular matrix* (PCM). Type VI collagen is a major component of the PCM and is only found in this part of the mature articular cartilage [16]. The PCM has a high concentration of macromolecules (type VI collagen, chondronectin, decorin, laminin and sulfated PG types) that link chondrocytes to the matrix. As negatively charged molecules are distributed densely in the PCM, it appears as an intensely basophilic area in conventional light microscopic images. Isogenious chondrocytes are embedded in a more remote part of the ECM, called *territorial matrix* (TM). As PGs are also present in a relatively high concentration in the TM, it is also basophilic, but the phenomenon is less intense in comparison with PCM. An isogenous group of chondrocytes and their territorial matrix forms the structural unit of cartilage traditionally termed as *chondron*. Finally, the *interterritorial matrix* (IM) is set between chondrons. In accordance with the tendency in the regional differences in the distribution of sulfated proteoglycans, IM has the lowest concentration of these molecules [17]. On the other hand, the closer packing of collagen fibers [18] is also a known characteristic of this region, which accounts for the eosinophilic staining of the area as well [7].

As **cartilage is an avascular tissue**, the exchange and transport of nutrients, gases and metabolites take place by continuous diffusion from the surrounding connective tissue and the perichondrium; while in the case of cartilage in our primary area of interest, synovial joints, the synovial fluid and the subchondral bone tissue are the main sources of supply. Cartilage, as a consequence, is regarded a bradytroph tissue that is characterized by a *low metabolic rate, slow renewal and by chondrocytes having an extremely long lifetime* [19]. The milieu required for diffusion is provided by the high water content of the tissue that is mostly bound to the sulfated GAGs of the ECM [20, 21]. As mentioned, the majority of water is bound to ECM components, thus it provides the tissue its ability to resist compression and return to its original state following deformation [22]. In addition, biomechanical forces resulting in such fluid movements are actually key factors in keeping mature cartilage in a healthy state, which can at least partly be attributed to the fact that they facilitate diffusion to and from the tissue [23].

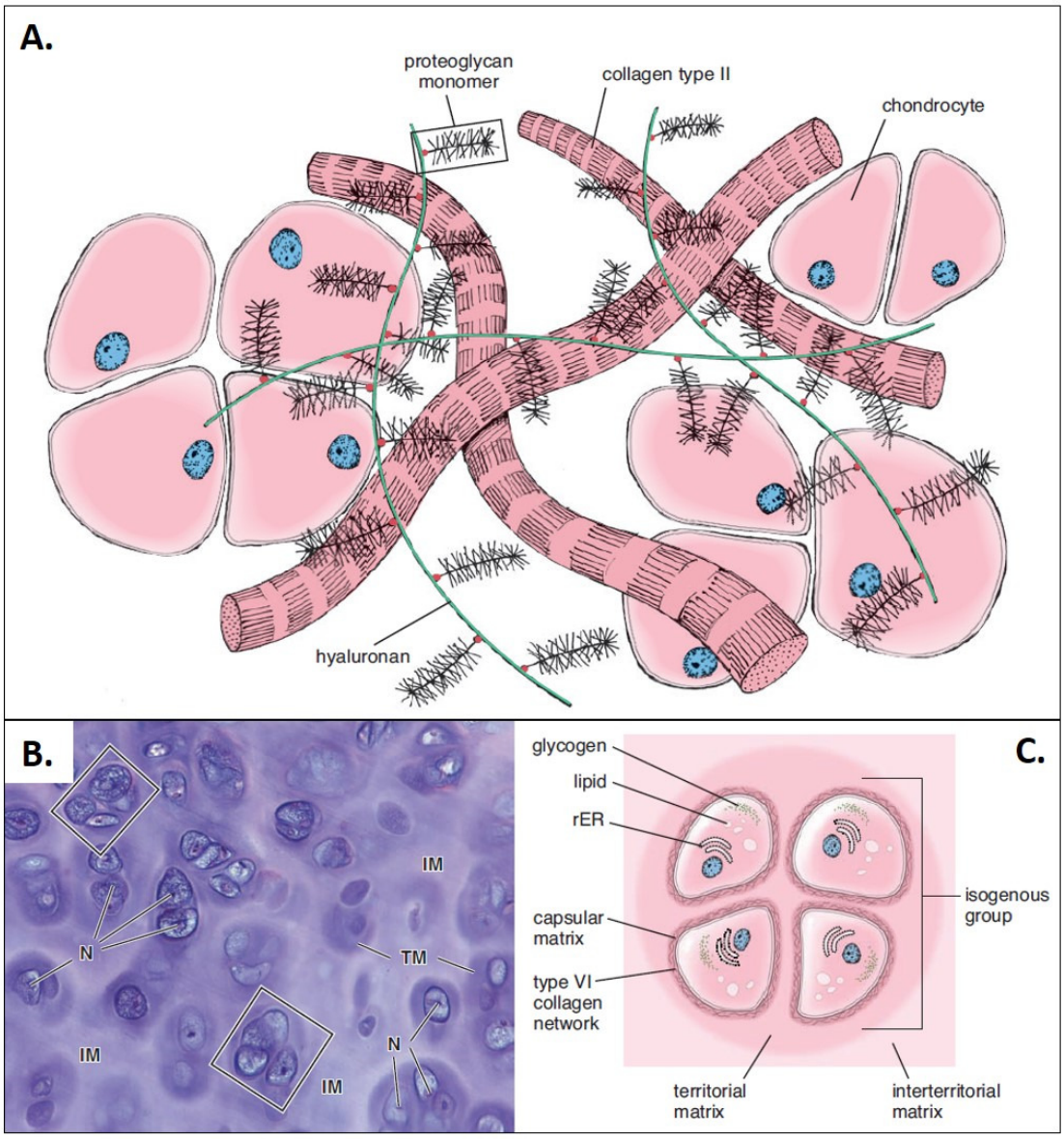

Fig. 2.2. Schematic [(A) and (C)] and light microscopic (B) structure of chondrons (in rectangles), the basic functional unit of hyaline cartilage. From the work of Ross and Pawlina [7].

As partly stated previously, resting chondrocytes of mature articular cartilage are incapable of dividing and have a low metabolic activity [7]. These facts alone provide some explanation for the very low regeneration potential of articular cartilage. Furthermore, the absence of the perichondrium along with the chondrogenic cells it contains in its inner layer from makes the picture even more complex. Exploring the possibility of cartilage regeneration is evidently a fundamental goal of cartilage research. Recent studies have identified a number of *mesenchymal stem cell (MSC) tissue reservoirs in adult humans* that include cartilage, bone marrow, adipose tissue, periosteum, and muscle [24]. Furthermore, migratory chondrogenic progenitor cells have been identified from repair tissue in later stage human osteoarthritis, which means that the tissue has healing capacity, although to a very limited extent [25] and the poor intrinsic regenerative ability is firmly outweighed by the catabolic

processes in pathological conditions that are detailed later in this chapter. Hyaline cartilage has a complex architecture and the repair tissue, even if it forms, is biomechanically inferior fibrocartilage in the majority of cases [26]. Proliferation and differentiation of pluripotent mesenchymal stem cells or chondroprogenitors into chondrocytes and the formation of cartilage tissue is a complex process that depends on numerous factors. Also, the chondrocyte phenotype is determined by a particular local microenvironment provided by the cartilage-specific ECM; the alteration or loss of this surrounding at any point during or after differentiation leads to dedifferentiation [27], making autologous implantation of chondrocytes a very difficult challenge [26].

2.2. Pathological Conditions of the Articular Cartilage, Osteoarthritis

Articular cartilage pathology consists of a range of conditions that are potentially debilitating and may have a dramatic impact on the well-being of an individual. These chondropathies present the main relevance of our work. Symptoms usually consist of persistent pain and decreased function of joints. Lesions of various joints are being diagnosed in increasing numbers every year [28, 29]. These lesions frequently progress to symptomatic osteoarthritis (OA) and a sort of functional impairment in otherwise healthy patients. As articular cartilage is an avascular and alymphatic tissue, it has a very limited natural healing capacity [30-32]. Therefore, *articular cartilage is isolated from the systemic circulation, so the normal inflammatory and reparative processes are not capable to assist the repair of injured cartilage in a synovial joint* [33]. In the meantime, healthy chondrocytes in the surrounding tissue are kept away by the extracellular matrix which prevents their migration to the damaged site [34]. Another adverse feature is that even though injuries that penetrate subchondral bone can promote the production of reparation tissue by multipotent bone marrow stromal cells, this tissue is usually *fibrocartilage*, which is biomechanically inferior to hyaline articular cartilage, partly because it is primarily composed of type I collagen [35, 36].

OA is a progressive, degenerative and disabling disease of synovial joints. It not only affects the elderly, but also younger, physically active individuals who usually engage in highly demanding activities (such as intense sports) [37]. OA may form in various sites, mainly in the large joints of the lower limb (knees, hips), but could also occur in hands and vertebral column. Its main characteristics are gradual destruction of articular cartilage by proteolytic degradation of the ECM, typically leading to remodeling of the affected joints. Therefore, among the earliest signs is the loss of PGs [38, 39], followed by reduction in the collagen network and decreased stiffness against compressive forces. [40]. These changes alter physiological deformation, metabolic activities and electromechanical events of articular chondrocytes under bodyweight [39, 41]. Risk factors include age, obesity, previous joint damage and joint malalignment. The importance of OA is highlighted by the fact that it is the leading

cause of disability in adults with more than 50 million adults reporting arthritis. In an ageing society where obesity rates also rise, the prevalence of OA is expected to further increase; by 2030, around 25% of the adult population of the USA is expected to suffer from this disease [42]. Along with the alteration of OA affected articular cartilage *(Fig. 2.3.)*, changes also occur in the menisci, synovium, ligaments, periarticular muscles and the subchondral bone. With the progression of OA, the changes in the joint become more severe and gradual loss of function occurs [43]. A notable step in OA development is the release of inflammatory factors by synovial macrophages and fibroblasts, which induce changes in chondrocytes that normally are responsible for the maintenance of the structural integrity of articular cartilage ECM (e.g. collagen and aggrecan). However, under OA conditions, these cells up-regulate the production of catabolic enzymes, such as matrix metalloproteinases (MMPs) and aggrecanases that degrade the ECM and release protein fragments. Depending on the severity of OA, these catabolic events cause a reduction in the osmolarity of the extracellular milieu of cartilage, which leads to deterioration of biomechanical properties and increased deformation during mechanical load [44, 45]. The released fragments then initiate further inflammatory responses building a positive feedback loop causing more and more severe cartilage destruction. Furthermore, inflammatory cytokines have derogatory effects on the adjacent synovium and bone, stimulating synovial inflammation and deregulation of subchondral bone remodeling.

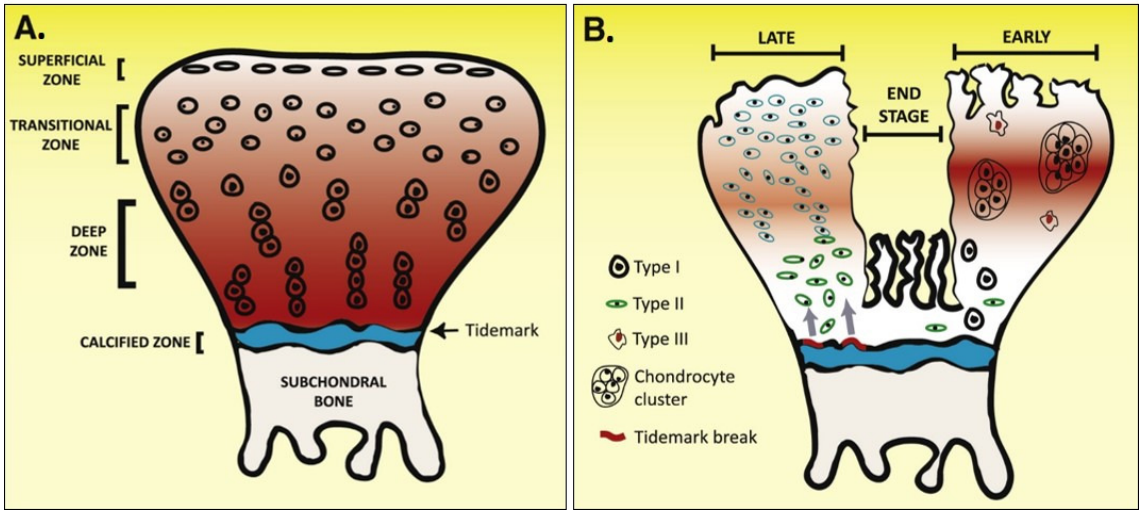

Fig. 2.3. (A) Articular cartilage under normal circumstances is composed of superficial, transitional, deep and calcified zones. The tidemark (blue line) forms connection between the deep and calcified zones, while the density of proteoglycans – mostly aggrecan – is shown by red color. (B) Influence of early to terminal phases of OA on the structure of articular cartilage [46].

2.3. Chondrogenic Models

In vivo study of chondrogenesis poses a very difficult challenge that we are currently yet to overcome. The majority of this hardship stems from the fact that differentiation of cartilage and a set of other tissues of mesenchymal origin takes place in early embryogenesis [47-49]. Therefore, as

presented below, numerous *in vitro* models have been developed during attempts to obtain data that can be translated into medicine. The broad spectrum of roles played by various types of cartilage tissue during fetal and adult life make it unsurprising that numerous conditions are known to be derived from abnormal development and function of cartilage. *Chondropathies* can result from defects of many genes that are somehow related to chondrogenesis [3]. The *initial condensation of mesenchymal cells* is a precondition of their differentiation. As a consequence, *in vitro* models aim to mimic these conditions by setting *high cellular density* (HD). HD brings about *cellular interactions* that are essential to promote chondrogenic differentiation of pluripotent mesenchymal cells, as well as chondroprogenitors. The well-established and reproducible avian model for studying hyaline cartilage formation was first proposed by Ahrens and colleagues [50]. The simplicity of this model lies in the limb bud-derived chondroprogenitor cells' innate ability to spontaneously differentiate into chondroblasts and then chondrocytes. Thus by day 6 of **HD culturing**, a significant amount of metachromatic ECM is produced *(Fig. 2.4.)*. In addition to the chondrogenic cell population, the cultures contain cells of the fibrogenic and myogenic lineages, but the number and ratio of these cells diminishes in later phases due to the conditions favorable to chondrogenesis [51]. A major advantage of this model in addition to its cost-effectiveness is the high yield of chondroprogenitor cells from embryos of the same developmental stage (Hamburger-Hamilton 23-24) [52] that are obtained by synced incubation of fertilized eggs. A drawback of the avian model that has to be taken into consideration is that differently regulated signaling pathways may exist when compared to mammalian systems. Although these digressions are not numerous, chondrogenesis in chick for instance, is influenced negatively by extracellular signal regulated kinase 1/2 (ERK1/2) [53, 54], one of the mitogen-activated protein kinases (MAPKs). Meanwhile in mouse cells ERK1/2 turns out to be a positive regulator of chondrogenesis in chondrocytes as well as in C3H10T1/2 cells [55, 56]. Further remarkable disadvantages of the chick model are the limited availability of antibodies, the lower number of published gene sequences and certain drugs that work well in a mammalian system, act with diminished or zero efficacy on avian targets [57]. Regardless of the above-mentioned factors, the relevance of the avian chondrogenic model is confirmed by many recent studies applying this system to describe important signaling mechanisms of chondrogenesis [57-63].

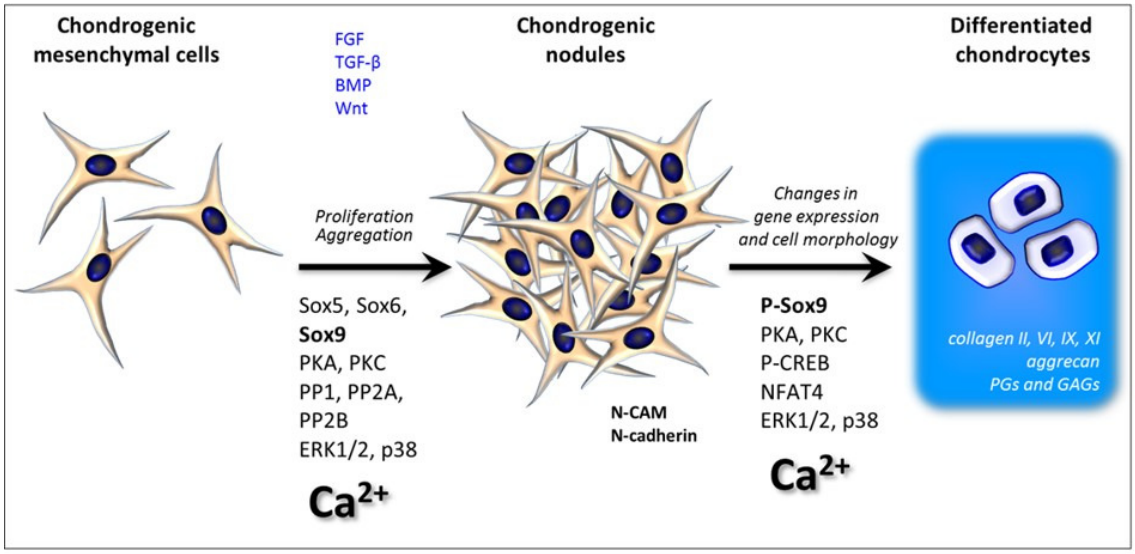

Fig. 2.4. Major events during chondrogenesis and the main signaling pathways that regulate differentiation. Chondroprogenitors are originally loosely organized and have a typical elongated morphology. In the condensation phase chondrogenic cells proliferate considerably and migrate to form precartilaginous nodules. Cell adhesion molecules like N-CAM and N-cadherin and soluble factors (such as FGF, BMPs, Wnt) are all required for this process. Following differentiation, cellular morphology becomes rounded and gene expression of the cells shifts in favor of cartilage-specific ECM synthesis. Calcium is vital for diverse pathways to function throughout each step of chondrogenesis [64].

Mammalian chondrogenic models offer a necessary replacement under circumstances when these limitations create an obstacle. One of the possible options is preparing mouse embryonic limb bud-derived micromass cultures in a technically highly similar fashion to the previously discussed avian one [65]. Nevertheless, they present a serious experimental difficulty in many aspects when compared with the previous model. Precise timing of the pregnancy is essential so that all of the embryos are in the same developmental stage, furthermore several pregnant mice are needed simultaneously in order to obtain a sufficient cell number. However, even with all these conditions fulfilled, there is an inevitable variation among experiments that is an inherent feature of **primary cell cultures**. Still, a considerable disadvantage and moral concern of this model is the necessity to sacrifice the mother animals.

On the other hand, transgenic and/or knockout animals can also be used as a cell source, thus creating a possibility to avoid the otherwise quite burdensome transfection, which is another axiomatic trait of HDC [66]. Similar primary cell cultures can also be established with the isolation of mature chondrocytes from articular cartilage or other tissues and organs containing hyaline cartilage (for instance trachea and nasal cartilage). Nonetheless, such cultures are not suitable for studying chondrogenic differentiation. It is also noteworthy that chondrocytes quickly lose their mature phenotype when taken out of their normal environment provided by the ECM, which is thus considered necessary to maintain their differentiated state [67, 68].

In the meantime the previously mentioned limitations posed by the application of primary cell cultures have been tackled by the establishment of diverse **cell lines with potential for differentiation in** most importantly **chondrogenic** – and other mesenchymal – **directions** [69]. The mouse cell line ATDC5 was isolated from a differentiating culture of AT805 teratocarcinoma [69], RCJ 3.1 is a clonal cell population derived from a 21-day-old fetal rat calvaria [70] and C3H10T1/2 is a multipotent mouse embryonic mesenchymal cell line [71]. The C3H10T1/2 cell line is quite an attractive model for studying chondrogenesis, because the cells can be expanded without the risk of unwanted differentiation, as they do not do so in a spontaneous fashion under normal culturing conditions. This, on the other hand, means that all experiments involving chondrogenic induction requires special media containing certain morphogens, such as BMP-2 or TGF-β1 [71, 72]. As a solution to ease this at least partly financial issue, a construct continuously overexpressing the human BMP-2 has been transfected into C3H10T1/2 cells [73]. The expressed morphogen drives *in vitro* chondrogenesis of this cell clone when cultured in high density as an autocrine-paracrine factor without any special media requirement other than the presence of puromycin to maintain the plasmid.

In order for the chondrogenic models to provide the best translation capacity for clinical application, a shift to use **human chondrogenic cell lines or hMSC** is unavoidable. The number of explored possibilities is already high, chondrogenic progenitor cells have been isolated from repair tissue [25] of late stage osteoarthritic articular cartilage. These cells were involved in experiments that demonstrate the necessity of purinergic signaling in their calcium oscillations [74] which is known as an essential feature of chondrogenesis [75] showing their true potential as a model for research in such area. Human adult MSCs or cells bearing stem cell properties can be isolated from a number of sources; synovial joint tissues such as articular cartilage [76, 77], synovial membrane [78], tendons [79] and infrapatellar fat pad [80], bone marrow [81], trabecular bone [82] and muscle [83]. These sources should be mentioned separately as due to their spatial characteristics, MSCs located in the proximity of articular cartilage may participate in natural regenerative processes of diseased joints. However, isolation of MSCs is also possible from tissues that are not necessarily in close relationship with articular cartilage, such as subcutaneous adipose tissue [84, 85] and Wharton's jelly [86]. It is noteworthy that most of these cells have been shown to successfully differentiate into cartilage *in vitro*, but the observation has to be handled with caution, as reproducing the unique architecture of articular cartilage is still a major challenge.

Regardless, the above-mentioned simple and cost-effective animal systems are used in several laboratories to date due to various reasons; identification of novel therapeutic targets for a host of

musculoskeletal diseases is simplified and made more effective, and also because drug candidates are usually tested for safety and efficacy using such models before proceeding to clinical trials.

2.3.1. Marker Genes of Mesenchymal Differentiation Pathways

Expression profiling of marker genes based on reverse transcription polymerase chain reaction (RT-PCR) is one of the best options available to determine the differentiation status of a cell culture; it is relatively cost-efficient, effective and can easily be verified in a comparative fashion. It can be even extended as a quantitative/semi-quantitative approach to follow expression level changes of various marker genes throughout the process of differentiation of a single or between multiple cell types. Therefore, this approach is an essential tool when assessing cell types – as in our case with cells of mesenchymal origin – that are theoretically capable of differentiating in multiple directions. The main goal for which we picked our set of marker genes for investigation is to determine the osteo- and chondrogenic differentiation potentials of the discussed cell types, but we also undertook to analyze their adipogenic potential and how much they retain from their stem cell characteristics.

2.3.1.1. Cartilage-Specific Markers

Certain members of the **SRY (sex determining region Y)-box (SOX) transcription factor family**, especially **SOX9** in cooperation with **SOX5 and 6**, serve as a key transcription factor trio of chondrogenesis that is regulated by a host of chondrogenic pathways and maintains a steady expression level over cartilage formation (see below). **Aggrecan (ACAN)** and **type II collagen (COL2A1)** are both essential and specific components of the hyaline cartilage ECM (for their description, see above). **HAPLN1** is a glycoprotein that exists as a monomer of 356 amino acids in mice. As in the case of all essential cartilage components, SOX9 is a key regulator of its expression. HAPLN1 stabilizes aggregates of aggrecan and HA [14]. **SNORC** (Small NOvel Rich in Cartilage) is a novel cartilage-specific transmembrane chondroitin sulfate proteoglycan, which is implied in the regulation of chondrocyte maturation and postnatal endochondral ossification. SNORC also has a glycosaminoglycan independent affinity to FGF2 and it inhibits FGF2-dependent cell growth of C3H101/2 cells [87], which is an important precondition of differentiation [88]. **Lubricin (PRG4)** is a glycoprotein amply expressed in the superficial zone of articular cartilage responsible for joint boundary lubrication. It has been noted as a potential preventive therapeutic for certain posttraumatic joint degenerative diseases due to its superior lubricant properties [89]. **Type X collagen (*Col10a1*)** is a marker expressed in calcifying parts of articular cartilage in the proximity of the subchondral bone, where it even participates in the formation of new bone. This collagen type is a key ECM component during endochondral bone formation. Consistently, the expression of this gene is an indication of mature, hypertrophic

chondrocytes. The medical application of this collagen type is also conceivable in inducing or mediating endochondral ossification in cases like the fracture healing of synovial joints [90].

2.3.1.2. Markers of Osteogenic Differentiation

Runt-related transcription factor 2 (RUNX2 or CBFA-1) is an important osteogenic transcription factor, which is necessary for inducing the expression of multiple osteogenic genes. Its function is carried out by binding to promoters of osteogenic genes and activating their transcription [91]. **Osterix (OSX)** is another essential transcription factor that is expressed in osteoblasts, which is fundamental for osteogenesis. It has been demonstrated to interact with RUNX2 in a physical and functional manner to regulate bone formation by osteoblasts [92]. **Collagen type I (COL1A1)** is the most abundant protein of the bone ECM; it accounts for 95% of the total bone collagen and 80% of the whole bone protein [93]. Although it is a highly ubiquitous ECM component of many tissue types, when it is considered in its context and along with other factors, it is a reliable marker of osteogenesis. **Osteocalcin (OC)** is a dependable osteogenic marker, as it has been found only in bones and in dentin. It is a non-collagenous bone ECM protein, which is chiefly synthesized by mature osteoblasts, odontoblasts and hypertrophic chondrocytes [93]. **Osteopontin (OP)** has been verified as a marker for osteoblasts that plays an important role in matrix mineralization and communication between cells. It was also found to be regulated by mechanical forces, which makes it a contributor to the mechanotransduction pathway [94]. **Alkaline phosphatase (AP)** is a ubiquitous enzyme attached to the outer cell surface. The physiological role of AP is the dephosphorylation various substrate molecules, it also clearly plays an important role in osteoid formation and mineralization. The total AP amount consists of numerous dimeric isoforms originating from diverse tissue types, such as liver, bone, intestine, spleen, kidney and placenta [95].

2.3.1.3. Adipogenic Lineage-Specific Marker Genes

Fatty acid binding protein 4 (FABP4) is a predominantly cytosolic protein that can reversibly bind saturated and unsaturated long-chain fatty acids with high affinity. As it is expressed in adipocytes, its suggested traditional function is facilitating the transport of lipids to specific compartments in the cell [96]. It has been recently reported that elevated serum level of FABP4 is associated with a host of diseases, such as obesity, insulin resistance, type 2 diabetes mellitus, hypertension, renal dysfunction and cardiovascular events, making *Fabp4* a possible candidate for diagnostic marker role [97]. **Peroxisome proliferator-activated receptor gamma 2 (PPARγ2)** is a critical component of adipogenic differentiation. PPARs are members of the nuclear hormone receptor family, which includes retinoic acid receptors, thyroid hormone receptors and vitamin D3 receptors

[98]. *Pparγ* has two isoforms, γ1 and γ2. *Pparγ1* is expressed in early adipogenic stages and in other cell types too, while *Pparγ2* has an expression that is limited to adipose tissue. Ablated expression of *Pparγ2* has been demonstrated to suppress adipogenic differentiation [99].

2.3.1.4. Pluripotency Factors

OCT4, SOX2 and NANOG are well-known key components of the core regulatory network that governs embryonic stem cell (ESC) pluripotency [100]. **Octamer-binding transcription factor 4 (OCT4)** is one of the earliest factors identified as obligatory for pluripotency maintenance [101]. *Oct4* displays a strong expression during mouse and human embryonic development as far as the stage of gastrulation, when its global level decreases rapidly, causing it to be limited to primordial germ cells [102]. The avian homolog of *Oct4*, which is similarly required for the maintenance of pluripotency and self-renewal of chicken ESCs, is known as ***PouV*** [103] *(Fig. 2.5.)*. **NANOG** (derived from Celtic mythological expression Tir na nÓg) is an atypical homeodomain protein that controls the proliferation of undifferentiated ESCs. *Nanog* mRNA expression can be detected from pluripotent mouse and human cell lines. Yet, its expression becomes diminished after differentiation [104]. **SOX2** is a transcription factor that belongs to the family of high-mobility group transcription factors. SOX2 is an essential factor for the development and preservation of undifferentiated ESCs. It also has a vital role in the establishment of induced pluripotent stem cells (iPSCs) from somatic cells (the primordial factors were **OCT3/4, SOX2, cMYC and KLF4** – the so-called **Yamanaka factors**) [105].

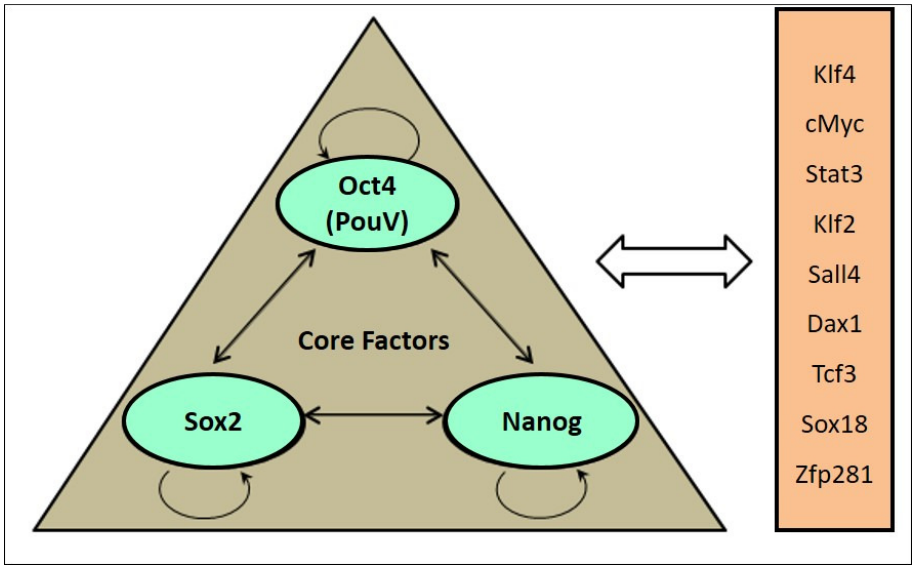

Fig. 2.5. Schematic image displaying the transcriptional regulation of core pluripotency factors and highlighting some of the extended factors. Modified based on the work of Bieberich and Wang [106].

2.4. The Process of Chondrogenesis

In the early stage of ontogenesis **chondrocytes differentiate from mesenchymal cells** of different origin via a complex multi-step process [107]. The cells arise from various sources throughout the embryonic body, notably, in the case of limb articular cartilages, its source mesenchyme originates from the lateral plate mesoderm. An initial and cardinal step is the **condensation** of cells into chondrogenic nodules without any morphologic change, making them indistinguishable from other mesenchymal cells. In chicken primary HDC, this contraction mainly takes place on day one of culturing, while the aggregated cells become chondrocytes during day two and three [50]. **Cell-cell interactions** mediated by N-cadherin are, at least partly, responsible for directing the process of cell condensation, as demonstrated by using neutralizing antibody to block the biological activity of N-cadherin *in vitro* in hMSC culture and *in vivo* during the limb bud formation [108]. N-cadherin presenting cells play an important role in chondrogenic pellet formation and tissue homogeneity [109]. The presence of FGF receptors and N-CAM on cell surfaces have also been indicated as a positive regulator in mesenchymal condensation [110, 111]. The condensation phase is also characterized by the appearance of gap junctions with an emphasis on Connexin-43. The blockade [112] or downregulation [113] of this junction results in decreased chondrogenesis in chick limb bud cultures, further highlighting the importance of intercellular communication during this process. Another major purpose of condensation into nodules is to increase the gradients of diffusible factors that are required for progression towards further developmental stages [114]. Once the cells formed their junctions and condensed into nodules, they undergo morphological changes. The **cytoskeleton reorganizes**, thus the formerly stellate, fibroblast-like cells become much more round-shaped [115] *(Fig. 2.4.)*. The importance of cytoskeletal remodeling is well highlighted by the finding that the modification of actin dynamics has an impact on chondrogenesis [116]. Out of the many factors that regulate chondrogenesis, nodule formation seems to be one of the most essential steps in the commitment of mesenchymal cells towards the chondrogenic lineage. As the above-mentioned connections become established, intracellular mechanisms become activated to facilitate the mature chondrocyte phenotype. **Multiple signaling pathways necessary for cartilage formation involve calcium ion as a second messenger** (see later). Cytokines, hormones and other morphogens such as bone morphogenic proteins (BMPs), transforming growth factor beta types (TGF-β), fibroblast growth factors (FGF), Wnt and sonic hedgehog (SHH) ligands, the parathyroid hormone-related protein (PTHrP) and the insulin-like growth factor (IGF) regulate chondrogenesis in various phases [117, 118]. On the other hand, the function of these proteins is complemented by steroid and other lipid factors in either a stimulatory (namely, prostaglandins [119] and sexual steroids within strictly-defined conditions and

concentrations [120, 121]) or an inhibitory (such as corticosteroids [118], retinoids [122]) fashion with respect to chondrogenesis.

In addition to the aforementioned changes, the **surrounding ECM also undergoes notable transformation during cartilage formation**. Up until the nodule-formation takes place, a significant amount of fibronectin is secreted and the cells express the fibronectin-binding integrin type α5β1 on their surface. The amount of both secreted fibronectin and integrin type α5β1 diminishes directly after aggregation as fibronectin is an inhibitor of later stages of chondrogenesis [123]. Tenascin-C, a typical matrix glycoprotein of embryonic tissues, is expressed selectively in chondrogenic mesenchyme and appears to undergo a pattern of temporal regulation with a peak unfurling around the time of condensation. Thrombospondins-1 and -2 display a distribution similar to tenascin-C in chondrogenic mesenchyme in the chick. They are both present during condensation, and expression is lost as chondrocyte differentiation advances, only being retained in the peripheral parts of the tissue [124]. Hyaluronan is not only a structural component of the ECM, but additionally interacts with cell surface receptors thus aiding cell proliferation, migration, and intracellular signaling. HA is a major component of the ECM of the developing limb bud where cells are undergoing proliferation. Although HA is synthesized by three HA synthase isoforms (HAS1, HAS2 and HAS3), the main source of HA during the early outgrowth and patterning of the limb bud is HAS2 [125]. However, the expression of HAS2 and therefore the production of HA itself are downregulated in the formation of the precartilage condensations of the skeletal elements, suggesting that downregulation of HA may be necessary for the proper advancement of the condensation phase [126]. Furthermore, pericellular HA surface coats are removed as a result of the receptor-mediated endocytosis of HA and its intracellular degradation by hyaluronidase enzymes, in particular Hyal1 [127]. Collagen type I also reaches a maximal density at the time of cartilage differentiation. The background of this phenomenon is likely clarified by a study that demonstrates that type I collagen substrates stimulate cell proliferation and cartilage differentiation in limb-bud mesenchyme cell cultures [128]. As cartilage differentiation advances, type I collagen is progressively replaced by type II collagen [129]. Even type II collagen itself undergoes a splice variant-switch for subsequent stages of maturation. During condensation type IIA mRNA is more abundant, later on type IIB mRNA dominates, which excludes an exon encoding a cysteine-rich domain in the amino-propeptide [130]. Hereinafter, the aggregated cells secrete cartilage-specific matrix components and receptors that enable binding them. **Metachromasia** – a characteristic phenomenon when staining mature cartilage ECM with a suitable dye such as dimethylmethylene blue (DMMB) – appears in the ECM during the third day of culturing in chick and mouse primary limb bud cultures and similarly, although to a lesser extent in a BMP-2 overexpressing mouse embryonic mesenchymal cell

line [131]. It is therefore clear that this distinguished composition of the cartilage ECM has an important role in maintaining chondrocytes in a differentiated status [132].

2.4.1. Intracellular Events of Chondrogenesis

As chondroprogenitor cells undergo changes in their phenotype, their gene expression pattern displays alterations as well; more specifically **SOX9**, a key transcription factor of chondrogenesis, which is regulated by members of the FGF, TGF-β, BMP and Wnt families displays a distinct increase in its expression [133]. The expression of this **master transcription factor** in committed chondroprogenitor cells is an initial step for chondrogenesis to occur. Subsequently, two other SOX transcription factors, SOX5 and SOX6 are activated, forming what is often referred to as the SOX trio. This group controls the expression of a multitude of ECM macromolecules, including collagen types II, VI, IX and XI and aggrecan [134]. Detailed understanding of the main intracellular signaling pathways that sway chondrogenesis is vital for attempts of externally influencing the formation of articular cartilage. The SOX transcription factors, SOX9 in particular, have a solid expression level throughout chondrogenesis as they are needed during the primary steps of condensation and also for maintaining the differentiating mesenchymal cells in a chondroprogenitor phenotype [135]. As SOX9 is a central component in the differentiation of chondroprogenitor cells, its activity is regulated by multiple molecules, such as Ser/Thr (L-serine/L-threonine) protein kinases.

Reversible protein phosphorylation is involved in an immense portion of cellular processes – including the regulation of gene expression – of the eukaryote cell. The phosphorylation status of any given protein is a direct result of a dynamic balance that exists between protein kinases (PK) responsible for phosphorylation and phosphoprotein phosphatases (PPPs) that are in turn responsible for removal of the phosphate group [136]. The modification itself mostly occurs via Ser/Thr amino acid side chains, while a minor portion receives the phosphate group by its Tyr (L-tyrosine) residue. All in all, the rapidity and easy reversibility of the process and the ubiquity of the phosphate group make this the most prevalent form of covalent protein modification. Protein kinase A (PKA) is one of the early regulators in chondrogenesis. It has long been established that cyclic adenosine monophosphate (cAMP) levels increase during the initial condensation of mouse and chick limb bud-derived HDC *in vitro* [61], furthermore, the addition of extrinsic cAMP derivatives resulted in enhanced chondrogenesis [137]. As a consequence, the cAMP/PKA pathway is now known to be a positive regulator of chondrogenesis with its action being exerted via multiple pathways. PKA mediates the positive effects of BMP on chondrogenic differentiation via phosphorylating Ser/Thr residues of key substrates [138] while through the binding of cAMP response element binding protein (CREB) to CRE sites of cAMP responsive genes, gene expression of multiple chondrogenic genes – including *Sox9* – is

also regulated [139]. In addition to controlling *Sox9* at the level of gene expression, PKA also phosphorylates it at Ser 211. This induces the protein to translocate into the nucleus, which causes an elevation in its transcriptional activity [140].

On the other part, PPPs are just as important governors of chondrogenesis. Our laboratory was the first to establish PP2A as a negative regulator of chondrogenic differentiation, its inhibitor okadaic acid modulates proliferation and cytoskeletal organization in a fashion that it increases chondrogenic differentiation [63]. We have also reported the presence of crosstalk with the PKA pathway, as inhibition of PP2A activity resulted in elevated protein level of PKA [141]. Moreover, CREB has been identified as a mutual target of both PKA and PP2A pathways, the phosphorylation and thus the response of CREB depends on the dynamic balance of their activity to a great extent [141]. Recent results of our laboratory while investigating chicken HDC demonstrate that cyclic mechanical load has an impact on the above-mentioned balance by targeting both pathways, increasing the activity of PKA and reducing that of PP2A [23]. On the other hand, PP2B – or calcineurin, a Ca^{2+}-calmodulin dependent phosphatase – is a positive regulator of cartilage formation in chick HDC; its inhibition by cyclosporine A (CsA) reduces both the amount of cartilage and the expression of mRNAs of aggrecan and the chondrogenic transcription factor *Sox9*. The proposed mechanism of action for calcineurin is via the ERK1/2 pathway, as phosphorylation of ERK1/2 was extremely elevated either by 1 mM H_2O_2 or 2 µM CsA, and both agents are known to decrease calcineurin activity [54]. The increase of $[Ca^{2+}]_{ic}$ during chondrogenesis is directly linked to the activation of calcineurin, which leads to the dephosphorylation, consequent nuclear transport and activation of nuclear factor of activated T lymphocytes 4 (NFAT4) [142]. The NFAT transcription factor family consists of five members NFATc1, NFATc2, NFATc3, NFATc4, and NFAT5 [143] out of which the first four are regulated by calcium signaling. NFATs are localized in the cytoplasm in a constant phosphorylated state in resting cells, at the time they become dephosphorylated by calcineurin, their nuclear localization signal becomes exposed leading to their nuclear translocation [144]. Most of the research regarding NFATs was directed on their role in cells of the immune system, what is known outside of this area is that they take part of the expression of certain cytokines, such as BMPs and cell surface receptors. Also, a number of studies suggest that NFAT signaling can induce catabolic genes (namely, ADAMTS4 and 9) in chondrogenic cells [145]. In chondrogenic mesenchymal cells activation of NFAT4 results in elevated BMP-2 synthesis, which facilitates the differentiation program. Accordingly, pharmacological inhibition of PP2B produces a decrease in chondrogenesis [54].

Members of the **TGF-β superfamily**, BMPs and TGF-βs in particular, are key components of multiple steps during embryonic chondrogenesis [146]. This pathway is often exploited to induce

chondrocyte differentiation in various cell cultures [131, 147]. TGF-β1 and TGF-β2 are both well-known co-ordinators of chondro- and osteogenesis, moreover BMP family members are also required during chondrogenic condensation and cell differentiation both *in vivo* and *in vitro* [131, 148]. TGF-β also causes a shift from proliferation to chondrocyte differentiation [88]. A possible treatment to repair damaged articular cartilage is under investigation developing suitable molecular scaffolds to deliver TGF-β to the site of injury [149]. In addition to the above-mentioned TGF-β types, proper development of joints also requires the action of numerous types of BMPs, most notably BMP-2, BMP-4, and growth and differentiation factor-5 (GDF5). In addition, it is suggested that the effects of these factors are dose-dependent. [131, 150, 151]. The primary pathway for transmission of TGF-β/BMP signals is via SMADs [146]. SMAD2/3 and SMAD1/5/8 signaling mediated by TGF-β family members has a fundamental role in the initiation of chondrogenic differentiation [88]. Upon receptor activation, type-specific receptor-SMADs (R-SMADs) are phosphorylated, activated SMAD1, SMAD5, and SMAD8 associate with SMAD4 causing translocation to the nucleus and the regulation of gene expression [152]. On the other hand, some SMADs, such as SMAD6 and SMAD7 are inhibitory (I-SMADs). As SMAD7 inhibits all R-SMAD signaling pathways, it is a potent inhibitor of chondrogenesis [153]. MAPK proteins p38, ERK1/2 and JNK are also possible targets of TGF-β family signaling aiding the differentiation step of cartilage formation [154]. While **TGF-βs** are mainly involved in the **initiation of cartilage differentiation**, **BMPs** are necessary for **different steps of chondrogenesis**: chondroprogenitor determination and/or condensation and subsequent differentiation into chondrocytes [155]. Before the onset of differentiation, FGF-mediated cell proliferation is inhibited by TGF-β [88], which is likely an indirect effect by causing the downregulation of Gremlin, which is an inhibitor of BMPs that can in turn throw off the proliferative effects of FGF [156]. BMP-2 itself has been shown to have anti-proliferative effects as well [157], plus TGF-β signaling not only inhibits Gremlin, but also activates cyclin D-dependent kinase (CDK) inhibitors, such as p16, p21 and p53 further supporting the anti-proliferative effects mentioned above [88]. This reveals an antagonistic relationship between FGF and TGF-β signaling. Furthermore, FGF2 has an inhibitory effect on the expression of TGF-β2 [158]. Expression of TGF-βR1 and SMAD3 demonstrates a steady increase in *in vitro* hMSC cultures over the course of a three-month-long period, indicating the constant progress of differentiation, which is accompanied by a decrease in proliferation [159]. Conditional knockout (CKO) mouse experiments inducing the loss of BMPR1A and BMPR1B or SMAD1 and SMAD5 expression during cartilage formation blocked endochondral skeleton formation, leading to the conclusion that BMPs take part in the process of chondrogenesis via the canonical SMAD signaling [148, 160]. Various BMP types, such as BMP-2, 4, 6, 7, 9, 13, or 15 can enhance type II collagen synthesis in chondrogenic cultures [131, 161, 162]. An important implication to bear in mind during medical attempts at regenerating articular cartilage is that following the differentiation of mature chondrocytes, members

of the TGF-β family induce the onset of hypertrophy by continued signaling via the canonical SMAD1/5/8 pathway [163]. It is also noteworthy that under certain conditions, BMP-2 induces adipogenesis by upregulating expression of *Pparγ2* in a SMAD1-dependent fashion and its transcriptional activity via the p38 kinase pathway independent of SMAD signaling [164].

The **protein kinase C (PKC) family** of enzymes consists of fifteen isozymes in humans [165], is yet another positive regulator of chondrogenesis [166]. Based on structural aspects, activation mechanisms and their second messenger requirements, they can be divided into three subfamilies: conventional (a.k.a. classical), novel, and atypical. Activation of conventional PKCs (i.e. α, β_I, β_{II} and γ) occurs by binding of diacylglycerol (DAG) and phospholipids to their C1 domains, as well as Ca^{2+}-dependent binding of phospholipids to their C2 domains, novel PKCs (including isoforms δ, ε, η, and θ) require DAG and phospholipids, but not Ca^{2+} for activation. As a result, conventional and novel PKCs have a mutual activation pathway with phosphoinositide phospholipase C (PLC). In the meantime, atypical PKCs (ζ and ι/λ – the last one is present in mice – isoforms) do not require Ca^{2+} or DAG, their activation mainly comprises phosphorylation steps. The fact that conventional PKCs require calcium ion for their activation makes them an ideal mediator of global and localized changes of cytosolic Ca^{2+} levels [167]. Beyond the above-mentioned means of activation, other regulatory processes – their own phosphorylation status – influences their function. This wide array of activation mechanisms, plus the modular nature of the family enable these enzymes to be arranged with diverse spatial and temporal characteristics. Protein kinase D (PKD, formerly known as PKCμ) is also worth mentioning as it is our laboratory that established the differentiation stage-dependent expression level of this enzyme in chick HDC [141]. Currently there is no available data to confirm whether there is a direct interaction between SOX9 and PKC. On the other hand, it is known that PKCs regulate the chondrocyte phenotype via the actin cytoskeleton. Furthermore, actin cytoskeleton plays a role in chondrocyte differentiation, as stated previously. Staurosporine and other PKC inhibitors such as compound H-7 [1-(5-isoquinolinesulfonyl)-2-methylpiperazine] are well-known for being able to swiftly disorganize the microfilament cytoskeletal network and induce consequent alterations in cell shape and adhesion [168]. ERK1/2 is a major mediator of pro-chondrogenic effects of PKC. In isolated rabbit articular chondrocytes, treatment with the potent PKC activator, PDBU (phorbol 12,13-dibutyrate) induced a more than 10-fold stimulation of ERK1/2 activity, with no effect on p38 and JNK activities [169]. Our laboratory also demonstrated the importance of the ERK1/2 pathway in the regulation of chondrogenesis while studying the function of the novel PKC isoform PKCδ in the process [170]. The data obtained with the application of the PKCδ inhibitor rottlerin and PKCδ shRNA (short hairpin RNA) suggested that PKCδ mainly stimulated chondrogenesis via influencing SOX9 and ERK1/2 phosphorylation. It is also notable that N-cadherin expression is an important target of ERK activity in

the process of PKC regulating chondrogenesis in chick HDC [171]. The pathway governing the regulation of N-cadherin expression is a site for cross-talk, as PKA was identified as a regulator via PKCα: inhibition of PKA with H-89 (N-[2-[[(E)-3-(4-bromophenyl)prop-2-enyl]amino]ethyl]isoquinoline-5-sulfonamide) resulted in the lack of activation of PKCα, furthermore, the pattern of N-cadherin expression correlated with the inhibition or downregulation of PKC isoforms [172]. It is likely that PKA is an upstream regulator of PKCα as selective inhibition of PKCs did not have an effect on PKA activity as it was the case with the application of H-89. There is another possible site for cross-talk, although it has not been demonstrated in chondrogenic models, PKC is known to phosphorylate CREB in the hypothalamic paraventricular nucleus [173]. Since the recent identification of the proteins that form the molecular machinery of **store-operated Ca^{2+} entry (SOCE)**; a mechanism, by which PKC regulates this process in HEK293 cells, has been proposed. According to this model, suppression of SOCE takes place by PKC phosphorylating ORAI1 – one of the key molecules needed for SOCE – by the N-terminal Ser-27 and Ser-30 residues, as the application of PKC inhibitors or knockdown of PKCβ were both followed by increased calcium entry [174]. However, the effect of PKC activation on SOCE is likely dependent on the expressed PKC isoforms and types of Ca^{2+} release-activated Ca^{2+} channels (CRACs) of the given cell type, as other research revealed the necessity of PKC activation for SOCE in mesangial cells [175]. The way PKC activity may influence chondrogenesis via SOCE is an intriguing and currently open question. In addition to SOCE, PKC has been with the modulation of an abundance of ion channels, such as inhibition of Ca^{2+}-activated K^+ channels [176] and modulation of voltage-dependent Ca^{2+} channels [177].

MAPKs conduct proliferation and differentiation by relaying extracellular stimuli creating cellular responses. Three major MAPK families have been identified to date in mammalian cells and an additional and less-known ERK5 group is also worth mentioning. Each of the MAPKs are activated by specific MAPKKs, furthermore each of the MAPKKs can be phosphorylated by multiple MAPKKKs. MAPKKKs themselves are regulated by multiple mechanisms [178] creating a network with multiple focal points of regulation and options for crosstalk. The three MAP kinases play a role in the regulation of chondrogenesis to an individual extent: the role of JNKs is a relatively uncharted territory, while it is reported that JNK phosphorylation is not affected during chondrogenesis, suggesting that JNKs play only minor roles in this process [179], more recent results imply these kinases with a more considerable role [180]. ERKs and p38s are key regulators of chondrogenic differentiation [181]. In chick HDC, p38 and ERK appear to play antagonistic roles: the p38 MAPK pathway promotes, ERK1/2 decreases *in vitro* cartilage formation [53]. This notion is in synchrony with previous findings of our laboratory that also corroborate the negative role of the ERK1/2 pathway in the regulation of *in vitro* chondrogenesis in the same chick limb bud model [54]. There is still a plenty of knowledge to be gained regarding

upstream regulators of the MAPK pathways in chondrocytes. As far as the extracellular signals are concerned, members of the TGF-β, FGF and EGF (epidermal growth factor) families, IGFs, retinoic acid and integrins are all implied with altered activity of p38 and ERK MAPK pathways [181]. Considering the fact that MAPKs relay extracellular stimuli to cellular responses, MAP kinase signaling is also likely involved in the transduction of mechanical signals in cartilage development. It has been established that shear stress and loading regulate MAP kinase signaling thus proliferation and differentiation in articular chondrocytes, potentially through integrin receptors [182].

2.5. Calcium as a Second Messenger

Calcium is a macroelement, the fifth most abundant element of our body. An average adult person has around one kilogram of calcium predominantly stored in bone, calcified cartilage and dental tissues; only the remaining portion – a miniscule one percent of the whole amount – serves to implement secondary signaling [183]. In the above-mentioned bound state, it has a low bioavailability. The way this can be overcome is through the process of bone resorption, when calcium is liberated into the bloodstream by osteoclasts. Resting state concentration of free ionized calcium within a typical cell cytoplasm is 100 nM in round numbers, but is subject to significant shifts as required by cellular functions. The extracellular space (with a calcium ion concentration of 1,4-1,5 mM) and intracellular calcium stores have a strong electrochemical gradient in the direction of the cytoplasm. Although the ER or its specialized form in muscle (the sarcoplasmic reticulum, SR) is mainly referred to when discussing **intracellular Ca^{2+} storage**, a great portion of other organelles also play a role in Ca^{2+} signaling/release: mitochondria [184], the Golgi apparatus [185], secretory vesicles [186] and others [187-189]. Cytosolic Ca^{2+}-rise can be the result of release from organelles or entry from the extracellular space; as well as it can be the combination of both factors. In all cases the electrochemical gradient of Ca^{2+} provides a sufficient propulsion for the transport process. Via a set of effector molecules that are tissue and differentiation stage-specific, the cell renders a characteristic response, which is then concluded by calcium elimination processes that utilize **Ca^{2+} pumps and/or exchangers** [190]. Therefore, Ca^{2+} functions as a second messenger during physiological processes of cellular life in a universal fashion. The earliest-described role of this ion is in the electromechanical coupling of skeletal muscle, since then a whole array of other functions have been uncovered, such as regulation of the cell cycle, differentiation, gene expression, apoptosis, enzymes, exocytosis/neurotransmitter release and cellular response to hormones. A major advantage of Ca^{2+} against other secondary factors is that its cytoplasmic concentration can be increased very rapidly due to its high electrochemical gradient, plus it does not require synthetic enzymes for its production, it is readily available in the extracellular milieu. **Temporal and spatial features of the Ca^{2+} signal are precisely regulated** and have

to be able to control fast processes, such as exocytosis (microseconds) or transcriptional gene expression, which – on the other hand – takes hours to show itself. As for the spatial regulation, some Ca^{2+} signals remain localized to restricted domains of cells [191] while others – like skeletal muscle contraction – produce a global increase in the cytoplasmic concentration of the ion [192]. So how is it possible to produce a diverse array of signaling functions with a single ion? The key to the answer lies in the target proteins that serve to mediate its actions. The collection of proteins that contribute to the regulation and upkeep of Ca^{2+} homeostasis in the cells is conceived as the global **Ca^{2+} signaling toolkit**. Cells express and apply the components that best suit their requirements for executing their function [193]. In a non-exhaustive fashion, the following members of this toolkit should be mentioned: plasma membrane (PM) receptors, G-proteins, voltage- and ligand-gated Ca^{2+} channels, receptors of the ER (inositol-1,4,5-trisphosphate receptors (InsP3Rs), ryanodine receptors (RyRs)), chaperons (calsequestrin, calreticulin), Ca^{2+} pumps (sarco/endoplasmic reticulum Ca^{2+} ATPase (SERCA), plasma membrane Ca^{2+} ATPase (PMCA)), and various effectors (calmodulin, classic PKC isoenzymes, NFAT and CREB transcription factors) [193]. As proliferation and differentiation are essential functions controlled by Ca^{2+} signaling [190], Ca^{2+} homeostasis of differentiating MSCs has become a focus numerous research groups, including ours. Although MSCs are non-excitable cells, their differentiation can also result in their conversion into excitable cell types, such as muscle and nerve cells [194]. Despite recent advancements regarding the Ca^{2+} homeostasis and ion channel pool of chondrocytes and chondrogenic cells, their contribution to the differentiation program and maintenance of physiological conditions still requires further research. Based on our current knowledge, **Ca^{2+} signaling pathways can be expected to play an essential role in conducting MSC differentiation**. Ca^{2+} channel composition is likely to change along with differentiation, as suggested by an already identified switch in voltage-gated K^+ channel expression, which acts as a modifier of Ca^{2+} oscillations [195], while it is also notable that MSCs and mature chondrocytes have different, but somewhat overlapping assortments of Ca^{2+} ion channels or receptors [64].

2.5.1. Sources of Elevated Cytoplasmic Calcium Levels

Ca^{2+} that enters the cytosol is derived from two major sources: either the extracellular space or intracellular Ca^{2+} stores. The abundance of **Ca^{2+} channels in the PM** enabling entry from the extracellular space is categorized into four classes: **voltage-dependent** calcium channels (L-, P/Q-, N-, R- and T-types), **ligand- or receptor-operated** calcium channels (e.g., ionotropic purinergic P2X Ca^{2+} channels, N-methyl-D-aspartate (or NMDA) type glutamate receptors and transient receptor-potential (TRP) channels), **second messenger-operated** channels (such as ARC – arachidonate-regulated Ca^{2+} channel) and **CRACs** that are activated when calcium ions are depleted from the ER [193]. Ca^{2+} release

from the intracellular stores may occur either via InsP3Rs or RyRs, which represent two distinct pathways, the latter one being exclusively expressed in excitable cells [64]. Ca^{2+} release from internal stores *(Fig. 2.6.)* is agonist-dependent and voltage-independent. SOCE is executed in succession of establishing an interaction between STIM (stromal interaction molecule, an integral Ca^{2+} sensor of the ER membrane) and SOC channels that form due to depletion of ER Ca^{2+} stores [196]. In the following parts – due to the nature of the results to be presented in this work – a detailed description will be provided on VDCC and SOCE pathways (CRACs, more precisely) *(Fig. 2.6.)*, with an emphasis placed on their role in differentiating cartilage.

2.5.1.1. Voltage-Dependent Ca^{2+} Entry Pathways

Undifferentiated hMSC were reported to carry two main Ca^{2+} entry channel classes, VDCCs and CRACs [197]. In most of the non-excitable cell types CRACs are the main mediators of Ca^{2+} entry, therefore the identification of a highly Ca^{2+}-selective store-operated Ca^{2+} current (I_{CRAC}) in undifferentiated hMSCs is not surprising [198]. VDCCs are large complexes consisting of several subunits (α_1, $\alpha 2\delta$, $\beta_{1\text{-}4}$, and γ), of which the α_1 subunit determines their type based on specific characteristics: L- ($Ca_V1.1$, 1.2, 1.3, 1.4), P/Q- ($Ca_V2.1$), N- ($Ca_V2.2$), R- ($Ca_V2.3$) and T-type ($Ca_V3.1$, 3.2, 3.3) [64]. Depending on biophysical and pharmacological properties, further classification of VDCCs into two major groups is the following: **high voltage-activated channels (HVA), which include L-, N-, P/Q- and R-type channels and low voltage-activated channels (LVA), consisting of T-type channels** [199]. The general observation is that the expression of L- and T-type VDCCs (but not P/Q- or R-VGCC) is identifiable in many types of stem cells (SCs). In hMSCs, L-type Ca^{2+} channel currents can be identified, while there is no sign of functional expression of N-type Ca^{2+} channels. These results are similar to the ones obtained with mouse ESCs (mESCs); again, SOCE appeared as the main Ca^{2+} entry form [200]. L- and T-type VDCCs were also detected by RT-PCR in human adipose tissue-derived stem cells (hASCs) [201]. Supporting the assumption that CRACs are the main sources of extracellular Ca^{2+} entry, mRNA expression of L-, T- or P/Q-type Ca^{2+} channels was undetectable in mESCs, further suggesting a less substantial significance for VDCCs in their Ca^{2+} homeostasis. However, the importance of VDCCs cannot be neglected, as their expression was also demonstrated in human ESCs (hESCs) [202] and rat MSCs [203]. While L-type VDCCs were reported to be involved in the upkeep of Ca^{2+} homeostasis of osteoblasts, experiments with the addition of the L-type Ca^{2+} channel blocker nifedipine to the culture media during their osteogenic differentiation suggest these channels are not necessary for osteogenic differentiation of hMSCs [204]. A possible resolution to the results indicating diminished roles and expression level of VDCCs during and after differentiation of SCs (stem cells) [199] is provided by Rodríguez-Gómez and colleagues, who claim that the modulation of T-type channels

that occurs during cell cycle progression may be a contributor to the maintenance of ESCs self-renewal capacity [205]. VDCCs were also reported to be expressed during chondrogenesis. In mouse limb bud organoid cultures, VDCCs appear to form mechanoreceptor complexes with beta1-integrin, Na/K-ATPase and epithelial sodium channels (ENaCs) [206]. Furthermore, immunoreactivity of the L-type $Ca_V1.2$ and T-type $Ca_V3.2$ subunits was detected during endochondral ossification in both osteoblasts and chondrocytes in mouse skeletal development from E14.5 throughout skeletal maturity. These results were verified by western blot and immunohistochemical assessment of *in vitro* cell culture models of osteogenesis and chondrogenesis [207]. VDCCs also have a well-described role interceding for IGF-1 in the elevation of cytoplasmic Ca^{2+} concentration in articular cartilage chondrocytes [208]. Based on recent results of our laboratory, we can propose an important role for VDCCs in chick HDC, as depolarization by high concentration of the potassium ion caused large Ca^{2+} transients [195]. This is in an apparent contradiction with results obtained with mESCs [200], which can be resolved by the more differentiated character of the previous cells. As further clarification in this field appears crucial, one of the major undertakings of this work is to provide a better understanding of the role of VDCCs in chondrogenic chick HDC.

2.5.1.2. Ca^{2+} Release from the ER and SOCE

It has been proposed in 1986 that SOCE, a mechanism for Ca^{2+} entry which is controlled by the Ca^{2+}-saturation of the intracellular Ca^{2+} stores [209]. This model provoked three decades of intense investigation and scientific debate about the means of communication between the Ca^{2+} stores and the plasma membrane and the characteristics of store-operated channels in the PM [210]. Before the complete identification of molecules participating in SOCE, strong evidence for the involvement of TRPC channels in SOCE have been presented for TRPC1, TRPC4 and TRPC6 (canonical TRP channels) [211, 212]. However, as TRPC channels form non-selective cation channels, which do not bear the same characteristics that have been measured for I_{CRAC}; therefore the identification of the CRAC remained a major challenge. The undertaking reached a milestone with the identification of **STIM1** as the Ca^{2+} sensor of the ER [213]. STIM1 was first described in 2005 as an essential SOCE component, decades after the initial observations of SOCE signals during Ca^{2+} measurements. STIM1 was found incapable of functioning as a CRAC or SOC channel by itself, as its overexpression did not enhance SOCE [214]. The identification of **ORAI1** as the pore-forming subunit of the CRAC is a major recent breakthrough [215]. The role of these proteins has been confirmed by co-transfection experiments, where ORAI1 and STIM1 have been found capable of restoring I_{CRAC} [216]. It has since been determined that the role of STIM1 is to mediate the communication of the Ca^{2+} stores and plasma membrane channels; STIM1 protein contains an EF hand motif, which is responsible for luminal Ca^{2+} binding and Ca^{2+} level

detection. Introduction of a point mutation (D76A) in this latter motif results in constitutive activation of SOCE, regardless of the amount of Ca^{2+} within the ER [217]. STIM1 is a transmembrane protein containing a single transmembrane segment its subcellular localization has been demonstrated in the ER, the PM and acidic stores [218, 219]. STIM2 is a homologue of STIM1, it is mainly implicated in maintaining basal cytosolic and ER Ca^{2+} levels. A long, alternatively spliced variant of STIM1 – STIM1L – has also been identified; its localization is mainly restricted to muscle fibers and myotubes, where it co-localizes with CRACs to enable brisk stimulation of SOCE, thus providing the molecular background of repetitive Ca^{2+} signals of muscle cells [220]. Upon store depletion, STIM1 relocates to form punctae in the proximity of the plasma membrane *(Fig. 2.6.)*, where it may cause the activation of highly selective CRACs composed of ORAI1 subunits, or unselective SOC channels that involve ORAI1 as well as TRPC subunits, leading to SOCE [221, 222]. The ER being closely positioned to the plasma membrane adjacent to the STIM1-ORAI1 clusters is a potent support also for the SERCA pumps to refill the ER Ca^{2+} store [223].

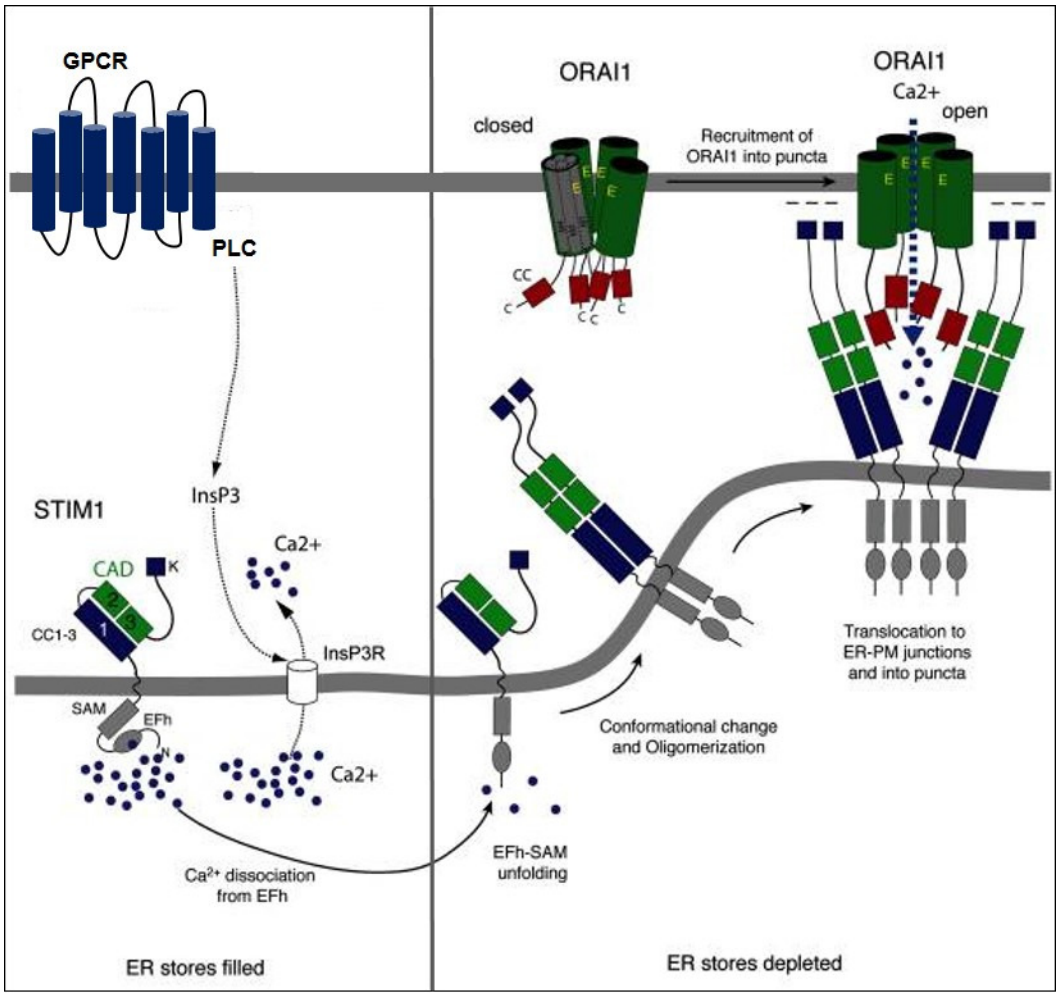

Fig. 2.6. While ER Ca^{2+} stores are full, Ca^{2+} is bound to the EF hand domain at the luminal end of STIM1. Stimulation of GPCRs, such as P2Y purinergic receptors, results in the production of InsP3 causing Ca^{2+} release from the ER through InsP3R. The decrease of ER Ca^{2+} concentration leads to the multimerization of STIM1 proteins due to conformation changes induced by the dissociation of Ca^{2+} from the luminal EF hand domain. These STIM1 multimers translocate and form puncta juxtaposed to the plasma membrane where they can recruit and activate ORAI1 CRACs by the cytoplasmic SOAR (also known as CAD) domain in the C terminus of STIM1 thus generating SOCE. Modified figure based on the work of Feske and colleagues [224].

It is also noteworthy that ORAI1 channels may form heteropentameric complexes with ORAI3, which function as ARCs, a store-independent channel with an active participation of STIM1 located in the PM [225]. ARCs are implicated to regulate the frequency of agonist-induced Ca^{2+} oscillations. Calcineurin appears to be an important downstream element that enables differential relay of signals from CRACs and ARCs. Calcineurin activation requires a sustained rise of cytoplasmic Ca^{2+} levels, thus it is not activated by oscillatory Ca^{2+} signals generated by ARCs, moreover, it even inhibits ARC function [226]. As ARCs have only recently been described, their presence in MSCs has not been validated up until now. However, experiments using hMSCs already demonstrated the presence of an unknown, novel Ca^{2+} entry pathway that is irrespective of store-depletion, which was active in hMSCs, and it also contributed to their Ca^{2+} oscillations [227]; ARCs are likely candidates for this role. Albeit ARCs have not been profiled in developing or mature chondrocytes, arachidonate metabolism is a well-known

regulator of *in vitro* chondrogenesis [228], thus it is plausible that ARCs will be identified as contributors in cartilage biology.

The other main source – besides influx from the extracellular space – that can cause significant elevation of cytoplasmic Ca^{2+} levels is Ca^{2+} release from intracellular stores, mainly the ER. InsP3Rs have been identified as the dominant mediators of Ca^{2+} release from the ER in MSCs (and in many other non-excitable cell types, for that matter), while RyRs did not prove to be functionally present [197] *(Fig. 2.6.)*. Similarly, InsP3Rs are the determinants of Ca^{2+} discharge from the ER in mESCs as well. All subtypes of this receptor (1, 2 and 3) have been confirmed at the level of mRNA expression, while the application of caffeine or ryanodine did not change cytoplasmic Ca^{2+} concentration, indicating the functional absence of RyRs [200]. In isolated bovine articular chondrocytes, inhibition of cytosolic Ca^{2+} elevation by neomycin implicates activation of PLC and InsP3 synthesis in the otherwise noticeable mobilization of Ca^{2+} from intracellular stores [229]. One study suggests that under pathological conditions (impact induced apoptosis) of equine articular cartilage explants, RyRs are involved upstream to the activation process of caspase 9 [230]. Data of our laboratory indicate the role of InsP3Rs, but not RyRs in differentiating chondrocytes of chick HDC; the PLC-InsP3R pathway was also found to be functional. Despite what is mentioned above, these cells store a relatively low amount of CPA-releasable Ca^{2+} in the ER. Regardless, the ER can still be a significant player in the Ca^{2+} signaling in these cells [75, 231]. It is therefore safe to assert that the prevalent form of Ca^{2+} entry in non-excitable cells is via CRACs, whose activation occurs following ER store-depletion [232]. As already mentioned, hMSCs – as prime examples of non-excitable cells – chiefly employ SOCE preferably over VDCCs [197]. To elicit the activation of CRACs during single cell Ca^{2+} measurements of MSCs, Ca^{2+} stores were depleted by the administration of SERCA inhibitors cyclopiazonic acid (CPA) or thapsigargin. **Canonical TRP (types 1, 2 and 4) channels** were identified as mediators of Ca^{2+} entry via SOC channels following store-depletion in multiple cell types, including mESCs [200]. Internal Ca^{2+} stores appear to play a chief role in the regulation of Ca^{2+} homeostasis without any major influence by extracellular influx in mature porcine articular chondrocytes [233]. Prior to our results that provide the foundation for this work as well, our laboratory already observed signs of SOCE in chick HDC during single cell Ca^{2+} measurements [231]. These observations indicate the more or less universal nature of SOCE in the regulation of cellular functions from undifferentiated pluripotent cells to committed chondroprogenitors and mature chondrocytes.

Although it is known that CRACs are essential mediators of Ca^{2+} entry in MSCs, their detailed characterization is yet to be performed in these undifferentiated cells. On the other hand, ORAI1 is clearly implicated in osteogenic differentiation of mouse bone marrow mesenchymal stem cells

(mbMSC); moreover, BMP signaling appears to be the pathway via which this takes place, as its activation was capable of rescuing the osteogenic differentiation capacity of *Orai1*$^{-/-}$ mbMSCs [234]. This result is of specific interest, as SMAD1/5/8, the immediate effector molecules of BMP signaling in mbMSCs are also involved chondrogenic differentiation (see above). At the same time, data regarding the expression and role of SOCE proteins is lacking in mature chondrocytes. Further analysis regarding the role of SOCE in chick chondrogenic HDC will take place in the discussion chapter.

2.5.1.3. Septins and their Role as Modulators of SOCE

Septins belong to a highly conserved family of small (30-65 kDa) **GTP-binding proteins that form hetero-oligomeric complexes and higher-order structures, including filaments and rings located in the proximity of the PM of eukaryotic cells** *(Fig. 2.7.)*. This group is the superclass of phosphate-binding loop (P-loop) NTPases, which also includes the RAS-like GTP-binding proteins [235]. Septins are increasingly recognized as **a novel component of the cytoskeleton**. These proteins are involved in an abundance of molecular functions as scaffolds for protein recruitment and as diffusion barriers for subcellular compartmentalization in numerous biological processes, such as cell division, cytoskeletal organization, membrane-remodeling events, host-microorganism interactions [236]. Since their discovery in yeast over four decades ago [237], these proteins have been identified in almost all eukaryotes, including humans [238]. The filamentous appearance and association of septins with cellular membranes, actin filaments and microtubules provides a background to them being recognized as cytoskeletal components. Most of the **13 human septin genes** undergo alternative splicing [239]. These genes are named SEPT1-SEPT12 and SEPT14; SEPT13 is a pseudogene which has been renamed as SEPT7P2. Some of these genes are ubiquitous, while some are tissue-specific. Septins are classified based on sequence similarity into four groups named after their originating members: SEPT2, SEPT3, SEPT6 and SEPT7 [240] *(Fig. 2.7.)*. The basic structure formed by *in vitro* oligomerization of human septins purified from Escherichia coli has been identified as a heterohexamer, however the details of their function remains mostly unknown [241]. Septins have been proposed to interact through their GTP-binding domain (called the G interface) and their N-terminal and C-terminal regions (called the NC interface) [242] *(Fig. 2.7.)*. After forming complexes, septins create a **non-polar filament**, which results in an important structural distinction from actin and microtubule filaments [236]. A study, in which the solved structure of a complex of three human septins (SEPT2, SEPT6 and SEPT7) has been described, reported the formation of a non-polar hexamer, with the symmetrical arrangement of two copies of each septin (SEPT7-SEPT6-SEPT2-SEPT2-SEPT6-SEPT7). This hexameric complex displayed the alternation of G and NC interfaces within the complex, which also accounts for the non-polar structure [241] *(Fig. 2.7.)*. As septins are GTP-binding proteins, the hydrolysis of GTP –

unsurprisingly – regulates septin-septin interactions and thus formation of complex structures. The hydrolysis of GTP induces conformational changes in the G and NC interaction surfaces. However, there is an important dissimilarity to classical small GTPases which cycle between an active GTP-bound state and an inactive GDP-bound state [243]; septins that belong to the SEPT6 group are incapable of hydrolyzing GTP to GDP due to the lack a key Thr residue (Thr78) from their G domains [242]. Thus, members of the SEPT6 group (SEPT6, SEPT8, SEPT10, SEPT11 and SEPT14) are constantly bound to GTP, thus their interaction interfaces are not regulated by GTP hydrolysis. This suggests that the SEPT2-SEPT6 interaction via SEPT6 G interface might be stable without affecting SEPT6-SEPT7 interaction via the SEPT6 NC interface, which is a possible major influence on septin complex formation [236]. **Interactions between septins and actin, microtubules, as well as phospholipid membranes have been identified**; these interactions are likely to influence the formation of complex septin structures and their specific assembly at given cellular locations [236].

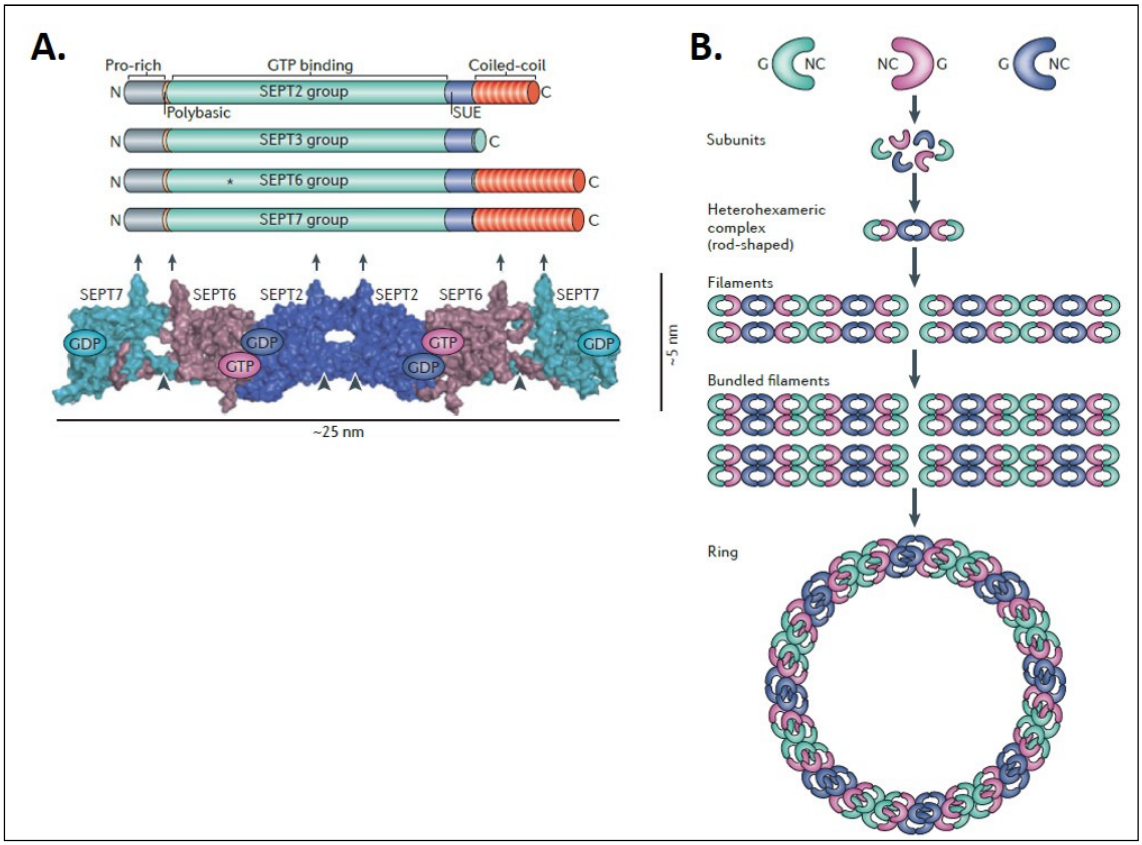

Fig. 2.7. Septin structure, assembly and cytoskeleton dynamics. (A) Typical septins consist of three major conserved domains: a GTP-binding domain, a polybasic phosphoinositide-binding region and the SUE (septin unique element). Septins in the SEPT6 group are uncapable of hydrolysing GTP to GDP (shown by asterisk). In a septin heterohexamer, two copies of each septin are symmetrically arranged (SEPT7-SEPT6-SEPT2-SEPT2-SEPT6-SEPT7). Polybasic regions are marked by arrowheads, while arrows show the position of coiled-coil domains. (B) Septin subunits that belong to different groups are indicated with different colors. Interaction between septin subunits occurs through the GTP-binding domain and also the amino- and carboxy-terminal regions. Heterohexamers can further polimerize to form non-polar filaments or they can associate laterally and form bundles. Bundles of septin filaments may also form higher-order structures, such as rings [236].

The initial observation regarding the modulatory role of septins in SOCE ensued in a large-scale siRNA screen based report to identify activators of NFAT nuclear translocation [2]. Members of the SEPT2 family emerged as candidates, as their ablation reduced NFAT nuclear signals to levels that are comparable to the results of siRNA-mediated depletion of *Stim1*. Total internal reflection fluorescence (TIRF) microscopy demonstrated aberrant ORAI1 distribution and cluster formation in the plasma membrane of *Sept2* family-depleted cells. Under resting conditions, septin 4 and ORAI1 are broadly distributed in the plasma membrane, while after store-depletion – as expected – STIM1 and ORAI1 colocalize; septin 4, on the other hand, forms distinct assemblies that do not colocalize with either ORAI1 or STIM1 at the ER-PM junctions. Interestingly, following an initial increase, septin 4 fluorescence at the TIRF layer starts to decrease, with a magnitude that shows a strong co-relation with Ca^{2+} influx. Simultaneously, ORAI1 clusters begin to form in a consecutive manner to the decrease in the level of septin 4 at the TIRF layer. Forchlorfenuron (FCF), a small molecule that disrupts normal septin dynamics by hyperpolymerizing and stabilizing septin filaments [244], inhibits ORAI1 cluster formation, STIM1-ORAI1 colocalization and SOCE. The reported results also indicate the formation of localized microdomains of phosphatidylinositol 4,5-bisphosphate (PIP_2) in the PM proximal to CRACs after ER Ca^{2+} store-depletion, which are shaped by septins [2]. According to another study, septin 7, on the other hand, was identified as a molecular brake on activation of ORAI channels in Drosophila neurons. Lowering the expression level of dseptin 7 by siRNA-mediated depletion was not only able to induce dORAI-mediated Ca^{2+} entry and higher cytosolic Ca^{2+}, but could also compensate for decreased functional expression of InsP3R or dSTIM. According to the model proposed by the authors, septin filaments can keep the recruitment of dSTIM to ER-PM junctions under control at resting conditions with normal dseptin 7 levels. This block is removed by the reduction in dseptin 7 levels in cells with completely replete ER and results in deregulated recruitment of dSTIM to ER-PM junctions. Furthermore, non-canonical modes of dORAI activation may also be suspected, as *dStim*-depletion did not seem to have a significant effect when *dseptin 7* was also depleted, which can unlikely be fully explained by the function of residual dSTIM proteins [245].

2.5.2. Elimination of the Cytoplasmic Ca^{2+} Signal

As stated before, the **typical resting state concentration of free ionized calcium in the cytoplasm is 100 nM**. Increased Ca^{2+} levels that provide signal for Ca^{2+}-dependent pathways require the existence of elimination processes to terminate these signals and restore resting Ca^{2+} levels. Calcium ions are eliminated towards the extracellular space primarily by PMCA and the Na^+/Ca^{2+}-exchanger (NCX). Concurrently, SERCA accumulates cytoplasmic Ca^{2+} in the intracellular stores, thus also contributing to decreasing cytoplasmic levels. Mitochondrial uniporters (mCU) are also notable

elements of cytoplasmic Ca^{2+} elimination; their role is to pump Ca^{2+} into mitochondria [184]. It is noteworthy that excess Ca^{2+} uptake by mitochondria triggers a bioenergetic failure of the organelle, which may lead to cellular death by apoptosis or necrosis [246]. Accordingly, mitochondrial Ca^{2+} homeostasis and its relationship with cytoplasmic levels via the mCU has been a major interest of numerous research groups [247].

It has been reported that extrusion mechanisms via PMCA and NCX are functionally expressed and contribute significantly to sustaining oscillations of cytoplasmic Ca^{2+} levels in hMSCs. According to a study published by the same group, functional expression of PMCA (1 and 4) and NCX (1, 2 and 3) is also detectable in mESCs based on confocal Ca^{2+} imaging systems, patch clamp techniques and RT-PCR [200]. NCX has also been reported to be functional in mature articular chondrocytes [248]. The importance of the Ca^{2+} extrusion pathways is greatly highlighted by a recent report, which demonstrates that overexpression of PMCA4b in the plasma membrane enhances Ca^{2+} clearance from BRAF mutant melanoma cells after SOCE. This, in turn, induced a marked inhibition of migration of these cells, which provides insight into an important crosstalk between Ca^{2+} signaling and the MAPK pathway through the regulation of PMCA4b expression [249]. Future studies of these proteins in chondrogenic models will surely uncover essential biological functions related to cartilage tissue, as SOCE is already turning out to be a significant contributor of this area. Notably, the amount of Ca^{2+} eliminated by SERCA and mCU is dwarfed by the activity of PMCA and NCX. Regardless of this ratio, an abundance of observations suggest the functional expression of SERCA in undifferentiated [197] and differentiating chondrogenic cell types [231].

3. Materials and Methods

3.1. Cell Culturing

3.1.1. Micromass Cultures Established from C3H10T1/2 Cells

C3H10T1/2 is an embryonic murine mesenchymal stem cell line that was purchased from the American Type Culture Collection (ATCC; Rockville, MD, USA). We have also obtained a modified version of this cell line that has been permanently transfected with the eukaryotic expression vector pMBC-2T-fl containing the cDNA encoding the human bone morphogenic protein BMP-2 as a kind gift from G. Gross. The long terminal repeat (LTR) promoter of the myeloproliferative sarcoma virus (MPSV) ensures constitutive transcription of the construct and termination signal is provided by a poly(A) site from SV40; clones were selected by cotransfection with pBSpACΔp plasmid that imparts resistance against puromycin [73]. Monolayer cultures of control and BMP-2 overexpressing C3H10T1/2 cells (for simplicity, abbreviated as c-C3H10T1/2 and b-C3H10T1/2, respectively, from this point onwards) were routinely maintained in standard 75 cm^2 cell culture flasks or to obtain sufficient cell numbers for high density culturing, in 150 cm^2 polystyrene tissue culture dishes (Orange Scientifique, Braine-l'Alleud, Belgium). Culturing of cells was performed in high glucose (4.5 $g \cdot L^{-1}$) Dulbecco's modified Eagle's medium (DMEM; Sigma-Aldrich, St. Louis, MO, USA) supplemented with 10% (v/v) fetal calf serum (FCS; Gibco, Gaithersburg, MD, USA), 0.5 mM alanyl-glutamine (Ala-Gln) as a more stable source of L-glutamine (Sigma-Aldrich), 6.6 $\mu g \cdot mL^{-1}$ ampicillin and 100 $\mu g \cdot mL^{-1}$ streptomycin (TEVA, Debrecen, Hungary). In addition, the culture medium of the b-C3H10T1/2 cells contained 5 $\mu g \cdot mL^{-1}$ puromycin (Sigma-Aldrich). Cultures were incubated in a humidified CO_2 incubator at 37 °C. Upon reaching approximately 80% confluency, cells were passaged with the application of 0.25% trypsin-EDTA (Sigma-Aldrich) dissolved in phosphate buffered saline (PBS) for 2 min at 37 °C.

To establish micromass cultures from c- and b-C3H10T1/2, cells were harvested by brief centrifugation (at 800 × g for 10 min) following trypsinization. Cells were counted using a haemocytometer and cellular density was set at 1.5 × 10^7 $cells \cdot mL^{-1}$ in high glucose DMEM supplemented with 10% FCS. Depending on their intended application, 30 or 100 µL droplets of the cell suspension were pipetted into 35 mm plastic tissue culture dishes (Orange Scientifique). Cells were allowed to attach to the surface at 37 °C and 5% CO_2 for 2 h, after which 2 mL of complete culture medium was added to the dishes, which then was changed every second day until the end of culturing. The day of plating was considered day 0 of culturing. Micromass cultures were maintained for up to 15 days. *C3H10T1/2 cells were cultured by Roland Ádám Takács and Csaba Matta*.

3.1.2. Chicken Primary Embryonic Mesenchymal Micromass Cultures

A widely applied and easy-to-reproduce *in vitro* experimental model to study hyaline cartilage formation was first described by Ahrens et al. [50]. In HDC, chondroprogenitor mesenchymal cells derived from chicken limb bud spontaneously differentiate to chondroblasts and chondrocytes on days 2 and 3 of culturing and a well-detectable amount of hyaline cartilage ECM is produced by day 6.

To establish primary micromass cell cultures of chondrifying mesenchymal cells, Ross hybrid chicken embryos of Hamburger-Hamilton developmental stages 22-24 (4.5-day-old) were used. Experimental work using early chick embryos *in vitro* does not require licensure from the Ethics Committee of the University of Debrecen. Distal parts of forelimbs and hindlimbs of embryos were isolated and then digested in 0.25% trypsin-EDTA (pH 7.4; Sigma-Aldrich) at 37 °C for 1 h. Equal volume of FCS has been added to terminate the enzymatic digestion and the digested solution of limb buds were filtered through a 20 μm pore size plastic filter unit (Millipore, Billerica, MA, USA) to yield a single cell suspension of chondroprogenitor cells. Following a brief centrifugation (at 800 × g for 10 min), cells were counted in haemocytometer, then resuspended in Ham's F12 medium (Sigma-Aldrich) supplemented with 10% FCS at a concentration of 1.5×10^7 cells mL^{-1} and droplets were placed into plastic cell culture plates (Orange Scientifique). After 2 h of allowing the cells to attach to the surface at 37 °C in a CO_2 incubator (5% CO_2 and 95% humidity), 2 mL of Ham's F12 supplemented with 10% FCS, 0.5 mM stable L-glutamine and antibiotics/antimicotics (penicillin 50 U mL^{-1}, streptomycin 50 μg mL^{-1}, fungizone 1.25 μg mL^{-1}; TEVA, Debrecen, Hungary) was added. The day of plating was considered day 0 of culturing. Cultures were kept at 37 °C in a CO_2 incubator up to 15 days with the medium being changed every other day. *Chicken primary limb bud cultures were established and cultured by Roland Ádám Takács, Tamás Juhász and Csaba Matta*.

3.1.3. Mouse Primary Embryonic Mesenchymal Micromass Cultures

Mesenchymal cell cultures derived from mouse embryonic limb bud were established according to the aforementioned protocol used by our laboratory on chicken high density cultures with slight modifications for mice. NMRI laboratory mice were mated overnight, following which, the presence of a vaginal plug confirmed mating. The time of detection of the vaginal plug was considered day 0 of gestation. Pregnant female mice were sacrificed by cervical dislocation on day 11.5 of gestation, according to the regulations defined by the University of Debrecen Committee of Animal Research (license number: 11/2010/DE MÁB). The uterus of each animal was removed and washed in sterile calcium and magnesium-free PBS (CMF-PBS) preheated to 37 °C. E11.5 embryos were then isolated from the uterus, pooled and washed several times in CMF-PBS.

To establish primary micromass cultures, distal parts of forelimbs and hindlimbs of embryos were isolated and collected in CMF-PBS. After all limb buds being collected, they were transferred into 0.25% trypsin-EDTA (Sigma-Aldrich) and incubated at 37 °C in a CO_2 incubator (5% CO_2 and 95% humidity) for 1 h. The enzymatic digestion was terminated by the addition of equal volume of FCS to that of the digestion mix. This digestion cocktail was then suspended by gentle aspiration using 5 mL plastic pipette tips until no aggregates remained and cells were filtered through a 20 µm pore size plastic filter unit (Millipore, Billerica, MA, USA) to yield a single cell suspension of chondrogenic mesenchymal cells. Following 10 min of centrifugation (at 800 × g), the cell pellet was resuspended in Ham's F12 medium supplemented with 10% FCS to yield a concentration of 1.5×10^7 cells mL^{-1} and 30 or 100 µL droplets were placed into 35 mm plastic tissue culture dishes (Orange Scientifique). After allowing the cells to attach to the surface for 2 h in a CO_2 incubator at 37 °C, 2 mL of Ham's F12 culture medium supplemented with 10% FCS, 0.5 mM Ala-Gln (Sigma-Aldrich) and antibiotics/antimicotics (penicillin, 50 U mL^{-1}; streptomycin, 50 µg mL^{-1}; fungizone, 1.25 µg mL^{-1}; TEVA, Debrecen, Hungary) was carefully added to each dish. The day of plating was considered day 0 of culturing. High density cultures were maintained at 37 °C in a CO_2 incubator for 15 days with the medium replaced every second day. *Mouse primary limb bud cultures were established and cultured by Roland Ádám Takács, Csilla Somogyi and Csaba Matta*.

3.2. Modulating either VDCC Function or SOCE by Channel-Specific Blockers, Inducing Septin Hyperpolimerization and Stabilization to Disturb Calcium Homeostasis

To evaluate long term effects of modulating Ca^{2+} homeostasis in chick differentiating chondrocytes, the following compounds were added to the culture medium of HDC. The L-type VDCC-blocker nifedipine was administered to the culture medium from the beginning of day 1 of culturing at a final concentration of 10 µM. For control experiments, equal volumes of the vehicle (dimethyl sulfoxide (DMSO); Sigma-Aldrich) was added to cultures. The role of internal Ca^{2+} stores has been ascertained following store depletion with 10 µM of the SERCA inhibitor cyclopiazonic acid (CPA; Sigma-Aldrich), SOCE was blocked by the simultaneous application of the non-specific TRPC antagonist YM-58483 (a pyrazole derivative, also known as BTP-2; Sigma-Aldrich) [250] and $LaCl_3$ (Sigma-Aldrich) [197] (1 µM and 500 µM, respectively). Treatments to address the role of internal stores were performed on culturing day 2 for 24 h. For control experiments equal volumes of the vehicles (DMSO and sterile water, respectively) were added to cultures. Septin reassembly was inhibited by the addition of forchlorfenuron (FCF; Sigma-Aldrich) to the culture medium at a final concentration of 200 µM [2] for 24 h on either day 1 or day 2 of culturing. We have applied matching volumes of the vehicle

(absolute ethanol) to the cultures for control experiments. *The above-described experiments were executed by Roland Ádám Takács and Csaba Matta*.

3.3. RT-PCR Analysis

On set days of culturing, HDC established from 100 µL droplets of each model were washed three times with RNase-free physiological NaCl, then the cultures were snap-frozen in liquid nitrogen and stored at −70 °C. TRIzol was used to dissolve cell cultures (Applied Biosystems, Foster City, CA, USA). Following the addition of 20% RNase-free chloroform (Sigma-Aldrich), samples were centrifuged at 10,000 × g for 15 min at 4 °C. The samples containing total RNA were incubated in 500 µL RNase-free isopropanol at −20 °C for 1 h followed by centrifuging for 20 min at 10,000 x g and 4 °C. After this step, the supernatant was gently removed and the pellet was purified by two cycles of adding 1 mL of 70% ethanol and centrifuging for 10 min at 10,000 x g and 4 °C. Finally, total RNA was dissolved in nuclease-free water (Promega, Madison, WI, USA), its RNA content was measured with NanoDrop 1000 spectrophotometer (Thermo Fisher Scientific, Waltham, MA, USA) and was stored at −70 °C.

Composition of the assay mixture (20 µL) for each reverse transcriptase (RT) reaction was the following: 1000 ng (or 500 ng in the case of chicken HDC) total RNA diluted in 14.2 µL of nuclease-free water; 0.25 µL RNase inhibitor; 2 µL random primers; 0.8 µL dNTP Mix (4 mM); 50 units (1 µL) of MultiScribe™ RT in 1× RT buffer (High Capacity RT kit; Applied Biosystems, Foster City, CA, USA). cDNA was reverse transcribed at 37 °C for 2 h.

Specific cDNA sequences were amplified using specific primer pairs designed by Primer Premier 5.0 software (Premier Biosoft, Palo Alto, CA, USA) based on mouse and chicken nucleotide sequences published in GenBank (National Institutes of Health, Bethesda, MD, USA, available online: https://www.ncbi.nlm.nih.gov/genbank/). The primer pairs were purchased from Integrated DNA Technologies, Inc. (IDT; Coralville, IA, USA) and their specificity was confirmed *in silico* using the Primer-BLAST service of NCBI (National Institutes of Health, Bethesda, MD, USA, available online: https://www.ncbi.nlm.nih.gov/tools/primer-blast/) before *in vitro* application. Nucleotide sequences of forward and reverse primers and further reaction conditions are shown in *Table 1*. PCR reactions were carried out in a final volume of 25 µL containing 1 µL forward and 1 µL reverse primers (10 µM), 0.5 µL cDNA, 0.5 µL dNTP Mix (200 µM) and 1 unit (0.2 µL) of GoTaq® DNA polymerase in 1× Green GoTaq® Reaction Buffer (Promega) in a programmable thermal cycler (Labnet MultiGene™ 96-well Gradient Thermal Cycler; Labnet International, Edison, NJ, USA) with the following protocol: 2 min at 95 °C for initial denaturation followed by 35 repeated cycles of denaturation at 94 °C for 30 s, primer annealing for 45 s at the optimised temperature for each primer pair *(see Table 1.)* and extension at

72 °C for 90 s. After the final cycle, further extension was allowed to proceed for another 7 min at 72 °C. Bands representing PCR products were documented with the FluoChem E gel documentation system (ProteinSimple, San Jose, CA, USA) after horizontal gel electrophoresis in 1.2% agarose gels containing ethidium bromide at 90 V constant voltage for 2 h. Optical density of PCR product signals was determined using ImageJ freeware version 1.46 (ImageJ, Image Processing and Analysis in Java, National Institutes of Health, Bethesda, MD, USA, available online: https://imagej.nih.gov/ij/). *The RT-PCR analysis, including primer designing, was performed by Roland Ádám Takács*.

Table 1. Nucleotide sequences, amplification sites, GenBank accession numbers, annealing temperatures and amplicon sizes for each conventional PCR primer pair are shown.

Gene	*Primer*	*Nucleotide sequence (5'→3')*	*GenBank ID*	*Annealing temperature*	*Amplicon size (bp)*
Mouse chondrogenic marker genes					
Sox9	sense	GTA CCC GCA TCT GCA CAA CG (378–397)	**NM_011448**	62˚C	521
	antisense	GTG GCA AGT ATT GGT CAA ACT CAT T (874–898)			
Aggrecan core protein (Acan)	sense	CGG GAA GGT TGC TAT GGT G (782–800)	**NM_007424.2**	59˚C	359
	antisense	CCT GTC TGG TTG GCG TGT A (1122–1140)			
Collagen II (Col2a1)	sense	AAA GAC GGT GAG ACG GGA GC (1900–1919)	**NM_001113515**	63˚C	289
	antisense	GAC CAT CAG TAC CAG GAG TGC C (2167–2188)			
Hapln1	sense	GGC TCA GGA ATC CAC AAA (217–234)	**BC066853**	55˚C	284
	antisense	GGA AAG TAA GGG AAC ACC A (482–500)			
Lubricin (Prg4)	sense	CGA GGT CAT TAT TTC TGG (64–81)	**NM_021400**	51˚C	340
	antisense	TCA TTG GCT CCT GTT TAT (386–403)			
Snorc	sense	CCC TGT GGA ACG AGC CTA T (101–119)	**NM_028473**	58˚C	165
	antisense	CAA GCG ATC CTC CAT CCT G (247–265)			
Chicken chondrogenic marker genes					
Sox9	sense	TCG AAG GAA GCT GGC TGA CC (473–492)	**NM_204281**	62˚C	302
	antisense	CGC TGA TGC TGG AGG ATG ACT (774–754)			
Sox9	sense	CCC CAA CGC CAT CTT CAA (713–731)	**NM_204281**	54˚C	381
	antisense	CTG CTG ATG CCG TAG GTA (1075–1093)			
Aggrecan core protein (Acan)	sense	TAC ATC GAC AGG CTA AAG GG (1999–2018)	**NM_204955.2**	57˚C	265
	antisense	TCT GGT TGT GGT GCT GGT AG (2263–2244)			
Aggrecan core protein (Acan)	sense	CAA TGC AGA GTA CAG AGA (276–294)	**XM 001232949**	54˚C	430
	antisense	TCT GTC TCA CGG ACA CCG (688–704)			
Collagen II (Col2a1)	sense	CAA CAC CGC CAG CAT CCA (3947–3964)	**NM_204426**	59˚C	342
	antisense	CCA ATA TCC ACG CCA AAC TCC (4288–4268)			

Collagen II (Col2a1)	sense	GGA CCC AAA GGA CAG ACG G (1191–1210)	**NM_204426**	59˚C	401
	antisense	TCG CCA GGA GCA CCA GTT (1573–1591)			
Hapln1	sense	AAG TAT CAG GGC AGA GTG TT (457–476)	**NM_205482.1**	54˚C	487
	antisense	TGG TTG GGT GTA TTA GGT AG (943–924)			
Mouse osteogenic markers					
Alkaline phosphatase (Ap)	sense	GAA GTC CGT GGG CAT CGT (474–491)	**NM_007431**	59˚C	346
	antisense	CAG TGC GGT TCC AGA CAT AG (801–820)			
Collagen I (Col1a1)	sense	GGG CGA GTG CTG TGC TTT (237–254)	**BC050014**	62˚C	388
	antisense	GGG ACC CAT TGG ACC TGA A (606–624)			
Collagen X (Col10a1)	sense	TTC TGG GAT GCC GCT TGT C (1602–1620)	**NM_009925**	61˚C	263
	antisense	TCG TAG GCG TGC CGT TCT T (1846–1864)			
Osteocalcin	sense	AGC AGG AGG GCA ATA AGG (110–127)	**NM_007541**	57˚C	165
	antisense	CGT AGA TGC GTT TGT AGG C (256–274)			
Osteopontin	sense	GCT GAA GCC TGA CCC ATC T (126–144)	**X51834**	59˚C	494
	antisense	TCC CGT TGC TGT CCT GAT (602–619)			
Osterix	sense	CCC TTC CCT CAC TCA TTT CC (271–290)	**AF184902**	59˚C	424
	antisense	CAA CCG CCT TGG GCT TAT (677–694)			
Runx2	sense	GGA CGA GGC AAG AGT TTC A (595–613)	**NM_001146038**	58˚C	249
	antisense	TGG TGC AGA GTT CAG GGA G (825–843)			
Chicken osteogenic markers					
Alkaline phosphatase (Ap)	sense	CGG GTC GGT CTC GTT GTT CCT (964–944)	**NM_205360.1**	64˚C	577
	antisense	TGC TTA CCT CTG CGG CGT CAA (388–408)			
Collagen I (Col1a1)	sense	CCC ACG CAA GCC ACC ATT (4023–4040)	**XM_025144131.1**	62˚C	266
	antisense	AGC AGC AGA GCC TTC TTC AGG (4288–4268)			
Collagen X (Col10a1)	sense	GGA GCC AAG GGT GAA AGA G (5527–5545)	**XM_004940290.3**	56˚C	455
	antisense	TAA CCT TCT GGG ATT GTG GA (5981–5962)			
Osteocalcin	sense	CAG TGC TAA AGC CTT CAT CTC CC (102–124)	**NM_205387.3**	61˚C	167
	antisense	TCT GGT CGG CCA ACT CGT C (268–250)			
Osteopontin	sense	CCT AGC AAG AGC CAA GAG G (378–396)	**NM_204535.4**	58˚C	129
	antisense	CCC ACG GTT GAA AGG TGT (506–489)			
Osterix	sense	GCC AAA GGG CAC CCG TCG (496–513)	**XM_015300329.2**	65˚C	151
	antisense	GGT GCA CGT CCC ACC AAG C (646–628)			
Runx2	sense	GCT GGG AAC GAC GAG AAC (1779–1796)	**XM_015285082.2**	60˚C	304
	antisense	AGT GAA TGG ACG GCG AAG (2082–2065)			

Mouse adipogenic markers					
Pparg2	sense	TGC CTA TGA GCA CTT CAC (62–79)	**AY208183**	52˚C	258
	antisense	TGA TCG CAC TTT GGT ATT (302–319)			
Fabp4	sense	AAA GAA GTG GGA GTG GGC (64–81)	**NM_024406**	58˚C	173
	antisense	CTG TCG TCT GCG GTG ATT (219–236)			
Chicken adipogenic markers					
Fabp4	sense	TTT GCT ACC AGG AAG ATG (116–133)	**NM_204290.1**	55˚C	191
	antisense	GTG CCA CTG TCT AGG GTT (306–289)			
Mouse pluripotency markers					
Nanog	sense	GCC CTG ATT CTT CTA CCA (194–211)	**AY278951**	54˚C	383
	antisense	AGA TGC GTT CAC CAG ATA G (558–576)			
Oct4 (Pou5f1)	sense	GCA CGA GTG GAA AGC AAC (286–303)	**NM_013633**	56˚C	453
	antisense	CGG GCA CTT CAG AAA CAT (721–738)			
Sox2	sense	AAC CAG CGC ATG GAC AGC (466–483)	**U31967**	63˚C	281
	antisense	TCG GAC TTG ACC ACA GAG CC (727–746)			
Chicken pluripotency markers					
Nanog	sense	AGA CCA CCC ATC TCA CCG (228–245)	**NM_001146142.1**	59˚C	429
	antisense	CCC TGC CCA TTC CCA TAA (656–639)			
PouV	sense	GCT CTG GGC ACG CTC TAT (604–621)	**NM_001309372.1**	58˚C	231
	antisense	CGT TCC CTT CAC GTT GGT (834–817)			
Sox2	sense	TTC ATT GAC GAA GCC AAA C (326–344)	**NM_205188.2**	57˚C	251
	antisense	ATC CCA TAG CCT CCG TTG (576–559)			
Mouse control gene					
Gapdh	sense	TGG CAA AGT GGA GAT TGT TG (69–88)	**NM_008084**	60˚C	486
	antisense	GTC TTC TGG GTG GCA GTG AT (535–554)			
Chicken control gene					
Gapdh	sense	CTG CCC AGA ACA TCA TCC CA (656–675)	**NM_204305**	58˚C	366
	antisense	CAC GGT TGC TGT ATC CAA ACT CAT (1021–998)			
Gapdh	sense	GAG AAC GGG AAA CTT GTC AT (238–258)	**NM_204305**	54˚C	556
	antisense	GGC AGG TCA GGT CAA CAA (775–793)			
Store-operated Ca^{2+}-entry (chicken)					
Orai1	sense	TAG CAA CGT GCA TAA TCT CAA (264–284)	**NM_001030658**	57˚C	257
	antisense	TCA GTC CAA AGG GAA CCA T (502–520)			
Stim1	sense	GGT GGT GTC CAT CGT CAT CG (426–445)	**NM_001030838**	62˚C	356
	antisense	GCT CCT TCT CGG CGT TCT TC (762–781)			
Stim2	sense	CAA TTA GCA ATC GCC AAA G (1177–1195)	**XM_420749**	57˚C	495
	antisense	CAC AGA AAG GAT GTC AGG GT (1652–1671)			

Voltage-operated Ca^{2+}-channels, α_1 subunits (chicken)					
$Ca_V1.2$ (Cacna1c)	sense	CAA CAG AGC CAA AGG ACT AAA (3054–3074)	**XM_416388**	54˚C	477
	antisense	GTG ACG ATG ACG AAA CCA A (3512–3530)			
$Ca_V1.3$ (Cacna1d)	sense	AGG CTC ATC AAT CAC CAC A (2704–2722)	**NM_205034**	54˚C	387
	antisense	AAA GAC GCA CTG AAC AAC G (3072–3090)			
$Ca_V2.2$ (Cacna1b)	sense	CTA CGC CAC GAC CCT ACA C (2442–2460)	**NM_204293**	61˚C	408
	antisense	TTC TCA ACG CCT TCT TCC A (2831–2849)			
$Ca_V2.3$ (Cacna1e)	sense	TCA CCA ACT CCG ACC GTA AC (3347–3366)	**XM_422255**	60˚C	500
	antisense	CAC CTC CAT CTT GTT CTT CTC AT (3824–3846)			
$Ca_V3.1$ (Cacna1g)	sense	CAC TGA ATC CGT CCA TAG CAT C (1989–2010)	**XM_001232653**	61˚C	423
	antisense	CTG TCT GAG TCC GTC TCG TTG T (2390–2411)			
$Ca_V3.2$ (Cacna1h)	sense	CCC TGG AAG GAT GGG TTG A (1256–1274)	**XM_414830**	61˚C	371
	antisense	CTG CCC GTT TGT GGT GTT G (1608–1626)			
$Ca_V3.3$ (Cacna1i)	sense	CTG AGG ACG GAT ACA GGA GAT (2281–2301)	**XM_425474**	59˚C	437
	antisense	TTG CGT GAA GAG TTG GAG AC (2698–2717)			

3.4. Detection of mRNA Levels with Quantitative PCR

The protocol for RNA isolation and reverse transcription was almost identical to what is described in the previous point except that 1000 ng of RNA isolated from FCF-treated chicken HDC was used to generate first strand cDNA, which – after reverse transcription – was diluted 1:5 before RT-qPCR experiments.

Target cDNA sequences were amplified with specific primer pairs designed using the Primer-BLAST service of NCBI (National Institutes of Health) based on chicken nucleotide sequences published in GenBank (National Institutes of Health). The primers were designed to produce an amplimer sized between 100 and 200 base pairs and span an exon-exon junction except where this latter preference resulted in products on potentially unintended templates *in silico*. The primer pairs were purchased from Integrated DNA Technologies, Inc. (IDT; Coralville, IA, USA). Nucleotide sequences of forward and reverse primers with additional reaction conditions are shown in *Table 2*. Relative gene expression levels of chondrogenic (*Sox9*, *Col2a1*, *Acan* and *Halpn1*) and pluripotency (*PouV*) marker genes and SOCE-mediating molecules (*Orai1*, *Stim1* and *Stim2*) were detected by a QuantStudio 3 Real-Time PCR System (Thermo Fisher Scientific) in 96-well microplates (Greiner Bio-One Hungary, Mosonmagyaróvár, Hungary) using 2 × GoTaq® qPCR Master Mix (Promega). Thermal cycling conditions were as follows: enzyme activation at 95 °C for 2 min, followed by 40 cycles of denaturation at 95 °C for 5 s and annealing/extension (and data collection) at 60 °C for 30 s.

For data normalization the following three reference genes were investigated: peptidyl-prolyl isomerase A (*Ppia*), 60S acidic ribosomal protein P0 (*Rplp0*) and glyceraldehyde-3-phosphate dehydrogenase (*Gapdh*). To determine the best normalizing gene, standard deviations (SD) of gene expression levels of the previously mentioned reference genes (*Ppia*, *Rplp0* and *Gapdh*) were determined between control and FCF-treated samples and *RPLP0* was found to show the lowest SD values. Therefore, *RPLP0* expression was used to determine relative gene expression levels calculated by the comparative Ct method. In the comparative or ΔΔCt method of qPCR data analysis, the Ct values collected from two different experimental RNA samples are directly normalized to that of the reference gene (*RPLP0* in our case) and then correlated. *Experiments with quantitative PCR method, including primer designing, were carried out by Roland Ádám Takács*.

Table 2. Nucleotide sequences, amplification sites, GenBank accession numbers and amplicon sizes for each chicken qPCR primer pair are shown. The temperature for annealing/extension was 60 °C in all cases.

Gene	*Primer*	*Nucleotide sequence (5'→3')*	*GenBank ID*	*Amplicon size (bp)*
Chondrogenic marker genes				
Sox9	sense	TTT CCG AGA CGT GGA CAT CG (929–948)	**NM_204281.1**	150
	antisense	GTA CCG CTG TAG GTG GTG AC (1078–1059)		
Collagen II (Col2a1)	sense	GGG ACC TCA AGG CAA AGT CG (1550–1569)	**NM_204426.1**	140
	antisense	TTC CAG GCT CAC CAT TAG CG (1689–1670)		
Aggrecan core protein (Acan)	sense	AGC AGT AGA TGC ACT GGG AC (5631–5650)	**NM_204955.2**	153
	antisense	GCC AGG TCG ATC TCA CAC AG (5783–5764)		
Hapln1	sense	AGA GTT CTG AGC GCA TCT CG (70–89)	**NM_205482.1**	183
	antisense	GCG GGG TCC ATT TTC TTC TTG (252–232)		
Store-operated Ca^{2+}-entry				
Orai1	sense	AGC GTA TGC ATC GGC ACA TT (483–502)	**NM_001030658.1**	141
	antisense	TGT TCT CAG CTG GGT CAA GG (623–604)		
Stim1	sense	CAT CAA GAA GCA GAA CGC GG (1117–1136)	**NM_001030838.1**	114
	antisense	GAT GAG CTG TGA GCA ACG TG (1230–1211)		
Stim2	sense	CAA GAC GCA ATG TTG TGC CA (1734–1753)	**XM_420749.6**	159
	antisense	CCT GTA CTT CCC ATT GTT TAT CAG C (1892–1868)		
Pluripotency marker				
PouV	sense	TAT CTC GAG CCA TTC ACC GC (186–205)	**NM_001110178.1**	162
	antisense	ATC TTC CCA TAG AGC GTG CC (347–328)		

Reference genes				
Rplp0	sense	GAA CGT GGG CTT TGT GTT CA (320–339)	**NM_204987.2**	158
	antisense	AGG AGG TCT TCT CAG GTC CG (477–458)		
Ppia	sense	GAG CTC TTC GCT GAC AAG GT (67–86)	**NM_001166326.1**	139
	antisense	GCG TAA AGT CAC CAC CCT GA (205–186)		
Gapdh	sense	ACT GTC AAG GCT GAG AAC GG (226–245)	**NM_204305.1**	100
	antisense	CAC CTG CAT CTG CCC ATT TG (325–306)		

3.5. SDS-PAGE, Western Blot and Protein BLAST Analysis

Total cell lysates of chick HDC for sodium dodecyl sulfate polyacrylamide gel electrophoresis (SDS-PAGE) were prepared by adding 1/5 volume of fivefold concentrated electrophoresis sample buffer (310 mM Tris-HCl pH 6.8, 10% sodium dodecyl sulfate (SDS), 50% glycerol, 100 mM DTT (dithiothreitol), 0.01% bromophenol blue) to cell lysates and boiled for 10 min. For each sample 50 µg of protein was separated by 7.5% SDS-PAGE gel for immunological detection of investigated molecules playing key roles in Ca^{2+} influx or release functions (i.e. pan α_1 subunit of VDCCs and STIM1), as well as the protein expression and phosphorylation status of the chondrogenic master transcription factor SOX9. Proteins were transferred electrophoretically to a nitrocellulose membrane. After blocking in 5% non-fat dry milk solved in PBS, membranes were incubated with primary antibodies overnight at 4 °C as follows: rabbit polyclonal anti-CaV pan α_1 subunit in 1:200, epitope: intracellular C-terminus (Alomone Labs, Jerusalem, Israel); and mouse monoclonal anti-STIM1 in 1:500, epitope: 25-139 in human (BD Biosciences, Franklin Lakes, NJ, USA) that has a high similarity to the chicken sequence (to which it has been applied); rabbit polyclonal anti-SOX9 antibody (Abcam, Cambridge, UK) in 1:600; rabbit polyclonal anti-P-SOX9 antibody (Sigma-Aldrich) in 1:800; rabbit polyclonal anti-actin antibody (Santa Cruz Biotechnology,Inc., Santa Cruz, CA, USA) and rabbit polyclonal anti-GAPDH antibody (Abcam). Following washing in PBST for 30 min, membranes were incubated with anti-rabbit IgG (Bio-Rad Laboratories, Hercules, CA, USA) conjugated to horseradish peroxidase (HRP) in 1:1000 dilution. Membranes were developed by enhanced chemiluminescence reaction (Millipore, Billerica, MA, USA) according to the instructions of the manufacturer and were recorded with the FluoChem E gel documentation system (ProteinSimple). Optical density of signals was measured using ImageJ 1.46. Protein BLAST (National Center for Biotechnology Information, U.S. National Library of Medicine, Bethesda, MD, USA, available online: https://blast.ncbi.nlm.nih.gov/) analysis of the 114-amino-acid-long human sequence (that has been used for the production of our monoclonal antibody against STIM1) versus the chicken protein sequence database has been performed according to the NCBI

BLAST tutorial. *The above-described experiments were implemented by Roland Ádám Takács, Adrienn Tóth and János Fodor*.

3.6. Histological Analysis

3.6.1. Conventional Haematoxylin and Eosin Staining

HDC were established from 30 µL droplets of the cell suspensions and cultured on the surface of round 30 mm coverglasses (Menzel-Gläser, Menzel GmbH, Braunschweig, Germany) placed into 35 mm plastic culture dishes. After washing with PBS, cultures were fixed with a 4:1 mixture of absolute ethanol and 40% formaldehyde on day 3 of culturing. After rehydration, cultures were stained with Gill's haematoxylin No. 2 and eosin Y (1% aqueous solution; Bio Optica Milano S.p.A., Italy). Briefly, cultures were first immersed in haematoxylin for 20 s, rinsed in running tap water for 5 min and after washing in distilled water, eosin was applied for 2 min. After washing eosin, cultures were dehydrated in graded concentrations of ethanol. Finally, after a wash in xylene (VWR International, Debrecen, Hungary), colonies were mounted onto glass slides using DPX mounting medium (Sigma-Aldrich). An Olympus DP72 camera on a Nikon Eclipse E800 microscope (Nikon Corporation, Tokyo, Japan) was used to take photomicrographs of the cultures. Images were acquired using cellSense Entry 1.5 software (Olympus, Shinjuku, Tokyo, Japan). *The above-described experiments were carried out by Roland Ádám Takács and Csaba Matta*.

3.6.2. Analysis of Cartilage Matrix Production by Qualitative and Semi-Quantitative Methods

Cartilage matrix of HDC were visualised by DMMB (Sigma-Aldrich) low pH metachromatic staining. Cultures were fixed in a 4:1 mixture of absolute ethanol and 40% formaldehyde for 30 min on respective days of culturing. Cultures were then stained with 0.1% DMMB dissolved in 3% acetic acid (pH 2.52) for 5 min and mounted in gum arabic. The semi-quantitative method we applied to determine the amount of sulfated matrix components is measuring the optical density of extracted toluidine blue (TB; Reanal, Budapest, Hungary) that is bound proportionately to the amount of glycosaminoglycans in six-day-old HDC. The cultures were fixed in a solution containing 28% ethanol, 4% formalin and 2% acetic acid, stained with 0.1% toluidine blue dissolved in glycine—HCl buffer (pH 1.8) for 15 min, the unbound toluidine blue removed by washing with glycine-HCl buffer for 1 h. Eventually, the dye bound to highly sulfated proteoglycans and glycosaminoglycans was extracted by 8% HCl dissolved in absolute ethanol and the absorbance of these samples was measured at 625 nm with a microplate reader (Chameleon, Hidex, Turku, Finland). *The above-described experiments were performed by Roland Ádám Takács and Csaba Matta*.

3.6.3. Analysis of Matrix Mineralization by Alizarin Red S Staining

Micromass cultures established from 30 µL droplets on 30 mm round coverglasses were used to ascertain the extent of matrix calcification. Cultures were fixed with a 4:1 mixture of absolute ethanol and 40% formaldehyde on respective days of culturing and then stained with 2% (w/v) Alizarin Red S (Sigma-Aldrich) dissolved in distilled water (pH 4.2; adjusted with 10% ammonium hydroxide) for 2 min. Excess dye was removed by aspiration, coverslips were blotted and were dehydrated by dipping 20 times into acetone (VWR International) and then an additional 20 times into acetone-xylene (1:1) mixture (VWR International). Eventually, coverglasses were mounted onto glass slides using DPX mounting solution (Sigma-Aldrich). Photomicrographs of the stained cultures were taken as described above. *The above-described experiments were executed by Roland Ádám Takács and Csaba Matta*.

3.6.4. Oil Red O Staining to Estimate Lipid Accumulation

Adipogenic differentiation and lipid accumulation in micromass cultures established from 30 µL of cell suspensions was assayed by Oil Red O staining on respective days of culturing. 10% formalin was used to fix cultures for 60 min at room temperature. Formalin was washed with distilled water and cultures were rinsed in 60% isopropanol (VWR International) for 5 min. Isopropanol was removed from cultures by aspiration, which was followed by the addition of 2 mL Oil Red O working solution for 5 min at room temperature. Preparation of working solution: first, 0.3% (w/v) Oil Red O (Sigma-Aldrich) stock solution was made using 99% isopropanol (VWR International); second, 3 volumes of Oil Red O stock solution was mixed with 2 volumes of distilled water. After incubation, the working solution was discarded, surplus dye was washed away by tap water and then Gill's haematoxylin No. 2 was applied for 20 s to provide background staining of nuclei. Haematoxylin was rinsed with tap water, then cultures were mounted with gum arabic. We took photomicrographs of the stained cultures as described above. *The above-described experiments were performed by Roland Ádám Takács and Csaba Matta*.

3.7. Determination of Cell Proliferation, Collagen Synthesis and Mitochondrial Activity

To determine the **proliferation rate** of cells in HDC, 15 µL droplets were pipetted into wells of opaque 96-well microtiter plates (Wallac, PerkinElmer Life and Analytical Sciences, Shelton, CT, USA). Ham's F12 medium containing 1 µCi mL^{-1} (185 GBq mM^{-1}), ^{3}H-thymidine (diluted from methyl-^{3}H-thymidine solution; Amersham Biosciences, Budapest, Hungary) was added to the wells for 16 h promptly after treatments, or for their 24 h duration in the case of inhibitory treatments of septin rearrangement. Subsequently, two washes were performed with PBS and ice-cold 5% trichloroacetic acid was applied to precipitate proteins, which was followed by another two washes in PBS. Eventually,

plates were placed in an exsiccator containing phosphorous pentoxide in order to occlude moisture. 50 µL scintillation solution (MaxiLight; Hidex) was added to each well directly prior to measurements and radioactivity was counted by liquid scintillation counter (Chameleon).

Collagen synthesis was measured very similarly, 15 µL droplets of HDC were grown in wells of opaque 96-well microtiter plates (Wallac). Simultaneously with 24 h FCF treatments starting either on day 1 or day 2 of culturing, the Ham's F12 medium also contained 1 µCi mL^{-1} (185 GBq mM^{-1}) ^{3}H-proline (diluted from proline [6-^{3}H] solution; American Radiolabeled Chemicals, St. Louis, MO, USA). Afterwards, wells containing the treated cultures were washed two times with PBS and ice-cold 5% trichloroacetic acid was applied for fixation. This was followed by two further washes in PBS. Finally, plates were exsiccated and 50 µL of scintillation solution (MaxiLight) was added to each well and incorporated radioactivity was determined using a liquid scintillation counter (Chameleon).

MTT-assay was applied to measure **mitochondrial dehydrogenase activity** following various treatments to obtain information on the metabolic and via that, indirectly, the vital status of chondrogenic cells. Cells were cultured in wells of 96-well microtiter plates and the assay was performed immediately after treatments. 10 µL MTT reagent [3-(4,5-dimethylthiazolyl-2)-2,5-diphenyltetrazolium bromide; 5 mg MTT mL^{-1} PBS] was added into each well. Cells were incubated for 2 h at 37 °C in MTT-containing Ham's F12 medium. This medium was aspired and 100 µL of MTT solubilizing solution (10% Triton X-100 and 0.1 M HCl dissolved in anhydrous isopropanol) was added. Optical density was measured at 570 nm by a microplate reader (Chameleon) after 10 min of shaking at 200 rev/min.

Untreated HDC from the same stage of culturing were used as controls in the case of the assays described above. Measurements were carried out using 6 samples of each experimental group in 3 independent experiments. *The assays were executed by Roland Ádám Takács*.

3.8. Confocal Microscopy

3.8.1. Line-Scan Analysis

We used an LSM 510 META Laser Scanning Confocal Microscope (Zeiss, Oberkochen, Germany) **to monitor** spontaneous **Ca^{2+} transients** and the effects of modified extracellular Ca^{2+} levels or various pharmacons on oscillations. All measurements were performed at room temperature. Prior to measurements, cells of 1- and 2-day-old chick HDC were incubated for 30 min at 37 °C with 10 µM Fluo-4-AM in Ham's F12 medium. Calcium imaging was carried out in normal (containing 137 mM NaCl, 5.4 mM KCl, 0.5 mM $MgCl_2$, 1.8 mM $CaCl_2$, 11.8 mM HEPES-NaOH, 1 g L^{-1} glucose, pH 7.4) or Ca^{2+}-free

(containing 5 mM ethylene glycol-bis(β-aminoethyl ether)-N,N,N',N'-tetraacetic acid (EGTA), without $CaCl_2$) Tyrode's solution. CPA was used at a final concentration of 10 µM in normal Tyrode's solution (stock: 10 mM, in DMSO). SOCE blockers YM-58483 and $LaCl_3$ were used at 1 µM and 500 µM final concentrations, respectively and were diluted in normal Tyrode's solution (stocks: 300 mM and 1 mM in distilled water and DMSO, respectively). (Application of these reagents was not possible in Ca^{2+}-free Tyrode's since this solution alone abolished Ca^{2+} oscillations, which would make the evaluation of the effects of these blockers impossible.) Line-scan images were recorded immediately after adding the test solution to the cultures. During measurements, only cells exhibiting Ca^{2+} oscillations were investigated, other, non-oscillatory cells were disregarded. Line-scan images were acquired at 0.8 ms/line, 512 pixels/line with 7 ms intervals, recording 8192 lines. We have used a 63× water immersion objective for the recording. Measurements were carried out on HDC from 3 independent experiments. Analysis of the images was performed using an automatic event detection software developed in the Department of Physiology of the University of Debrecen, Faculty of Medicine. *The analysis was completed by Beatrix Dienes, János Fodor, Roland Ádám Takács and Csaba Matta*.

3.8.2. X-Y Monitoring

1- and 2-day-old Fluo-4-loaded HDC were examined by LIVE 5 Laser Scanning Confocal Microscope (Zeiss, Oberkochen, Germany) using EC Plan-Neofluar 20×/0.50 M27 objective with 2× digital zoom. X-Y image series were recorded after selecting random visual fields. **Calcium imaging** was performed in normal and Ca^{2+}-free Tyrode's solutions (see above). All measurements were performed at room temperature. $LaCl_3$ (500 µM), YM-58483 (1 µM) and nifedipine (10 µM) were diluted in normal Tyrode's solution (containing 1.8 mM Ca^{2+}; see above). The rate of frame acquisition was 10 s^{-1}. A total number of 1000 images were recorded under control conditions on days 1 and 2. In experiments testing the effects of treatments on spontaneous Ca^{2+} transients during time series recordings, we have kept the same visual fields of each culture 1, 3 and 5 min after replacing the bath solution from normal Tyrode's to the test solution (containing $LaCl_3$ and YM-58483 or nifedipine). A total of 500 X-Y scans were recorded at each time point in these experiments. Zeiss Enhanced Navigation (ZEN 2009) software was used for data analysis. The location where round-shaped chondrocytes were identified was considered the region of interest (ROI) for each visual field. An automatic event detection software has been developed in the Department of Physiology to analyze the time-dependent fluorescent intensities of ROIs. *The monitoring was implemented by Beatrix Dienes, János Fodor, Roland Ádám Takács and Csaba Matta*.

3.9. Single Cell Fluorescent Measurements to Assess Cytosolic Free Ca^{2+} Levels

Measurements were performed using the calcium dependent fluorescent dye Fura-2 on day 2 of culturing. Cultures were fed with 2 mL fresh Ham's F12 medium containing 10 µL Fura-2-AM (10 µM) and 4 µL neostigmin (0.3 nM) in order to inhibit extracellular cholinesterase activity. After 60 min of incubation at 37 °C in a CO_2 incubator, cultures were washed twice in normal Tyrode's solution (see above) to remove excess dye attached to the extracellular matrix. Fura-2-loaded cells were then viewed using a 40× oil immersion objective on the stage of an inverted fluorescent microscope (Diaphot; Nikon, Kowasaki, Japan). Measurements were carried out in normal and Ca^{2+}-free Tyrode's solutions. $LaCl_3$ (500 µM), YM-58483 (1 µM) and CPA (10 µM) were diluted in Ca^{2+}-free Tyrode's solution. Excitation wavelength altered between 340 and 380 nm (F340 and F380) generated by a microcomputer-controlled dual-wavelength monochromator (DeltaScan; Photon Technologies International, New Brunswick, NJ, USA). Emission was monitored at 510 nm with a 10 Hz acquisition rate using a photomultiplier. Background fluorescence was subtracted automatically from the signals by the data acquisition software. Intracellular [Ca^{2+}] was calculated from the ratio of measured fluorescence intensities (R = F340/F380) as described by Grynkiewicz et al. [251]. The measuring bath was continuously perfused with normal Tyrode's solution at a rate of 2 mL min^{-1} (EconoPump; Bio-Rad Laboratories, Hercules, CA, USA) during measurements. Test solutions were directly applied to the cells via a perfusion capillary tube (Perfusion PencilTM; Auto-Mate Scientific, San Francisco, CA, USA) with an internal diameter of 250 µm at a rate of 1.5 µL s^{-1}, using a local perfusion system (Valve BankTM 8 version 2.0, AutoMate Scientific). All measurements were performed at room temperature. *The measurements were executed by Tamás Oláh, János Fodor, Roland Ádám Takács and Csaba Matta*.

3.10. Statistical Analysis

All data are representative of at least three independent experiments. Averages are expressed as mean ± SEM (standard error of the mean; *n*, number of cells measured). Statistical analysis was performed using Student's *t*-test. Threshold for statistically significant differences as compared to respective control cultures was set at $*P < 0.05$. *The analysis was performed by Roland Ádám Takács, János Fodor and Csaba Matta*.

4. Results

4.1. Comparative Analysis of Diverse Types of Chondrogenic HDC

4.1.1. Micromass Cultures Derived from Embryonic Limb Buds and the C3H10T1/2 Cell Line Demonstrate Different Morphologies

We analyzed if the investigated models displayed condensation and precartilaginous nodule formation, as these are the earliest *in vivo* signals of chondrogenesis from the embryonic connective tissue [252]. To observe the cellular morphology of the investigated cultures, we performed haematoxylin-eosin (HE) staining on day 3 of culturing, which is a time point by when nodules are known to appear in chick limb bud cultures. The appearance of the cell line-based cultures demonstrated a considerably distinct morphology when compared with the primary HDC *(Fig. 4.1.)*. Unlike in C3H10T1/2-based cultures, nodules defined by multiple layers of cells were observable in both primary limb bud cultures (marked by arrows), while the internodular areas exhibited a low cell density. The contrast between these distinct areas appeared less resolute in the case of the chick HDC. In accordance with the literature [50], our results obtained with DMMB staining suggest that chondroprogenitors prefer these densely populated locations to proceed with differentiation into chondroblasts; unlike nodules, internodular areas did not contain metachromatic ECM *(Fig. 4.2.)*. On the other hand, no nodules or internodular areas were visible in case of the C3H10T1/2-based cultures; the central territories were homogeneous and cells were compactly arranged *(Fig. 4.1.)*. Moreover, cells of primary HDC reacted differently to high density culturing: only a small portion of these cells migrated to the periphery of the culture, while a considerable portion of the cells shifted to the periphery in the cell line-based HDC; so much that multiple layers formed in certain areas.

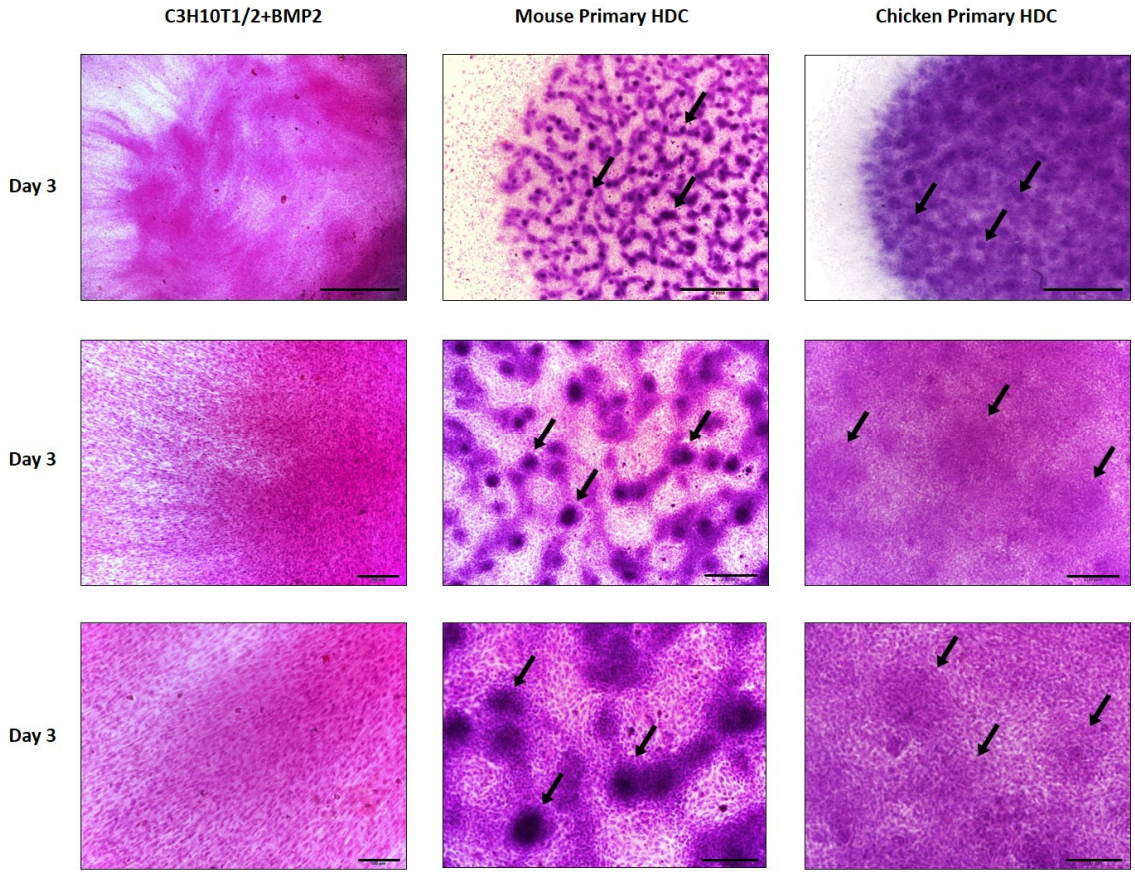

Fig. 4.1. Histological structure of 3-day-old HDC established from b-C3H10T1/2, chick and mouse primary embryonic mesenchymal cells following HE staining. Original magnification was 2× (upper panels), 10× (middle panels) and 20× (lower panels), while scale bars represent: 2 mm, 200 µm and 100 µm, respectively. The upper panels display both the peripheral (left) and central (right) regions of HDC. Precartilaginous nodules in primary micromass cultures are shown by arrows. Presented images are representative photomicrographs of 3 independent experiments.

4.1.2. Examined Models Undergo Various Levels of Chondrogenesis

We have adopted acidic **DMMB staining** to cultures harvested on selected days of culturing to determine the volume of **metachromatic ECM synthesis**. As the sulfated GAG containing PGs that are liable for this staining phenomenon do not occur in sufficient amounts in other tissues to produce the same effect, metachromatic staining is a well-accepted method to confirm cartilage ECM formation. *Fig. 4.2.* provides a distinct evidence that the volume of metachromatic ECM increases along with the progression of differentiation. On the other hand, it is noteworthy that the studied models display different temporal arrangements in terms of this process. As soon as day 3 of culturing, we saw the limb bud-derived HDC embodying large metachromatic territories within their nodules, while the C3H10T1/2-based cultures showed primarily orthochromatic ECM staining. By later stages of culturing, the gap further increased between the primary and cell line-based HDC, as seen on days 6 and 10 of culturing in *Fig. 4.2.* Despite this, cultures obtained from b-C3H10T1/2 cells displayed a higher volume of metachromatic ECM when compared to control cultures. By the end of the 15-days-long culturing

period of both primary HDC, their ECM completely turned metachromatic, its total volume has increased and cells reminiscent of hypertrophic chondrocytes were also present. Although b-C3H10T1/2 colonies also demonstrated an increase in the amount of metachromatic ECM, it was significantly below the level represented by primary HDC at the same time point. In the meantime, c-C3H10T1/2 cultures exhibited no metachromatic territories even at the end of their culturing period. Another conspicuous difference between limb bud-derived and BMP-2 overexpressing cell line-based cultures is expressed in the appearance of metachromatic territories following DMMB staining; the former ones displayed definite, strongly metachromatic areas that resembled chondrogenic nodules, while in the latter case fainter and more uniform metachromasia was observable. In addition, b-C3H10T1/2 colonies exhibited extensive orthochromatic territories from the start of culturing as far as day 15. While our results were exceedingly similar in case of chick and mouse limb bud HDC, it is noteworthy that metachromatic ECM accumulation appears more extensive by day 15 in chick cultures, likely due to their faster pace of embryonic limb development.

We have also examined **mRNA expression profiles** of representative chondrogenic marker genes through the same culturing period *(Fig. 4.3.)*. The transcription factor *Sox9*, a master regulator of cartilage formation, was detected to be expressed from the earliest stages of culturing at a relatively constant degree in the primary colonies and the b-C3H10T1/2 cultures. Our results regarding *Sox9* mRNA expression of c-C3H10T1/2 cultures are quite intriguing; relatively robust bands were visible at the initial periods, but a progressive and marked decrease could be observed until day 15 of culturing. *Col2a1*, the gene that codes for the alpha-1 chain of type II collagen, exhibited a constant mRNA expression level in all examined micromass cultures – including the c-C3H10T1/2 ones – suggesting that the activation of this gene may occur in a *BMP-2 signaling-independent fashion.* mRNA expression of the gene encoding the core protein of aggrecan, *Acan*, on the other hand, was completely absent in c-C3H10T1/2 cultures; furthermore, its strong level of expression in primary limb bud cultures was not seen in b-C3H10T1/2 colonies. *Hapln1*, the gene coding for the hyaluronan and proteoglycan link protein that – as mentioned earlier – connects proteoglycan core proteins to hyaluronic acid, displays a substantial expression in both primary and BMP-2 overexpressing colonies without the signs of ample expression in c-C3H10T1/2 cultures. Interestingly, in the case of *Snorc,* a cartilage-specific small transmembrane proteoglycan in differentiating and articular chondrocytes, a marked increase of mRNA amount could be detected from day 3 of culturing in the mouse primary and the BMP-2 overexpressing colonies, when cartilage matrix producing chondroblasts form. In the meantime, expression of this gene was almost undetectable in c-C3H10T1/2 cells. *Prg4,* which encodes the secreted protein specifically expressed by superficial zone chondrocytes and joint capsule synoviocytes, has an expression pattern where strong signals are exclusive to post-day 6 limb bud

derived HDC; meanwhile only a weak band is detectable in the BMP-2 overexpressing cell line-based model at the end of culturing. This important detail suggests a closer relation on the molecular level between articular cartilage and the limb bud derived HDC, than in the other case. Chicken mRNA sequences were unfortunately not available in any of the searched nucleotide databases (NCBI, DDBJ and EMBL-EBI) for *Snorc* and *Prg4*. Primary cultures expressed *Col10a1*, the marker gene coding for the alpha-1 chain of type X collagen expressed by hypertrophic chondrocytes, in a steadily, or slightly increasing fashion, while the cell line-based colonies had low expression levels and an indistinct temporal pattern for this gene.

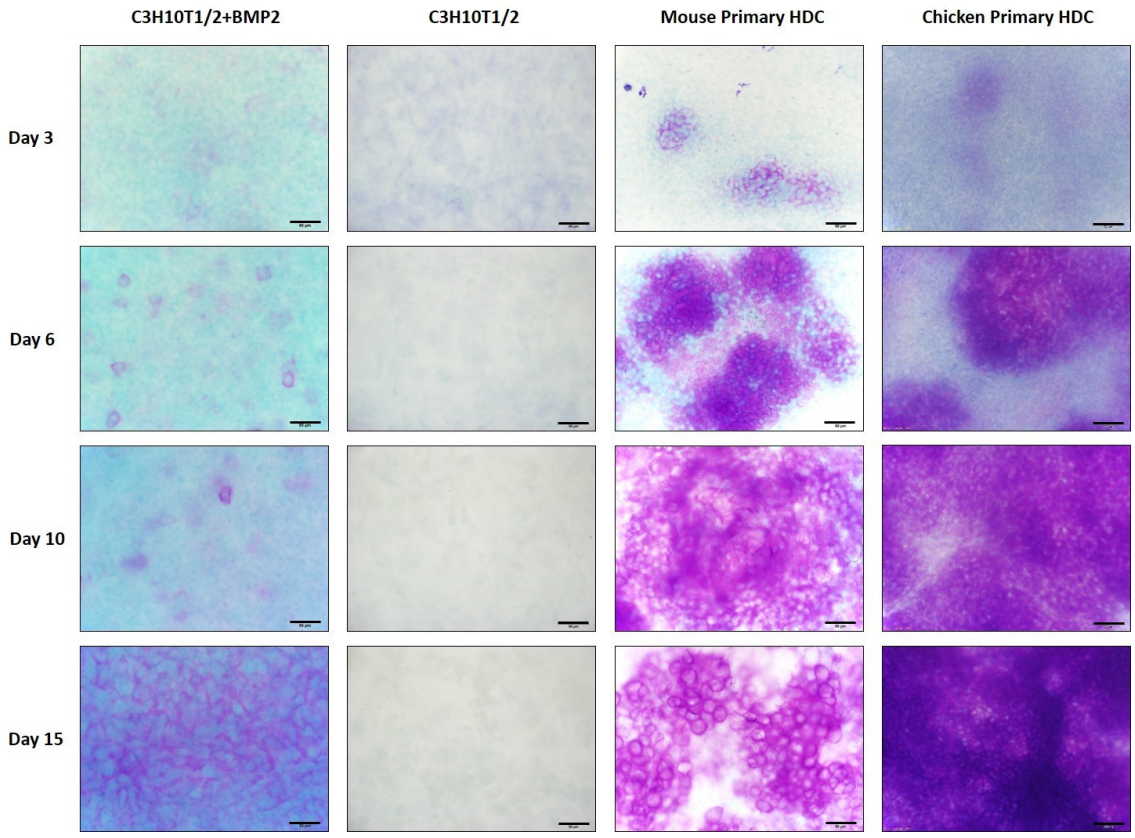

Fig. 4.2. Metachromatic cartilage areas on different days of culturing in HDC visualized with 0.1% DMMB dissolved in 3% acetic acid (pH 2.52). Original magnification was 40× for each photomicrograph. Scale bar: 50 µm. Purple areas coincide with cartilage matrix rich in sulphated GAGs. Presented images are representative photomicrographs of 3 independent experiments.

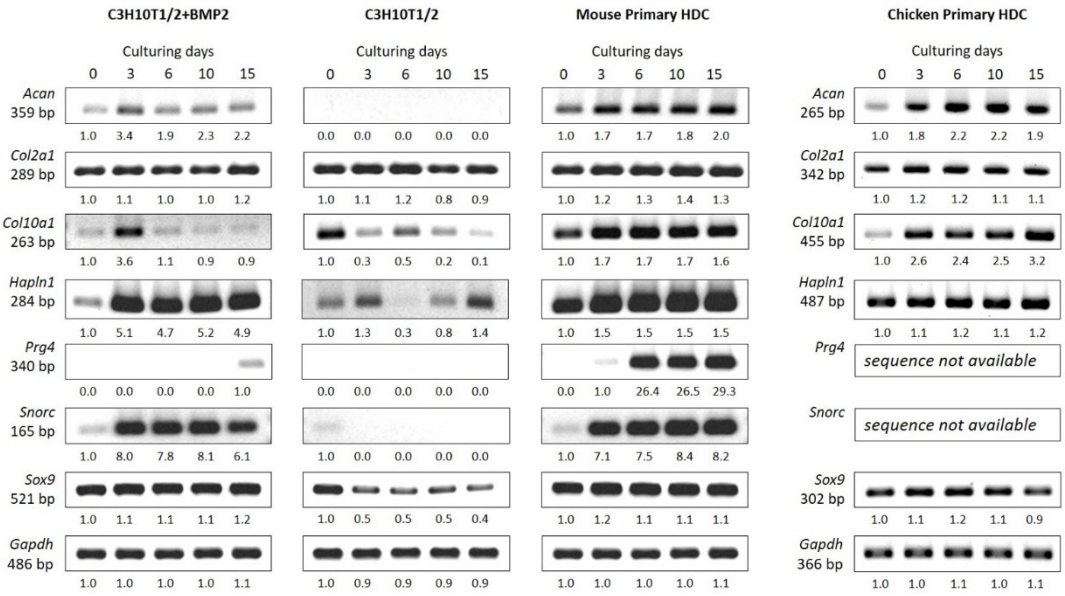

Fig. 4.3. Chondrogenic marker gene mRNA expression in cells of micromass cultures on various days of culturing. *Sox9* codes for the main chondrogenic transcription factor; *Acan* and *Col2a1* are cartilage-specific ECM components; *Hapln1* encodes the hyaluronan and proteoglycan link protein, another specific ECM component; *Prg4* is a characteristic proteoglycan, expressed by chondrocytes in the superficial zone of articular cartilage; *Snorc* is a recently identified cartilage-specific small membrane proteoglycan in chondrocytes; *Col10a1* is a marker of hypertrophic chondrocytes. *Gapdh* was used as a control. Integrated densities of signals established using ImageJ 1.46 are shown as numbers below gel images; data were normalized to the value detectable on the earliest day of culturing (making day 0 = 1.0, where applicable). Shown data are representative of 3 independent experiments.

4.1.3. Assessment of Osteogenic Differentiation

Calcified matrix accumulation was appraised by the application of Alizarin Red staining method to limb bud-derived HDC and cell line-based colonies. c-C3H10T1/2 cultures did not display signs of calcification, but we could observe a strong positivity in the BMP-2 overexpressing version of the same cell line from day 6 of culturing *(Fig. 4.4.)*. Primary micromass cultures, on the other hand, displayed substantial calcification exclusively within their cartilaginous nodules and only from day 10 (or day 6 in the case of chick HDC). Therefore we can assume that all micromass colonies – with the exception of the c-C3H10T1/2 ones – undergo maturation and hypertrophic transformation of chondrocytes and the following matrix calcification, leading to endochondral ossification. Furthermore, since multiple BMPs, including BMP-2, BMP-6, BMP-7 and BMP-9 are known to promote osteogenic differentiation both *in vitro* and *in vivo* [253], we were intrigued to perform the conventional RT-PCR analysis of osteogenic lineage-specific genes to observe this pathway of differentiation. *Runx2*, a key osteogenic transcription factor related to osteoblast differentiation, evinced a stable expression level in all differentiating HDC, but exhibited a progressive decrease in c-C3H10T1/2 colonies. By comparison, expression of *Osx*, which is an essential osteoblast-specific transcription factor that is downstream of RUNX2, has a deranged pattern and a relatively weak signal in c-C3H10T1/2 HDC, but shows strong signals from day 3 in the mouse primary and b-C3H10T1/2

colonies *(Fig. 4.5.)*. On the other hand, chick primary cultures display a slow increase in *Osx* expression throughout the culturing period with the strongest band being identifiable on day 15. The pattern for *Col1a1* mRNA expression appears similar to that of *Runx2*; a substantial and constant expression was visible in primary and b-C3H10T1/2 colonies, while c-C3H10T1/2 cultures displayed a slightly more noticeable weakening in signal strength by the late stages of culturing. The mRNA expression of *late osteogenic markers, OC and OP*, reveals a disorganized pattern and weak expression in c-C3H10T1/2 HDC and increasing signal fortitude (especially in the case of OP) in mouse limb bud-derived and BMP-2 overexpressing colonies by the end of culturing. Chicken HDC, similarly to the case of *Osx*, display a steady expression, with a slight increase towards later phases of culturing. Another important marker of osteoblast activity is *AP*; it was completely undetectable in c-C3H10T1/2 micromass cultures, while a strong upregulation appeared in the other mouse models, which was biphasic with an even more pronounced elevation by day 15 in mouse limb bud HDC. At the same time in chicken HDC, the expression of *Ap* is marked in the early phase with an apparent decrease by day 10 of culturing.

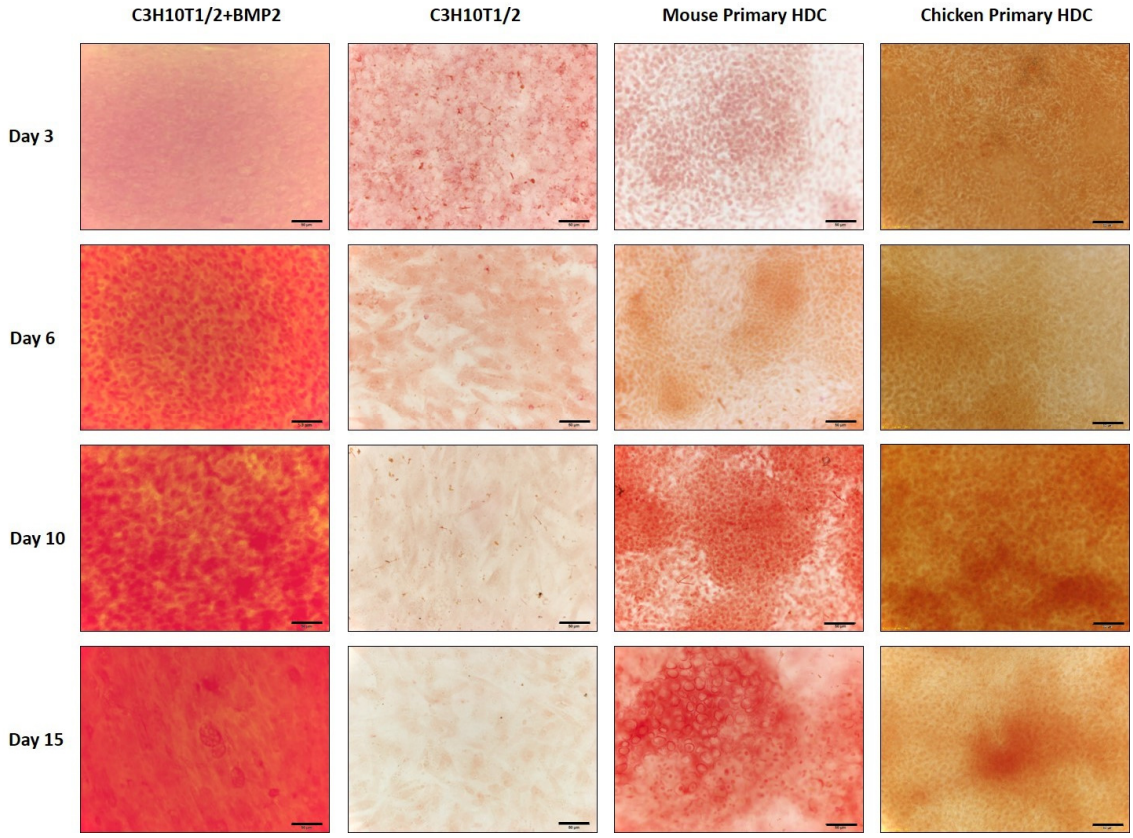

Fig. 4.4. Visualisation of calcified matrix accumulation in HDC on different culturing days with Alizarin Red staining. Original magnification was 40× for all photomicrographs. Scale bar: 50 µm. Extracellular matrix rich in calcium deposits correlate with orange-red areas of HDC. Presented images are representative photomicrographs of 3 independent experiments.

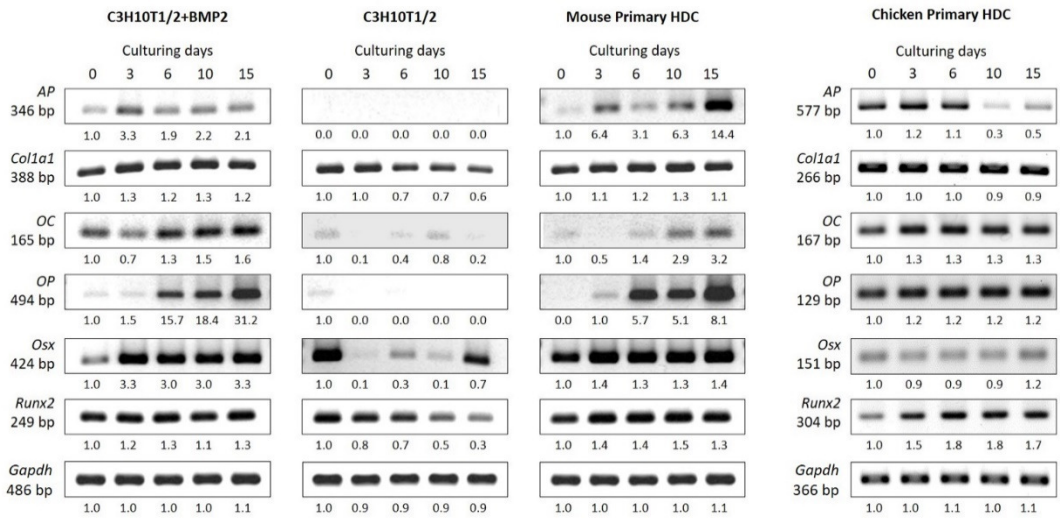

Fig. 4.5. Osteogenic marker gene mRNA expression patterns in cells of HDC on various days of culturing. *Runx2* and *Osx* constitute major osteogenic transcription factors; *Col1a1* codes for the main type of collagen in bone; osteocalcin (*Oc*) and osteopontin (*Op*) are signatures of late osteogenic development; alkaline phosphatase (*Ap*) marks osteoblast activity. *Gapdh* was used as a control. Integrated densities of signals established using ImageJ 1.46 are shown as numbers below gel images; data were normalized to the value detectable on the earliest day of culturing (making day 0 = 1.0, where applicable). Shown data are representative of 3 independent experiments.

4.1.4. Adipogenic Differentiation also Appears to Take Place in HDC

When investigating mesenchymal cells, other differentiation directions also demand consideration; adipogenesis being the primary option in this regard. **Oil Red O staining** procedure was applied to our chondrogenic models on specific days of culturing to observe whether they underwent adipogenic differentiation and started accumulating lipid droplets in their cytoplasm. Haematoxylin was co-applied with this formula to produce a nuclear staining that tags cells. Even by day 15 of culturing, limb bud-derived micromass cultures did not exhibit large lipid droplets *(Fig. 4.6.)*, only small ones that are consistent with the normal structure of chondrocytes [254]. The C3H10T1/2 cell line-based cultures, on the other hand, contained cells with Oil Red O-stained droplets of substantial size and number, particularly in the later phase of culturing. Even c-C3H10T1/2 HDC contained numerous adipocyte-like cells *(Fig. 4.6.)*, which is an unexpected result from an apparently non-differentiating model. To test whether the supposed accumulation of lipid droplets is an ongoing process in b-C3H10T1/2 micromass cultures, we have cultured them for an extended period and stained them after 25 days of culturing; large cells with multiple lipid droplets – likely precursors of white adipocytes – further increased in ratio, essentially outnumbering other cell types at the periphery and in the superficial layer over the center of these HDC (data not shown). Next, conventional RT-PCR analysis of adipogenic lineage-specific genes was performed to assess this aspect of differentiation (with the exception of *Pparγ2* in the chicken HDC model, for which, the mRNA sequence was unfortunately not available in any of the searched nucleotide databases: NCBI, DDBJ and EMBL-EBI). Adipocyte-specific *Fabp4* mRNA transcripts could be observed in all examined HDC, a marked upregulation was apparent

in both the b-C3H10T1/2 colonies and limb bud-derived HDC by the advanced phases of culturing *(Fig. 4.7.)*. Nevertheless, *Pparγ2*, an adipocyte-specific nuclear hormone receptor and key regulator of adipocyte differentiation showed little or no expression in all models except in the late stages of culturing of the b-C3H10T1/2 derived micromass cultures, where it exhibits a sudden and robust upregulation. This observation is in a good co-relation with our results obtained with Oil Red O staining *(Fig. 4.6.)* and the literature regarding possible adipogenic actions of BMP-2 [164].

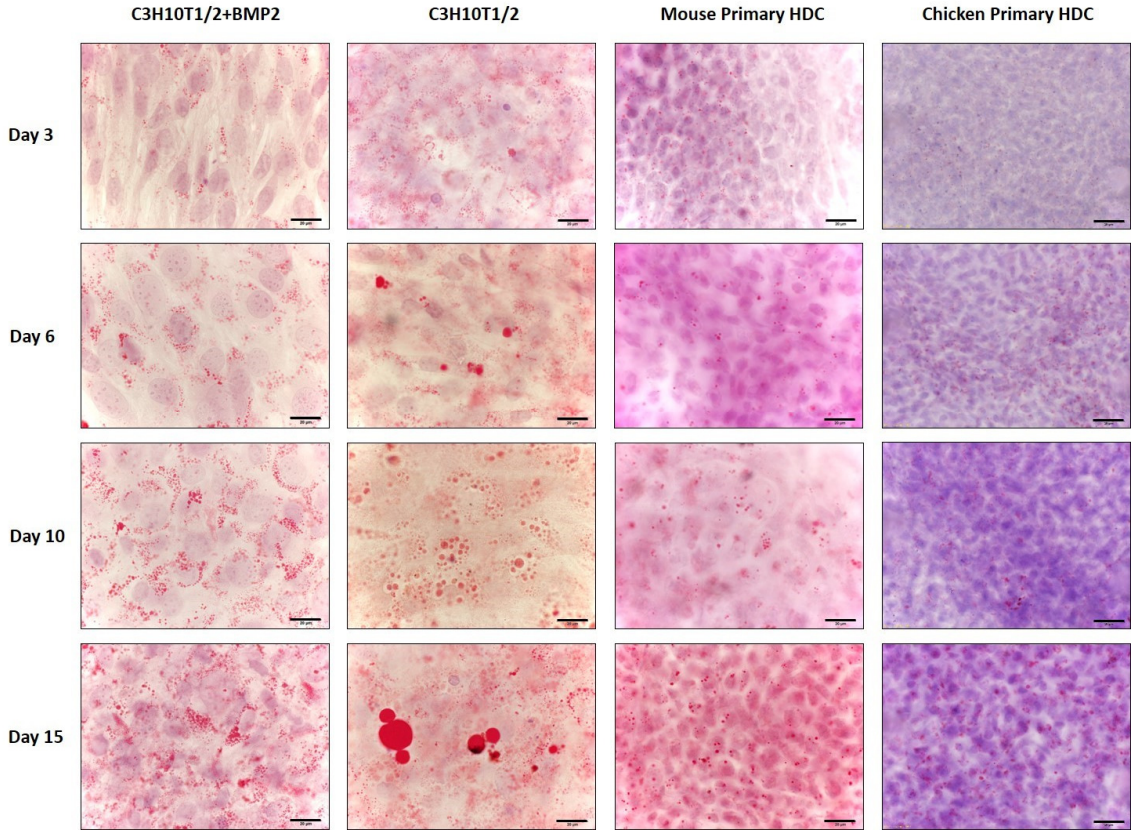

Fig. 4.6. Analysis of adipogenesis in micromass cultures on selected days of culturing following application of Oil Red O to selectively stain cytoplasmic lipid droplets in red color. Nuclear counterstaining with haematoxylin shows nuclei in blue color. Original magnification was 100× for all photomicrographs. Scale bar: 20 µm. Presented images are representative photomicrographs of 3 independent experiments.

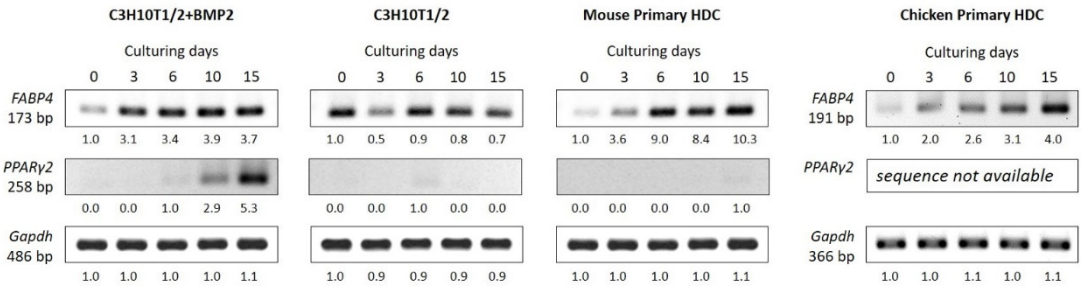

Fig. 4.7. Adipogenic marker gene mRNA expression patterns in micromass cultures on various culturing days. *PPARγ2* codes for a nuclear hormone receptor, which is a key regulator of adipocyte differentiation; *Fabp4* encodes a carrier protein for fatty acids primarily expressed in adipocytes and macrophages. *Gapdh* was used as a control. Integrated densities of signals established using ImageJ 1.46 are shown as numbers below gel images; data were normalized to the value detectable on the earliest day of culturing (making day 0 = 1.0, where applicable). Shown data are representative of 3 independent experiments.

4.1.5. Pluripotency Factors are Expressed in Micromass Cultures even at Later Stages

A further feature of significance is whether any of the cells in HDC persevere in a pluripotent state. Accordingly, we have evaluated the **mRNA expression patterns of key ESC genes – *Nanog*, *Sox2* and *Oct4*** (or in the case of the chick HDC model, its **avian homologue: *PouV***) – in our models *(Fig. 4.8.)*. *Oct4*, a homeodomain transcription factor that is essential to maintain self-renewal of ECSs, was not detectable in any of the mouse HDC samples. Nevertheless, *PouV* appeared distinctly in the avian model, displaying a firmly decreasing tendency towards later stages of culturing. However, *Nanog* and *Sox2* were identifiable in all mouse models and demonstrated mixed expression sequences. *Sox2* was found to be expressed in BMP-2 overexpressing cultures and in both limb bud-derived HDC at moderate levels in the beginning of culturing, but became downregulated as differentiation advanced with a modest rise at day 15 in mouse primary HDC. Meanwhile, *Nanog* underwent a robust upregulation in mouse differentiating models, especially in the BMP-2 overexpressing HDC, with no detectable expression in the avian colonies. Ultimately, in the case of c-C3H10T1/2 micromass colonies, we could not determine a definite expression pattern for any of these markers.

Fig. 4.8. Temporal pattern of mRNA expression of pluripotency markers during micromass culturing. *Oct4* (or *PouV* in the avian model), *Nanog* and *Sox2* are key genes essential to maintain self-renewal and pluripotency in ESCs. *Gapdh* was used as a control. Integrated densities of signals established using ImageJ 1.46 are shown as numbers below gel images; data were normalized to the value detectable on the earliest day of culturing (making day 0 = 1.0, where applicable). Shown data are representative of 3 independent experiments.

4.2. Investigating Ca^{2+} Signaling Processes that Maintain the Ca^{2+} Oscillations in Differentiating Chick HDC

4.2.1. Cells of Differentiating Chick HDC Display Rapid Spontaneous Ca^{2+} Oscillations

LIVE confocal microscopy was combined with Fluo-4 fluorescent Ca^{2+} imaging technique to study spontaneous repetitive transient cytosolic Ca^{2+} concentration increases of single cells of embryonic chick limb bud-derived HDC on days 1 and 2 of culturing. Due to the heterogeneous cellular nature of these cultures (muscle progenitors and epithelial cells are also present, but with morphology, which differs from the main osteochondroprogenitors that are round shaped [195]), only spherical cells were involved in our measurements. On days 1 and 2 of culturing, we have recorded series of X-Y images of randomly selected visual fields of Fluo-4-loaded chondrifying cultures. Cell cultures were kept at room temperature in agonist-free Tyrode's solution containing 1.8 mM Ca^{2+} to document the Ca^{2+} oscillations. *Fig. 4.9.* presents four representative X-Y images that were recorded at 6.5, 18.3, 29.6 and 54.4 s from cells of a Fluo-4-loaded culture during measurements on day 2 of culturing. The detected oscillations comprised a wide spectrum of amplitude and frequency *(Fig. 4.9.)*. While on day 1 of culturing, 45 of the 240 studied cells (19%) displayed spontaneous Ca^{2+} oscillations, by day 2, the fraction of cells to exhibit transient increases in cytosolic Ca^{2+} concentration presented an ample escalation to 55% (175 of 317 cells) *(Fig. 4.10.)*. Naturally, parameters other than the pure percentage of oscillatory cells demonstrated significant modifications concurrently with the progress of chondrogenesis *(Fig. 4.10.)*. Although the frequency of oscillations manifested a significant decrease by day 2 (0.06 ± 0.003 Hz; n = 175) when compared to day 1 (0.08 ± 0.01 Hz; n = 45; P = 0.01) *(Fig. 4.10.)*, the mean amplitude of these transient cytoplasmic Ca^{2+} concentration changes increased significantly as differentiation progressed from day 1 (expressed as F/F0: 0.97 ± 0.11; n = 45) to day 2 (1.27 ± 0.06; n = 175; P = 0.03) *(Fig. 4.10.)*. The values of full time at half maximum (FTHM), the

parameter tested in order to characterize the extent of individual spontaneous transients did not show significant difference between the two investigated culturing days (2.37 ± 0.29 s; n = 45 on day 1 vs. 2.57 ± 0.15 s; n = 175 on day 2; P = 0.55) *(Fig. 4.10.)*.

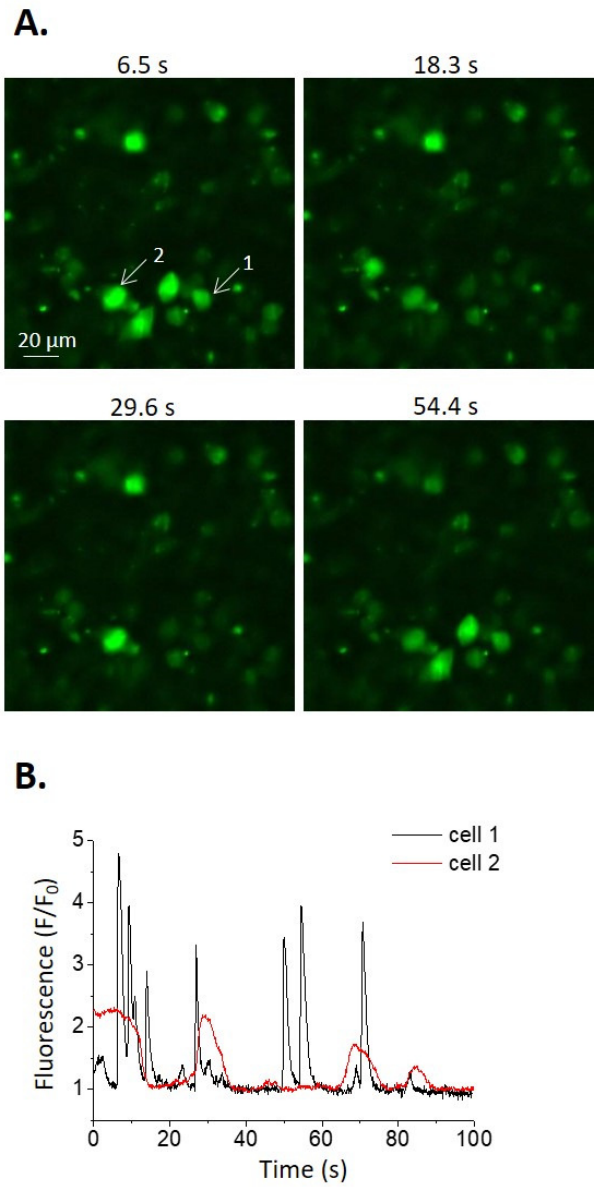

Fig. 4.9. Cells of primary chick micromass cultures display spontaneous Ca^{2+} oscillations on day 2 of culturing. Prior to measurements, cells were loaded with Fluo-4-AM for 30 min Ca^{2+} oscillations were observed without agonist stimulation in Tyrode's solution containing 1.8 mM Ca^{2+} at room temperature. (A) Series of X-Y images display Fluo-4-AM-loaded cells from random visual fields of chondrifying cultures recorded with Zeiss LIVE 5 Laser Scanning Confocal Microscope. Four representative frames were acquired during measurements at 6.5, 18.3, 29.6 and 54.4 s. Chondrogenic cells with repetitive intracellular Ca^{2+} oscillations are marked by arrows. (B) Chart showing fluorescence intensities of the cells indicated by arrows in panel (A). Fluo-4 fluorescence intensity values normalized to baseline fluorescence (F/F0) are plotted against time. A wide range of frequency and amplitude was observed in the culture.

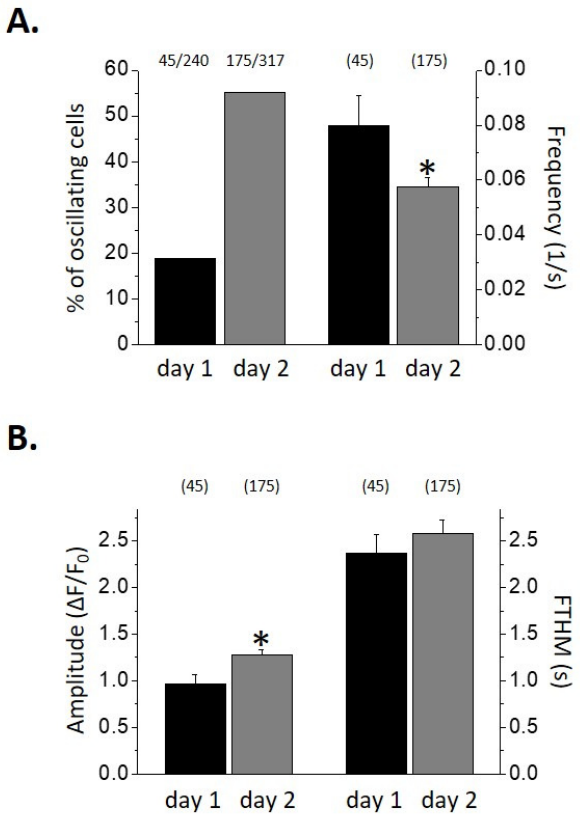

Fig. 4.10. Pooled data of Ca^{2+} oscillations acquired from random visual fields of Fluo-4-loaded chick HDC on culturing days 1 and 2. Data were obtained from series of X-Y images recorded with Zeiss LIVE 5 Laser Scanning Confocal Microscope. (A) Oscillatory cell ratio and frequency (s^{-1}) of Ca^{2+} transients on days 1 and 2 of culturing. Numbers above bars express the number of oscillating cells against all recorded cells. (B) Detailed parameters of day 1 and 2 Ca^{2+} oscillations (amplitude and full time at half maximum (FTHM)) in chondrogenic cells of chicken HDC. In all cases, while considering the parameters of Ca^{2+} oscillations, only round, chondroblast-like oscillating cells were analyzed. Measurements were carried out on cultures from 4 independent experiments. Data represent mean ± standard error of the mean (SEM). Numbers in brackets above graphs indicate the number of cells analyzed. Asterisks (*) mark significant differences (*P < 0.05) between measured parameters.

4.2.2. Ca^{2+} Oscillations are Transformed by the Modification of Extracellular Ionic Milieu and/or the Application of Ca^{2+} Entry Blockers

Next, we have studied the properties of spontaneous Ca^{2+} oscillations in 2-days-old cultures by registering X-Y image series. After appointing a random visual field of oscillatory cells, we started collecting frames under control conditions at the 0 time mark (the medium was normal Tyrode's solution containing 1.8 mM Ca^{2+}), then following the addition of the test solutions (either 10 µM nifedipine, or 500 µM $LaCl_3$ and 1 µM YM-58483), further frames were collected 1, 3 and 5 min into the treatment. Normal Tyrode's solution was not changed throughout the collection of frames at time points 0, 1, 3 and 5 min into the measurement on random visual fields of cultures. As all of the examined parameters of Ca^{2+} oscillations (namely, ratio of oscillating cells, amplitude and frequency of oscillations) underwent a progressive deterioration throughout the 5 min observation period regardless of the addition of test solutions, every single parameter was normalized to the control value

(data not shown) obtained at the same time point. Treatment with 10 µM nifedipine, an effective dose of the dihydropyridine L-type Ca^{2+} channel blocker did not induce a compelling shift in the percentage of oscillatory cells in comparison to control values recorded at 3- and 5-min time points (80.93 ± 25.78% [P = 0.56]; and 91.73 ± 28.95 [P = 0.84], respectively; n = 43 for all time points) *(Fig. 4.11.)*. The effects of nifedipine treatment were similarly insignificant on the amplitude of oscillations (87.58 ± 11.89% [P = 0.5]; 69.44 ± 10.26% [P = 0.16] and 75.83 ± 6.26% [P = 0.13] at 1-, 3- and 5-min time points; n = 25, 16 and 11, respectively) *(Fig. 4.11.)*. However, the frequency of Ca^{2+} oscillations was found to be reduced by the same inhibitor; we have identified a significant divergence from control values at the 3-min time point (53.97 ± 8.52% [P = 0.01] and 64.46 ± 12.88% [P = 0.15] at 3- and 5-min time points; n = 16 and 11, respectively) *(Fig. 4.11.)*. The above-described results suggest that the main parameter of oscillations influenced by nifedipine is their frequency, the other factors, namely, the ratio of oscillating cells and the amplitude of these transients are nearly unaffected. These observations suggest that VDCCs are possibly influential, but likely not the main mediators of oscillations. SOCE blockers, on the other hand, caused a significant decline compared to control values at all three time points in the proportion of oscillatory cells (11.59 ± 6.95% [P = 0.0006]; 23.05 ± 13.58% [P = 0.008] and 0.0% [P = 0.0] at 1-, 3- and 5-min time points, respectively; n = 29 for all time points) *(Fig. 4.11.)* and most importantly, no Ca^{2+} transients were observable in any of our random visual fields after 5 min. Furthermore, we have detected a simultaneous reduction in the amplitudes (45.35 ± 7.53% [P = 0.24] and 58.33 ± 12.85% [P = 0.34] at 1- and 3-min time points; n = 2 and 3, respectively) *(Fig. 4.11.)* and at the 3-min time point, in the frequency of the Ca^{2+} oscillations (45.45 ± 22.72% [P = 0.13]; n = 3) *(Fig. 4.11.)*. Following the above observations that imply the definitive role of ER Ca^{2+} stores in the regulation of these repetitive transients in cells of chondrogenic chick HDC, the next logical step was to further dissect the effects of SOCE blockers and Ca^{2+} free extracellular milieu on line-scan charts with a higher temporal resolution. Exclusively round-shaped chondrogenic cells with conspicuous repetitive Ca^{2+} transients were considered for the following evaluation. Line-scan images were registered from 2-days-old cultures maintained in normal Tyrode's solution *(Fig. 4.12.)*. The acquired value of the frequency and the amplitude of oscillations in the 46 cells investigated was 0.08 ± 0.007 Hz and 1.44 ± 0.15, respectively. Control measurements were followed by the replacement of the bath solution with the test solutions, after the addition of $LaCl_3$ and YM-58483, Ca^{2+} oscillations ceased (n = 10). In addition to terminating transients, SOCE blockers also induced a serious disturbance in cytoplasmic Ca^{2+}; arrhythmic fluctuations with a small amplitude replaced the regular Ca^{2+} oscillations. As a consequence, we could not establish a numerical analysis of these phenomena *(Fig. 4.12.)*. The co-application of the SERCA-blocker CPA with SOCE blockers to study their effects on cells with depleted ER Ca^{2+} stores led to the prompt abolishment of Ca^{2+} oscillations (n = 10); we could not detect changes in cytosolic Ca^{2+} levels even with Ca^{2+} being present in the extracellular space *(Fig. 4.12.)*. In

Ca^{2+}-free Tyrode's solution the oscillating cells (n = 10) displayed a progressive decline in the amplitudes of their oscillations; it is evident from the representative line-scan chart *(Fig. 4.12.)* that the repetitive Ca^{2+} transients have disappeared 3 min after the replacement of normal Tyrode's solution with its Ca^{2+}-free version.

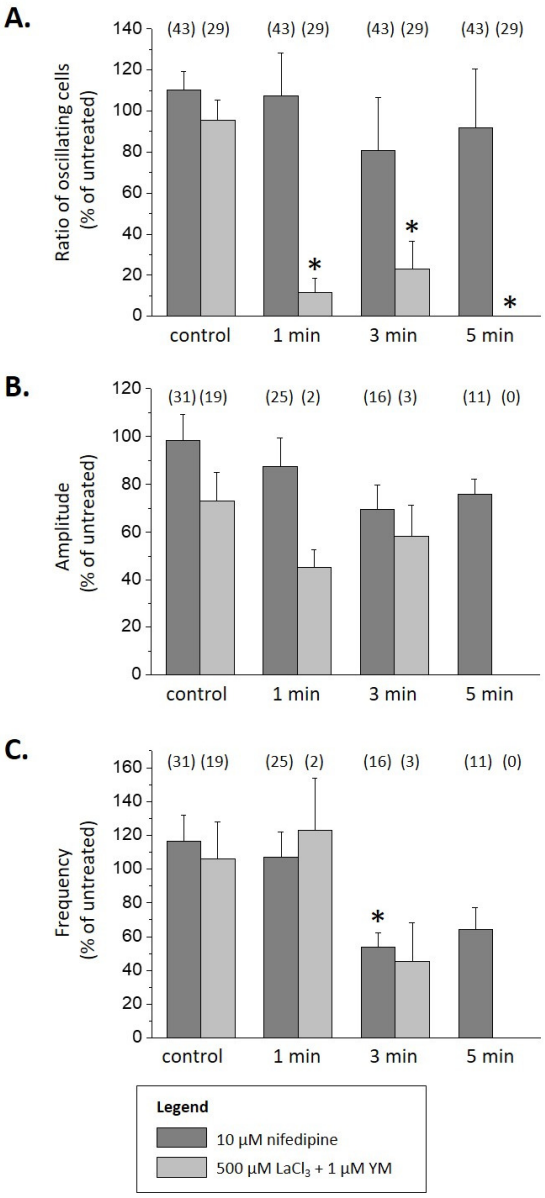

Fig. 4.11. Mean values (± SEM) of parameters describing Ca^{2+} oscillations in response to various treatments. Data were obtained from series of X-Y images acquired during measurements with Zeiss LIVE 5 Laser Scanning Confocal Microscope from Fluo-4-loaded HDC. At each time point and visual field, a total number of 500 images were recorded with a frame acquisition rate of 10 s^{-1}. (A) Oscillatory cell ratio under control conditions and 1, 3 or 5 min after blockade of VDCC or SOCE. Values were normalized to untreated cells measured at identical time points. Numbers in brackets above bars show the number of cells analyzed. (B) Amplitude of Ca^{2+} oscillations normalized to those of untreated cells. Numbers in brackets above bars show the number of oscillating cells analyzed. (C) Frequency of Ca^{2+} oscillations normalised to the control. Numbers in brackets above bars show the number of cells analyzed. In all cases, chondrogenic oscillatory cells of the corresponding random visual field were recorded at each time point. Individual HDC were used for a single series of measurements. Combined data from measuring random visual fields of 5 colonies in each of 3 independent experiments are displayed in the graphs. Asterisks (*) indicate significant differences (*P < 0.05) between measured parameters of treated cells against control ones at specific time points.

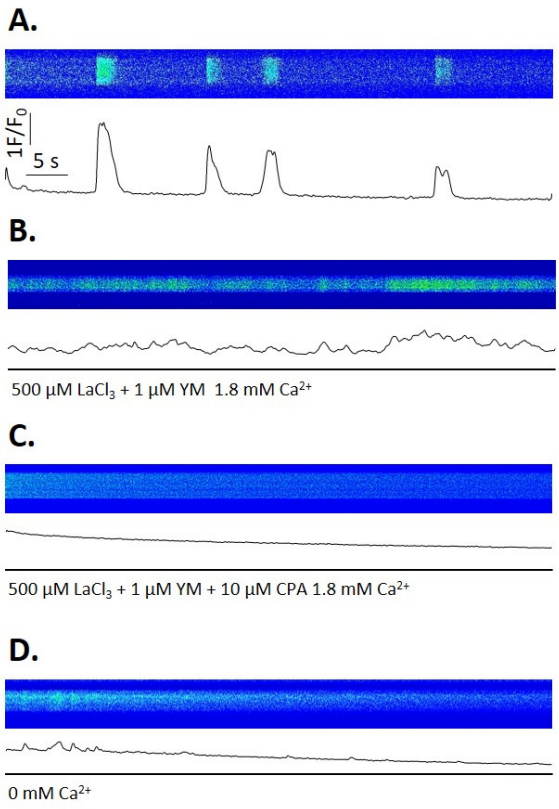

Fig. 4.12. Effects of pharmacological intervantions and altered extracellular ionic milieu on spontaneous Ca^{2+} oscillations of Fluo-4 loaded chondrogenic cells of 2-day-old chick HDC. Each panel contains representative confocal line-scan images and timelines of Fluo-4 fluorescence intensities; all traces in panels (A)-(D) share the same horizontal and vertical calibrations. Horizontal lines under traces display the span of either pharmacon treatments or altered extracellular ionic composition. Acquisition of line-scan images directly followed changing of the bath solution on the cultures. Prior to changing solutions, baseline functions were detected in every case. (A) Spontaneous Ca^{2+} oscillations in normal ($[Ca^{2+}]_e$ = 1.8 mM) Tyrode's solution. (B) Application of SOCE blockers in normal ($[Ca^{2+}]_e$= 1.8 mM) Tyrode's caused Ca^{2+} oscillations to cease, however, irregular changes in basal cytosolic Ca^{2+} concentration persisted. (C) The co-administration of the SERCA-blocker CPA (10 µM) with SOCE blockers in normal Tyrode's eliminated Ca^{2+} oscillations completely. (D) No periodic Ca^{2+} oscillations were detected 3 min after changing the bath solution to Ca^{2+}-free Tyrode's. The displayed line-scan diagrams are representative data of 4 independent experiments.

4.2.3. Components of the CRAC and the VDCC Pore-Forming Subunit are Expressed in Cells of Chick HDC

Based on our above findings regarding the lowering effects of nifedipine on the frequency of repetitive Ca^{2+} oscillations, plus previous results where the addition of 120 mM KCl stimulated large Ca^{2+} transients in the same model [195], we decided to map the expression of VDCCs in differentiating chondrocytes. Although functional VDCCs are composed of a diverse set of subunits, the Ca^{2+} selective pore-forming α_1 subunit has a principal role in governing the character of the assembled channel.

Accordingly, using the NIH genetic sequence database, GenBank we downloaded available mRNA sequences of chicken VDCC subtype α_1 subunits, and used each type to design specific primer pairs with Primer Premier 5.0 software (Premier Biosoft, Palo Alto, CA, USA) and carry out RT-PCR reactions. We were able to identify specific bands in the case of certain L- (*$Ca_V1.2$* and *$Ca_V1.3$*), R- (*$Ca_V2.3$*) and T-type (*$Ca_V3.1$*, *$Ca_V3.2$* and *$Ca_V3.3$*) ion channel subunits. In the case of L-type α_1 subunits *$Ca_V1.2$* exhibited a steady and robust level of expression, whereas *$Ca_V1.3$* displayed a peak-like pattern, as signals on culturing days 2-4 were practically 5 times as strong as in the beginning of this period *(Fig. 4.13.)*. At the same time, *$Ca_V2.3$*, the R-type subunit showed a progressive weakening of the band representing its mRNA expression to almost zero levels suggesting little to no role for this subtype in mature chondrocytes. Peculiarly, T-type VDCC subunits adhered to a similar mRNA expression figure to that of L-type ion channels; we have revealed a relatively stable expression in case of *$Ca_V3.1$* and *$Ca_V3.2$* with a slight downregulation (especially for *$Ca_V3.2$*) by day 6 of culturing, while *$Ca_V3.3$* showed elevated signal levels specifically during the days of differentiation (days 2-4) *(Fig. 4.13.)*. As the next connected step, we turned our attention to identifying VDCC α_1 subunit expression at the protein level. We were able to identify immunoreactive bands at the anticipated molecular mass (approx. 130 kDa) following the application of an anti-Ca_Vpan α_1 subunit polyclonal antibody. The level of expression remained robust for the entire culturing period in the chondrogenic HDC lysates *(Fig. 4.13.)*. Ultimately, we can conclude that the body of our results from Ca^{2+} imaging, RT-PCR and western blot experiments provide a stable foundation to confirm the functional expression of VDCCs in differentiating HDC. Identification of the precise roles played by specific subtypes requires further research.

In parallel with investigating VDCCs, we also started the characterization of CRAC subunits. Even though ORAI1 and STIM1 have been known as essential components of the CRAC for over a decade [255], there is no available data regarding their expression and function in mature chondrocytes. It is notable that since our results obtained from developing cartilage (described below) have been published, a Japanese research group revealed abundant expressions of ORAI1, ORAI2 and STIM1 proteins in a human chondrosarcoma cell line (OUMS-27) [256]. We were able to observe a stable expression pattern during the whole culturing period in the case of *Orai1*, *Stim1* and *Stim2* mRNA *(Fig. 4.13.)*, which is a definite indication of their fundamental role in the Ca^{2+} homeostasis of chondrogenic HDC. In addition, we could also validate the constant protein expression order of STIM1 throughout the complete culturing period from HDC total cell lysates with elevated levels represented by the bands at important days of differentiation *(Fig. 4.13.)*. Unfortunately, the identity of the upper immunogenic band at ~85 kDa can only be speculated. Protein BLAST search for the previously mentioned 114-amino-acid-long human STIM1 sequence against the chicken protein sequence database suggests that in addition to STIM1 (with a molecular weight of ~70 kDa), STIM2 (its predicted isoform X1 weighs ~83

kDa in chick) may also be recognized by the same antibody, as there are multiple regions where identical or chemically highly similar 6-amino-acid-long sequences exist in both the query and these hits. It is also noteworthy that the search resulted in no other hits than STIM1 and two predicted STIM2 isoforms. We could not perform western blot analysis in the case of ORAI1 on account of the lack of commercially available chicken-specific antibodies for this protein.

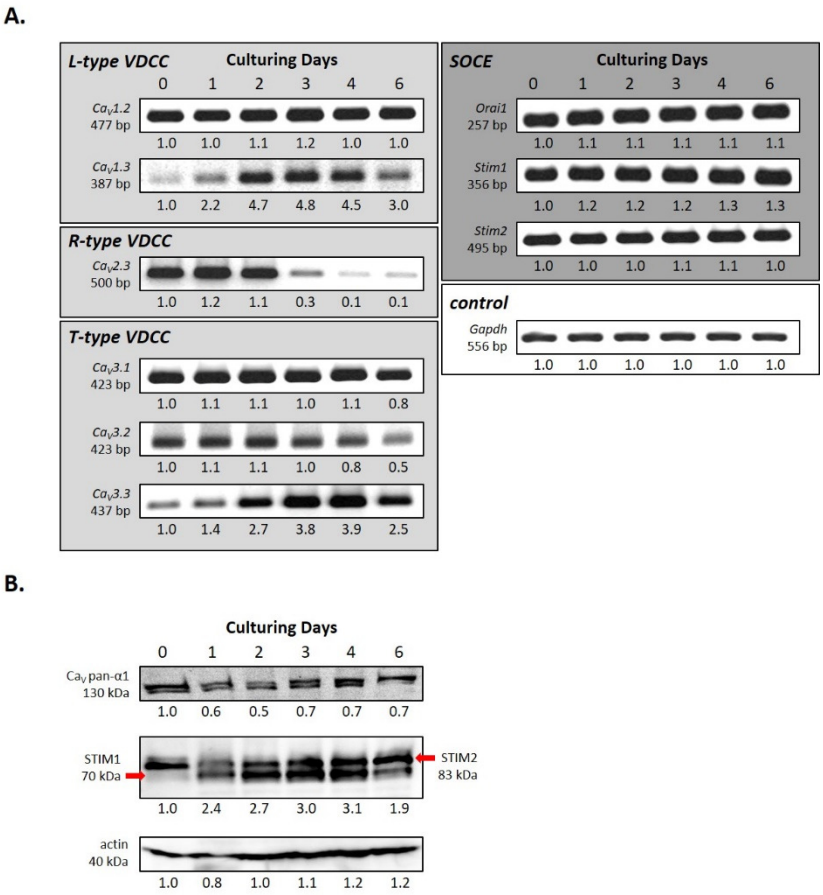

Fig. 4.13. Temporal expression pattern of selected key molecules of Ca^{2+} homeostasis. (A) VDCC α_1 subunit mRNA expression detected by RT-PCR. (B) mRNA and protein-level expression profiles of key organizers of the SOCE mechanism and protein expression of the Ca^{2+} selective pore-forming α_1 subunit of VDCCs on various days of culturing, detected by RT-PCR and western blot, respectively. In the STIM1 immunoblot, the lower band represents the expected (70 kDa) molecular weight of STIM1 (marked by arrow on the left side of figure), while the upper band (~83 kDa) is predicted to correspond to STIM2 (marked by arrow on the right side of figure). *Gapdh* was used as internal reaction control for PCR reactions shown in both panels (only shown in panel B), while β-actin served as control for western blots. Integrated densities of signals established using ImageJ 1.46 are shown as numbers below gel images; data were normalized to the value detectable on the earliest day of culturing (making day 0 = 1.0, where applicable). Shown data are representative of 3 independent experiments.

4.2.4. Precise Operation of VDCCs and SOCs is Required for Chondrogenesis of the Experimental Model

Afterwards, we were interested in the cartilage matrix production-related long-term responses to the effective dose of nifedipine (applied continuously from day 1) or SOCE inhibition combined with ER Ca^{2+} store depletion (by 500 µM $LaCl_3$, 1 µM YM-58483 and 10 µM CPA administered on day 2 for

24 h). Notably, combined treatments including ER Ca^{2+} store depletion and SOCE blockers that lasted longer than 24 h completely inhibited cartilage formation (data not shown). As we were interested in the consequences of SOCE inhibition on the differentiation step of chondroprogenitor cells, we have chosen day 2 to determine this effect. Metachromatic staining procedures displayed a seriously abated cartilage matrix production by day 6 of culturing in the case of continuous nifedipine treatments *(Fig. 4.14.)*. A similarly noticeable inhibition of chondrogenesis was observed following only 24 hours of ER Ca^{2+} store depletion along with the application of SOCE blockers on culturing day 2 *(Fig. 4.14.)*; a clear **indication of the importance of both plasma membrane Ca^{2+} entry pathways and Ca^{2+} release from the internal stores in the biology of chondrogenic cells**. Next, we harvested day 3 samples to investigate the effects these treatments had on mRNA and protein expression of basic chondrogenic markers. The mRNA expression of *Col2a1* and *Acan*, as well as the protein expression and phosphorylation status of SOX9 were analyzed by RT-PCR and western blot methods, respectively. Nifedipine did not cause any significant alteration in the mRNA expression of the monitored genes, however, we could detect a notable reduction in SOX9 protein expression without considerable decrease in the amount of its phosphorylated form *(Fig. 4.14.)*. On the other hand, combined inhibition of SOCE with ER Ca^{2+} store depletion was found to distinctly diminish ECM component mRNA expression without a similar effect on *Sox9* transcript levels *(Fig. 4.14.)*. SOX9 responded similarly at the protein level as in the case of nifedipine treatments; its total protein levels decreased to approximately half of the control amount, but the quantity of phospho-SOX9 remained almost completely unmodified *(Fig. 4.14.)*. These observations suggest that – at least to a certain extent – a decreased amount of SOX9 protein is capable of producing the detected amount of the active, phosphorylated isoform, which is necessary to maintain its function. Therefore, the changes in the ECM gene expression are likely to be the consequence of an at least partly SOX9-independent pathway. As our treatments are – in addition to their previously discussed effects – inclined to alter the metabolic activity and/or the cell cycle of differentiating chondrocytes, we have carried out MTT tests and ^{3}H-thymidine incorporation assays on day 3 to measure their mitochondrial activity and rate of proliferation, respectively. Notably, none of our tested treatments (10 µM nifedipine or the combination of 500 µM LaCl3, 1 µM YM-58483 and 10 µM CPA) caused a significant shift in the results of the metabolic activity assay, but almost completely inhibited cell proliferation *(Fig. 4.14.)*. Therefore, we must note that the compelling inhibition of cell proliferation needs to be considered as a significant part of our observed long-term responses.

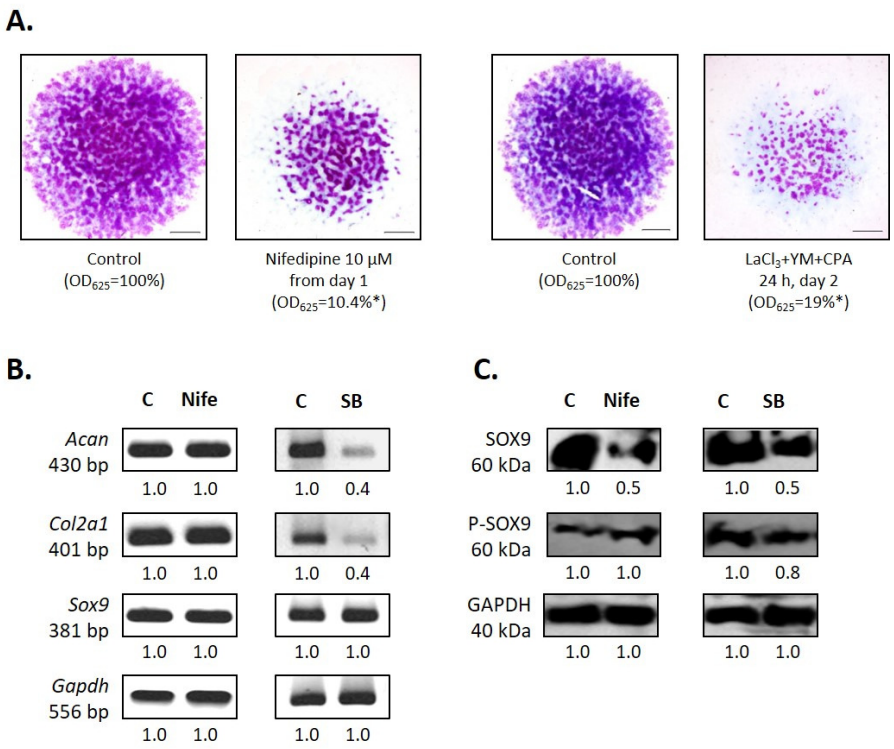

Fig. 4.14. Effects of continuous treatment (from day 1) with the L-type VDCC blocker nifedipine and the response to combination of SOCE blockers with SERCA inhibition (added on day 2 for 24 h) on cartilage ECM production *in vitro*. (A) Metachromatic cartilage areas on day 6 of culturing in HDC visualized with 0.1% DMMB dissolved in 3% acetic acid (pH 2.52). Original magnification was 2× for each photomicrograph. Scale bar: 1 mm. Purple areas coincide with cartilage matrix rich in sulphated GAGs. Presented images are representative photomicrographs of 3 independent experiments. Absorbance (OD625) was measured from supernatants of 6-day-old cultures containing toluidine blue extracted with 8% HCl dissolved in absolute ethanol. (B) RT-PCR analysis of mRNA transcripts of key chondrogenic and ECM marker genes on day 3. *Gapdh* was used as internal reaction control. (C) SOX9 protein expression and phosphorylation status in 3-day-old cultures. GAPDH was used as a control. (D) Mitochondrial enzymatic activity and proliferation rate in day 3 chick HDC detected by MTT test and ^{3}H-thymidine incorporation assays, respectively. Statistically significant (*$P < 0.05$) differences between absorbance (OD625) or in rate of proliferation are marked by asterisks (*). Abbreviations used for panels (B)-(D): C, control; Nife, nifedipine; SB, SOCE blockers combined with CPA. Shown data are representative of 3 independent experiments.

4.2.5. Inhibition of Septin Rearrangement Deteriorates Chondrogenic Differentiation of Chick HDC

For a different approach that targets SOCE [2] in order to corroborate other results suggesting the importance of SOCE in the process of chondrogenic differentiation, we have tested the effects of

FCF treatment – without depleting the intracellular Ca^{2+} stores – on the proliferation, mitochondrial activity, cartilage extracellular matrix production and chondrocyte-specific marker gene mRNA expression of chicken limb bud cultures. To investigate the consequences of SOCE inhibition on not only the differentiation step of chondroprogenitor cells, but also during the preceding proliferation stage, we have applied 24 h FCF treatments on day 1 or 2 on separate cultures to determine the response. Prior to pharmacological modulations targeting septins, we have verified the mRNA expression of relevant septin types according to literature [2] in chick chondrogenic HDC by conventional RT-PCR experiments (data not shown). Metachromatically stained colonies displayed a definite decrease in cartilage matrix production by day 6 of culturing in the case of both treatment timings, with 24 hours of FCF treatment on day 1 consistently resulting in a more prominent reduction compared to the respective vehicle control *(Fig. 4.15.)*. To determine whether our treatment also exerts an effect on cartilage ECM formation via altering mitochondrial metabolic activity and/or the proliferation of chondrogenic cells, we have carried out MTT tests and ^{3}H-thymidine incorporation assays directly after the treatments to measure their mitochondrial activity and rate of proliferation, respectively. Interestingly, both treatment timings resulted in a significantly increased mitochondrial metabolic activity, but similarly to previous SOCE inhibition experiments, the rate of proliferation displayed a dramatic decrease. According to ^{3}H-proline incorporation assays, collagen synthesis also declined significantly in both groups compared to their respective vehicle controls, further suggesting that the decreased amount of cartilage-specific ECM is not the consequence of altered mitochondrial activity, but presumably has a strong tie to cell proliferation *(Fig. 4.15.)*. However, it is noteworthy that on both treatment days, the drop in proliferation rate is larger than that of collagen synthesis, which suggests the lack of linear relationship between the number of cells and the amount of produced collagen.

Relative gene expression levels of chondrogenic (*Sox9*, *Col2a1*, *Acan* and *Halpn1*) and pluripotency (*PouV*) marker genes and SOCE-mediating molecules (*Orai1*, *Stim1* and *Stim2*) were monitored following 24 hours of FCF treatment on day 1 or day 2 of culturing *(Fig. 4.15. and 4.16.)*. On both days, FCF caused a marked decrease in the expression of all investigated chondrogenic marker mRNAs when compared with respective solvent control levels. Following treatments, all examined markers reached only approximately 20% of their mRNA expression observed in the control group. On the other hand, *Stim1* mRNA levels only slightly decreased after FCF treatment – on day 2 in particular – only *Stim2* expression demonstrated a robust level of suppression following application of the pharmacon on day 2. Furthermore, *Orai1* expression remains almost unaltered following FCF treatment on day 1, but a strong elevation is caused by the same pharmacological modulation on day 2. At the same time, the major investigated pluripotency marker, *PouV*, is substantially upregulated in

both cases, but, the relative increase is even more prominent on day 2, when most of the differentiation is expected to take place.

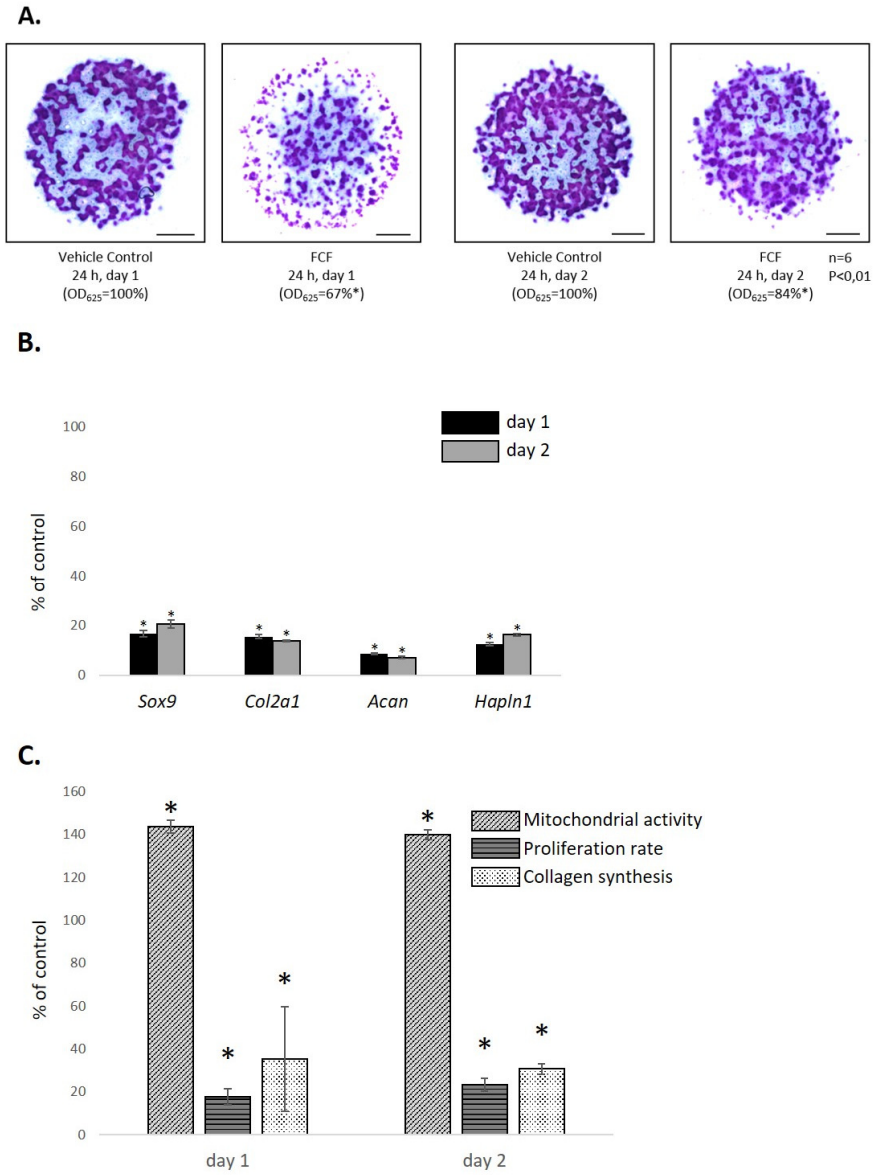

Fig. 4.15. Effects of inhibition of septin reorganization by treatment with 200 µM FCF (added on day 1 or 2 for 24 h) on various aspects of *in vitro* chondrogenesis. (A) Metachromatic cartilage areas in 6-day-old high density colonies visualized with 0.1% DMMB dissolved in 3% acetic acid (pH 2.52). Original magnification was 2× for each photomicrograph. Scale bar: 1 mm. Purple areas represent cartilage matrix rich in sulphated GAGs. Presented images are representative photomicrographs of 3 independent experiments. Absorbance (OD625) was measured from supernatants of 6-day-old cultures containing toluidine blue extracted with 8% HCl dissolved in absolute ethanol. (B) Relative mRNA expression levels of the chondrogenic marker genes *Sox9*, alpha-1 chain of type II collagen (*Col2a1*), core protein of aggrecan (*Acan*) and hyaluronan and proteoglycan link protein (*Hapln1*) immediately after 24 h treatments starting on days 1 or 2 using RT-qPCR. Relative gene expression levels were normalized to *Rplp0* (60S acidic ribosomal protein P0). (C) Mitochondrial enzymatic activity, proliferation rate and collagen synthesis in chick HDC immediately after 24 h treatments starting on days 1 or 2 detected by MTT test, ^{3}H-thymidine or ^{3}H-proline incorporation assays, respectively. Statistically significant (*P < 0.05) differences between gene expression levels, absorbance (OD625) and rate of proliferation or collagen synthesis are marked by asterisks (*).

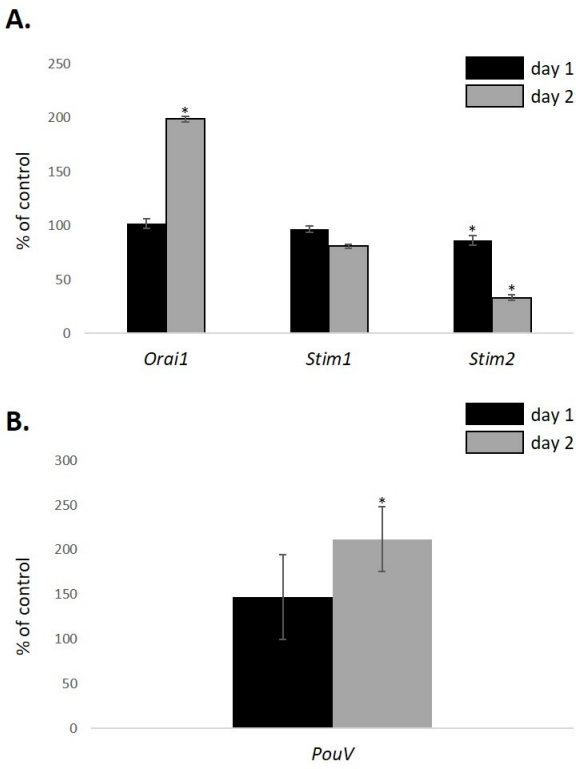

Fig. 4.16. Effects of inhibition of septin reorganization by treatment with 200 µM FCF (added on day 1 or 2 for 24 h) on mRNA expression of SOCE-related genes and a major factor of pluripotency. (A) *Orai1* codes for the pore-forming subunit of the CRAC and *Stim1* for the main Ca^{2+} sensor of the ER. (B) *PouV* is the avian homologue of *Oct4*, a key gene which is essential to maintain self-renewal and pluripotency in ESCs. Statistically significant (*P < 0.05) differences between gene expression levels are marked by asterisks (*).

4.2.6. Fluorescent Single Cell Ca^{2+} Measurements Demonstrate Reshaped SOCE Characteristics Following Combined Application of $LaCl_3$ and YM-58483

Fluorescent intracellular Ca^{2+} assessments were carried out with Fura-2-loaded colonies on day 2 of culturing to determine the parameters of generated SOCE Ca^{2+} transients without *(Fig. 4.17.)* and with the addition of SOCE blockers (500 µM $LaCl_3$ and 1 µM YM-58483) *(Fig. 4.17.)*. We have depleted the internal Ca^{2+} store of each cell at the beginning of measurements by pre-treatment with the CPA (10 µM) dissolved in Ca^{2+}-free Tyrode's bathing solution (data not shown), then re-established the normal extracellular Ca^{2+} concentration (1.8 mM) and recorded the resulting changes in cytosolic Ca^{2+} concentration of individual cells. A significant reduction could be seen in the presence of SOCE blockers in both the amplitude (114.4 ± 15.6; n = 16 vs. 58.4 ± 5.6; n = 10; P = 0.01) *(Fig. 4.17.)* and the maximal rate of rise (3.9 ± 0.5; n = 16 vs. 1.5 ± 0.2; n = 10; P = 0.001) *(Fig. 4.17.)* of the transient when compared to control values.

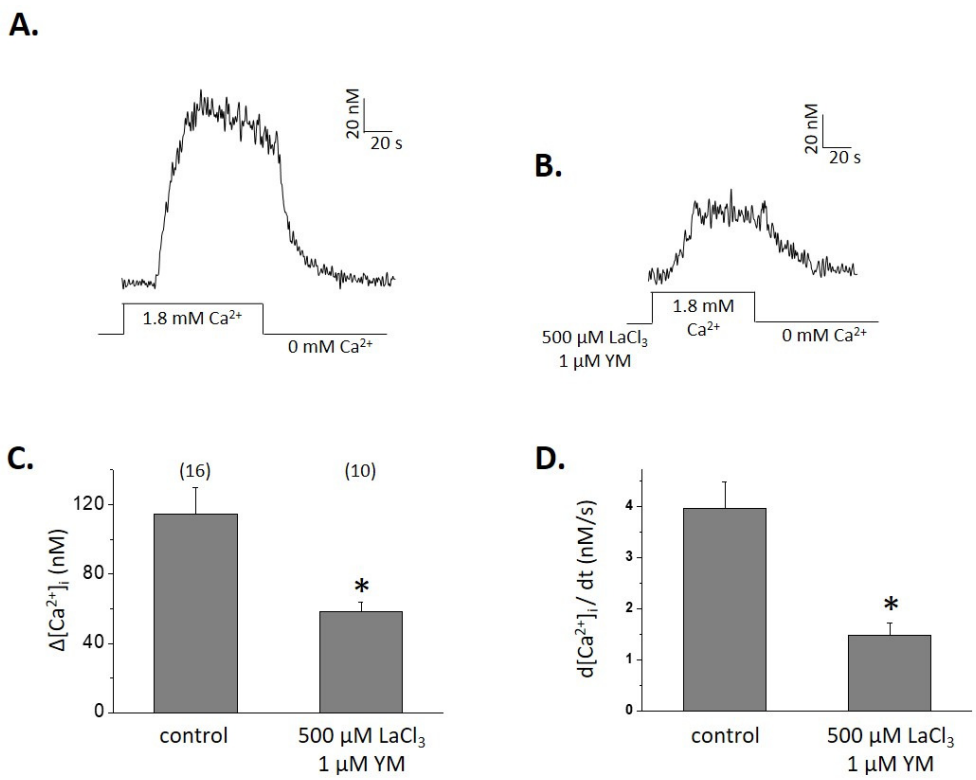

Fig. 4.17. Single-cell fluorescent Ca^{2+} measurements during SOCE inhibition in Fura-2 loaded chondrogenic cells of 2-day-old HDC. Prior to shown part of the records, ER Ca^{2+} stores were depleted by treatment with 10 µM CPA in Ca^{2+}-free Tyrode's for 5 min, which appears as a marked decrease in $[Ca^{2+}]_i$ preceded by a prominent increase. (A) A large transient increase in $[Ca^{2+}]_i$ can be observed after changing $[Ca^{2+}]_e$ back to normal (1.8 mM), which demonstrates SOCE. (B) Blocking SOCE by pre-treatment with $LaCl_3$ and YM-58483 for 5 min caused a significant decrease in the amplitude and maximal rate of rise of this Ca^{2+} entry. (C) Combined data of amplitudes of Ca^{2+} transients. (D) Mean values of the maximal rate of rise of $[Ca^{2+}]_i$ after the re-addition of external calcium. Numbers in brackets specify the number of cells measured. Asterisks (*) mark significant(*$P < 0.05$) differences between control and pre-treated cultures. Panels (A) and (B) display representative traces of 16 and 11 records, respectively.

5. Discussion

5.1. Comparative Analysis of Primary Chick and Mouse as well as the C3H10T1/2 Cell Line-Based Chondrogenic HDC

A detailed investigation of chondro-, osteo- and adipogenic differentiation is provided in this work by juxtaposing these widely employed micromass models. First, control C3H10T1/2 cell line and its modified version were investigated, in the latter, the cells contained a plasmid that maintains a constant BMP-2 overexpression and secretion into the culture medium that is independent of external sources [73]. All of these models are known to be broadly investigated for both early and late phases of cartilage formation [63, 71-73, 257, 258]. However, a comparative analysis that involves considering their differentiation potentials in multiple mesenchymal directions by involving some recently described target genes, standardized circumstances and sample collection times is a vital complement to our existing knowledge. Also, the direct comparison of mRNA expression profiles from such a broad spectrum of chondrogenic, osteogenic, adipogenic and pluripotency marker genes is a novelty.

A wide array of signaling pathways play a key role in the complex process of cartilage formation which precedes endochondral ossification, for an account on the most notable ones, see literature review chapter. The BMP pathway has been implicated in the *in vitro* differentiation of mesenchymal cells mainly in the direction of bone and cartilage [259]. More specifically, BMP-2, a type that has been reported to be expressed in the condensing mesenchyme of embryonic limbs and even vertebrae, plays an essential role in the patterning and development of the skeleton, according to current hypothesis [260]. As it was mentioned earlier, it is important to remark that depending on a set of parameters, in addition to enhancing chondro- and/or osteogenic differentiation, BMP-2 may also induce adipogenesis of C3H10T1/2 cells via the SMAD1-dependent upregulation of PPARγ2 expression [164]; a firm reason for us to include markers of this lineage in our study.

5.1.1. Morphological Comparison of Examined Chondrogenic Models

The presence or lack of prechondrogenic nodules was one of the most straightforward differences between the limb bud-derived and the cell line-based HDC that was apparent by morphological analysis following conventional HE staining. It can be assumed that primary micromass cultures express a relatively high number of intercellular junctions [261], mainly N-cadherins, that provide a more original representation of *in vivo* tissue, where similar nodules also appear. Nevertheless, N-cadherins are also expressed by C3H10T1/2-derived colonies [262]. Another feature we may trace back to N-cadherin expression is the migratory potential of different types of cultures; the embryonic limb bud-derived cells remained densely organized at their original position in the

culture, while the c-C3H10T1/2 cells displayed such a propensity for of migration that made the colony edges blurry after a few days of culturing. In the meantime, the b-C3H10T1/2 cells were also motile (mainly at the periphery), but not as much as the control ones, since cellular density remained high in the center of colonies. These perceptions are in a good accordance with results demonstrating that induction by BMP-2 is necessary for the upregulation of N-cadherin expression [262]. Indeed, it is possible to assume a consecutive relationship between the detected differences in migratory characteristics and the diverse morphology of various HDC.

5.1.2. Uncovering the Chondrogenic Capacity of Involved Micromass Cultures

In line with the leading objective of our comparative study, next, we sought to inspect the extent and quality of cartilage formation by comparing chondrocyte-specific marker gene mRNA expression patterns. We have detected a steady mRNA expression profile for majority of the essential chondrocyte-specific genes (namely, *Sox9*, *Acan*, *Col2a1* and *Hapln1*) in both the primary and the BMP-2 overexpressing micromass models. In addition, Snorc, a novel chondrocyte-specific transmembrane chondroitin sulfate proteoglycan [87, 263] displays a characteristic upregulation with robust expression levels from culturing day 3 in the examined differentiating models (we did not consider c-C3H10T1/2 HDC as differentiating due to the lack of necessary stimuli). Nevertheless, *Prg4*, encoding an important protective secretion of the superficial zone of *in vivo* articular cartilage [264], only demonstrated a strong expression in mouse limb bud-derived colonies (unfortunately, no mRNA sequence was available for *Snorc* and *Prg4* for chicken in any of the searched nucleotide databases: NCBI, DDBJ and EMBL-EBI), which is a substantial indication that these cultures have a better coincidence with native articular cartilage. Analysis of metachromatic ECM morphology, arrangement and quality further verified this observation. Notably, *Col10a1* expression was robustly detectable for the entirety of culturing in primary cultures, while the C3H10T1/2-based models exhibited a much fainter expression, at least for the majority of the course. Although this gene is primarily expressed by hypertrophic chondrocytes, it is certainly conspicuous that type X collagen has been reported as a natural structural supporting component of mouse articular cartilage which is associated with development and growth among other processes [265].

5.1.3. Our Differentiating Models Undergo Notable Osteogenic Differentiation Involving Matrix Calcification

Partly based on the observation provided by the robust expression of type X collagen, a marker of chondrocyte maturation and hypertrophy during endochondral ossification [266], a detailed comparative analysis of osteogenic marker genes was incorporated into this work. Our results

regarding the mRNA transcript levels of prominent osteogenic transcription factors that are both required for osteoblast differentiation, *Runx2* and *Osx* [267], imply that osteogenesis takes place as soon as the outset of culturing in all but the c-C3H10T1/2 colonies. In the control cell line-based cultures expression of these factors is also measurable, but both display a strong downregulation for later periods of culturing. Previous studies already confirmed the osteogenic potential of both primary micromass [268, 269] and BMP-2 treated C3H10T1/2 [270] micromass colonies. The relatively early onset of osteogenesis is further reinforced by the mRNA expression of *Col1a1* and *Ap* that can be detected at the starting point of culturing. *Ap* displays a strong upregulation in limb bud-derived HDC, which is likely the consequence of increased OSX activity, as increased stability of OSX by mutation of certain ubiquitination sites has been directly linked to elevated alkaline phosphatase expression in C2C12 cells [271]. Another group using the same mouse limb bud-derived micromass model also noticed the upregulation of *Ap* mRNA levels in later phases of culturing [258]. Still, stronger signals – especially in mouse limb bud cultures – were mostly limited to the second half of culturing in the case of late osteogenic markers *Oc* and *Op*. Our data regarding *Oc* expression agree aptly with results of other groups in both the case of mouse primary [258, 268] and BMP-2 (as well as BMP-7) induced C3H10T1/2 cultures [272]. In the case of chicken HDC, our *Oc* expression results could not be directly compared to others due to the lack of previous observations; one study in connection with inorganic phosphate and vitamin C induced mineralizing cultures found that relative expression of *Oc* increases compared to non-mineralizing control values, especially in late phases of culturing [269]. It is notable that according to the publication of Shea et al., *Op* mRNA levels in C3H10T1/2 colonies respond differently to BMP-2 and BMP-7 treatments; they saw a biphasic mRNA expression pattern in the case of BMP-7, while BMP-2 caused upregulation of *Op* only from later time points, the latter one being in a precise accordance with our own results. While in primary embryonic limb bud colonies *Op* mRNA expression patterns have not been examined earlier, chicken HDC displayed elevated protein levels of OP as culturing time progressed by western blotting [273]. Unfortunately, other than the investigated type of molecule (protein instead of mRNA), the time scaling in the experiments by Boskey et al. also makes it impossible to compare these to our own data. Still, our results regarding *Oc* and *Op* mRNA levels are in excellent conformity with previous data using the same b-C3H10T1/2 HDC system [73]. Based on the above results, it can be determined that all of our differentiating models express mRNAs of the same osteogenic markers on a comparable temporal scale. On the other hand, chicken HDC only weakly appear to display late stage elevations of osteogenic marker mRNAs, which may just indicate the importance of translational regulatory mechanisms, since phenotypically ECM calcification can be observed similarly to the case of other differentiating models. Therefore, Alizarin Red staining to visualize ECM calcification suggests a similarity between the rate and the pathway how these cultures reiterate embryonic endochondral bone formation. Curiously, the expression of articular cartilage

markers (such as *Snorc* and *Prg4*), was not separated temporally from bone markers (namely, *Oc* and *Op*), suggesting that chondro- and osteogenesis do not follow a sequential pattern as in the case of *in vivo* limb formation. However, data published by Stanton et al. imply that caution should be applied during the interpretation of marker mRNA expression level data: firstly, *Runx2*, *Osx* and *Oc* are also reported as regulators of late chondrocyte differentiation with distinguished expression in prehypertrophic and hypertrophic chondrocytes; secondly, *Oc* mRNA expressing cells appear to be mainly located in internodular areas of primary limb bud-derived micromass cultures, which means these cells are practically separate from chondrocytes of the nodules [268].

5.1.4. Adipogenic Differentiation of HDC – an Ambiguous Attribute

As development of C3H10T1/2 cells into adipocytes has also been observed following induction by BMP-2 [73], we decided to look for adipogenic signs in the case of all our investigated models. To this end, mRNA expression levels of the adipocyte-specific factors *Fabp4* and *Pparγ2* were monitored (with the exception of the chicken HDC model, for which, the mRNA sequence of *Pparγ2* was unfortunately not available in any of the searched nucleotide databases: NCBI, DDBJ and EMBL-EBI). In general, FABPs are expressed in a relatively ubiquitous fashion, but FABP4 is considered an adipocyte-specific component, which is an adipocyte precursor-marker at the same time [274]. We were able to detect *Fabp4* mRNAs in all of our micromass models with an apparent upregulation at later stages that was exclusive to the differentiating cultures and was not seen in the case of c-C3H10T1/2 colonies. As our Oil Red O staining protocols were also able to demonstrate that lipid droplet-containing cells reside in all examined types of colonies, a sound correspondence can be noted. On the other hand, our results regarding *Pparγ2*, a fundamental regulator of adipogenesis [275], imply that adipocyte differentiation only takes place in late phases of culturing in b-C3H10T1/2 colonies, since its expression is not discernible in other stages and/or in other models. With a view to this result, we have collected b-C3H10T1/2 HDC for Oil Red O staining on day 25 of culturing where we could observe an immense number of single, large lipid droplet-containing cells (most likely adipocytes) in the superficial layer at the center and also at the periphery of the colonies (data not shown). Remarkably, lipid droplet-accumulating cells were also seen in c-C3H10T1/2 cultures, while limb bud-derived colonies contained cells with small and infrequent lipid droplets; these are presumably mature chondrocytes and lipid droplets are present as their natural structural components [254].

5.1.5. Pluripotency Factors and their Possible Role in Micromass Cultures

In addition to investigating differentiation towards the above three lineages, a novel concept emerged; we were interested in ascertaining whether a portion of the cells in HDC maintain a

pluripotent condition. Accordingly, we have evaluated mRNA expression of *Sox2*, *Nanog* and *Oct4* (or the avian homologue of *Oct4*, *PouV*) pluripotency markers – all of them are critical to the self-renewal [276] of undifferentiated ESCs – in our models. Interestingly, *Oct4* did not produce identifiable levels in any of the mouse models, but its homologue displayed a well-detectable expression level in chick primary HDC, with a prominent downregulation as chondrogenic differentiation progressed making it the seemingly most reliable marker of differentiation from the group of genes investigated. On the other hand, *Sox2* was identifiable in all models, whereas in differentiating ones, it featured a relatively firm expression at the beginning of culturing and became downregulated later. In the meantime, *Nanog* – the expression of which was not detectable in chick primary HDC – was strongly upregulated from day 3 onwards in differentiating cultures. In c-C3H10T1/2 colonies, no particular tendencies could be observed in the case of the two expressed pluripotency markers. These results provide an important indication that not all cells in our investigated models undergo differentiation towards the above-discussed lineages, some cells may actually stay in an undifferentiated status.

5.1.6. Which Chondrogenic Model does Above Data Make Preferable?

According to the results seen so far, evidence for the presence of all three examined major mesenchymal differentiation pathways and for cells maintaining a pluripotent state can be seen by both morphological and mRNA expression analyses in the investigated differentiating micromass cultures. Implicitly, cells in these *in vitro* cultures become committed and differentiated towards disparate lineages in a simultaneous manner, instead of a sequential pattern. Moreover, key osteo- and chondrogenic lineage-specific transcription factor mRNAs (i.e. *Runx2*, *Osx* and *Sox9*) are promptly identifiable from day 0 of culturing, while the adipogenic *Pparγ2* expression can only be observed in the second half of culturing and exclusively in b-C3H10T1/2 colonies. On the other hand, an upregulation of marker gene transcripts for all three lineages (namely, *Snorc* and *Prg4* for articular cartilage; *Ap*, *Oc* and *Op* for bone; and *Fabp4* for adipocytes) was noticed by day 15 in primary mouse limb bud HDC. In primary chicken limb bud HDC, similar tendencies can be inferred, albeit certain genes could not be investigated (*Snorc* and *Prg4*, due to not being available in scanned databases) and late stage osteogenesis is best represented in Alizarin Red stained cultures. mRNA expression of previously noted markers in chicken HDC displays a less notable upregulation, if any, still, *Runx2* – a key osteogenic transcription factor – exhibits a prominent elevation. The apparent heterogeneity of the cultures has to be considered during data analysis; especially in the case of b-C3H10T1/2 HDC, as these cultures demonstrate the most convincing signs of adipogenesis, while our observations in both limb bud-derived micromass colonies likely indicate lipid droplets and associated components that are natural constituents of mature chondrocytes. It is also noteworthy that c-C3H10T1/2-based micromass

cultures did not express the majority of either chondrogenic or osteogenic marker genes (except for *Col2a1*) other than the varying, but mainly decreasing levels of lineage-specific transcription factors; which testifies for the fundamental role played by the autocrine/paracrine secreted factors (in our case, BMP-2) in lineage-specific differentiation. Moreover, adipogenesis appears to be the default pathway for C3H10T1/2 cells in HDC, as certain signs of adipogenesis (and the absence of such signs in case of chondro- and osteogenesis) were observable in unstimulated colonies without any additional factors.

As a matter of course, heterogeneity is a more ubiquitous issue that is experienced in the whole area of mesenchymal stem cell research. Although the stem cell niche of cartilage requires further characterization, progenitor cells with differentiation potential into hyaline cartilage ECM-secreting cells have already been reported [25]. Therefore, creating a chondrogenic mesenchymal stem cell line capable of assembling functional hyaline cartilage *in vivo* is still considered the Holy Grail of cartilage research [277]. Still, considering our data regarding the late-stage appearance of hypertrophic chondrocytes and the morphology in the case of primary HDC provides a solid confirmation to support that the embryonic limb bud-based models produce a closer recapitulation of embryonic cartilage formation followed by endochondral ossification. Other reports also came to coherent conclusions [258], thus the primary micromass models should still be handled as well-founded platforms to study *in vitro* chondrogenesis. Among limb bud-based systems, the avian model offers an immense convenience due to its simplicity, reproducibility, high yield and cost-effectiveness; unless some of the known disadvantages (converse regulation of certain pathways, lack of available antibodies or sequences, inefficiency of particular drugs) [53, 55, 57] compromise the experiments or the interpretability of gathered data, these advantages easily outweigh other factors. Ultimately, we advise considerable caution during the interpretation of these results that we gained by a particular set of experimental methods to assess *in vitro* differentiation of mesenchymal cells towards different lineages, even though these models provide a compelling apparatus to determine the relationship between prominent regulators of mesenchymal differentiation; as the transcriptome of these cultures does not inevitably match their proteome, further studies involving proteomic methods are likely to provide a more precise picture on these characteristics.

5.2. Intracellular Calcium Oscillations and their Regulation in Chondrogenic Cells

5.2.1. Ca^{2+} Homeostasis in Differentiating Chondrocytes

Ca^{2+} is broadly acknowledged as the most adaptable second messenger. There is growing data to indicate that non-excitable cells, such as MSCs and chondrocytes, are utilizing Ca^{2+} signaling pathways as pivotal mediators throughout the course of differentiation. Differentiation of MSCs into adipocytes has been linked to maintained elevation of cytosolic Ca^{2+} concentration with a biphasic regulatory role; early stages of adipogenesis were inhibited, while late stages were advanced by the phenomenon [278]. Similarly, chondrogenic differentiation of mesenchymal cells is also coordinated by Ca^{2+} dependent pathways; increased extracellular Ca^{2+} levels were associated with enhanced cartilage differentiation in chicken micromass cultures [279]. An ostensible contradiction is that low concentrations of Ca^{2+} implemented chondrogenesis in chicken embryonic calvaria in another case where extracellular Ca^{2+} was linked with a modulatory role during skeletogenesis [280]. As L-type VDCC-specific blockers nifedipine and verapamil abated cartilage differentiation in mouse limb bud-derived micromass cultures, the significance of these plasma membrane Ca^{2+} channels is already established in this model [281]. Previous results of our laboratory are in agreement with the above; during the time of final commitment of differentiating chondroprogenitors, cells of chicken HDC display a sustained rise in the concentration of cytosolic free Ca^{2+}, which appeared to be a necessary condition to their chondrogenesis [231].

5.2.1.1. Ca^{2+} Influx via VDCCs in Chondrogenic Chicken HDC

The preceding set of data clearly indicates the **importance of Ca^{2+} dependent signaling**, more specifically **extracellular Ca^{2+}, as a source of influx via plasma membrane Ca^{2+} channels in chondrogenesis**. Actually, multiple laboratories – including ours – were able to establish diverse Ca^{2+} entry mechanisms in both developing and mature chondrocytes; such as purinergic (P2X and P2Y) and NMDA receptors, TRP channels and ARCs [57, 64]. As mechanotransduction pathways are vital aspects in chondrocyte biology, NMDA receptors and TRPV channels – essential mediators of biomechanical signals – are of particular importance [282, 283]. In addition to these ligand-operated Ca^{2+} entry mechanisms, expression of VDCCs has also been reported in chondrogenic cultures [284]. Further information regarding VDCC subunits, types and their previous implications in cartilage can be found in the Literature Review chapter.

Nevertheless, differentiating chondrocytes were an uncharted area with regards to a comprehensive molecular characterization of correlated VDCC types. Certain cues for the association of VDCCs with *in vitro* chondrogenesis were already available from our previous work, especially that

high extracellular K^+ concentrations were able to induce large Ca^{2+} transients [195]. Accordingly, we have completed a comprehensive characterization of Ca_V α_1 subunit mRNA expression to be able to identify **detectable transcript levels in the case of two L-type (*$Ca_V1.2$* and *$Ca_V1.3$*), an R-type (*$Ca_V2.3$*) and all three T-type (*$Ca_V3.1$*, *$Ca_V3.2$* and *$Ca_V3.3$*) Ca^{2+} channels**. Moreover, we have found an indication for the role of VDCCs throughout the differentiation of chondroprogenitor cells to chondroblasts and mature chondrocytes based on the continuous presence of Ca_V α_1 subunit proteins in total cell lysates over the complete culturing period. Expression of α_1 subunits was first reported in mouse limb-bud chondrocytes by Mobasheri et al. [206]. Subsequently, expression of Ca_Vs in chondrocytes has been verified, and moreover, their connection with mechanotransduction pathways has also been proposed [285]. Notably, L- and T-type VDCCs were detected in both differentiating hMSCs and embryonic limb-bud-derived chondroprogenitor mesenchymal cells; a feasible indication of their regulatory role during differentiation. Albeit VDCCs have been functionally characterized in ossifying hMSC cultures [204], no comparable data have been available from chondrogenic models prior to ours.

Results gained by the continuous application of the L-type channel specific inhibitor nifedipine from day 1 on differentiating HDC suggest that VDCCs play a substantial role in chondrogenesis; both cartilage-specific ECM production and SOX9 protein expression were markedly reduced by the treatments. As noted before, administration of nifedipine also exerted an inhibitory effect on cartilage formation of mouse embryonic limb bud mesenchymal cells, which correlates well with our results [281]. However, interestingly, nifedipine treatment did not result in diminished osteogenesis of hMSCs [204], which is presumably due to the differences that exist between the molecular architecture regulating osteo- and chondrogenesis, as well as the steps required for differentiation of adult hMSCs and embryonic chondroprogenitor cells; the former one is a multipotent, while the latter one is a committed chondrogenic cell type. Recent results gained from investigating the Ca^{2+} homeostasis of mouse and chicken embryonic limb buds and their derived micromass cultures strongly underline the importance of the L-type VDCC, $Ca_V1.2$ in the chondrogenesis of developing limbs [286]. In accordance with this finding, our results regarding *$Ca_V1.2$* mRNA expression suggest that this type displays a stable and robust expression through the full length of the examined culturing period.

It has been well established that various VDCC types (especially L- and T-type) govern the cell cycle [287]. This dependence is a long-established aspect, but some elements are still disputed; both influx and release are reported to take place in regulating proliferation however, there seems to be a significant variance between different cell types in that in what ratio they rely on these mechanisms. This difference is apparently connected with the amount of Ca^{2+} stored in the ER [288]. T-type VDCCs are particularly likely to play a major role in regulating the cell cycle of non-excitable cells due to their

low voltage-dependent activation/inactivation and slow deactivation characteristics, which enables them to allow a membrane potential-sensitive and constitutive influx of Ca^{2+} [288]. Remarkably, **all three T-type channels are constantly expressed** throughout the whole culturing period of chondrogenic chicken micromass cultures, which is a definite indication of their influence in Ca^{2+} homeostasis through the course of cartilage formation. As high cellular density is an already highlighted requirement of *in vitro* chondrogenesis, it was arguably expectable that restricting cellular proliferation by blocking VDCCs would impede chondrogenic differentiation of HDC. Indeed, nifedipine demonstrated the anticipated antiproliferative effects as determined by measuring ^{3}H-thymidine incorporation into the newly synthesized DNA of differentiating chondrocytes. Consequently, we conclude that **VDCCs not only contribute to basal Ca^{2+} levels, they are likely influential regulators of cell division**; which has been previously emphasized as a prerequisite to the condensation phase in mesenchymal chondrogenesis.

5.2.1.2. SOCE in Differentiating Chondrocytes of Chicken HDC

In general, an additional source of cytosolic Ca^{2+} elevation to Ca^{2+} entry across the plasma membrane can be Ca^{2+} release from ER Ca^{2+} stores via either InsP3R or RyR channels [224]. The amount of Ca^{2+} to be found in the ER at any given time point is mainly determined by the balance between the activities of SERCA and NCX, the buffering capacity of luminal Ca^{2+} binding proteins and Ca^{2+} release. Ca^{2+} release mainly occurs via InsP3R activation in non-excitable cells [289]. In agreement with this assertion, application of the strong agonist of RyR – caffeine – procured no Ca^{2+} release in differentiating [231] or mature chondrocytes [290], as well as human and murine mesenchymal and embryonic stem cells [197, 200]. In addition, mRNA and/or protein expression in hMSCs and differentiating chondrocytes of HDC also reflected the above-described; InsP3R mRNA and protein was detectable in these models, while no RyR mRNA transcripts could be identified [197, 231]. **Signaling pathways leading to InsP3 production may easily deplete the ER Ca^{2+} store of cells of chicken limb bud cultures, since these stores are relatively small in non-excitable cells**. As a consequence of store depletion, **CRACs become activated to refill the ER stores, SOCE is thus implemented** [224]. There is plenty of evidence in the literature to corroborate the importance of SOCE in maintaining the Ca^{2+} homeostasis in non-excitable cells, such as OUMS-27, the human chondrosarcoma cell line [291], or in rat primary chondrocytes [292]. Moreover, during the course of previous experiments, our laboratory also demonstrated that ER store depletion by the SERCA pump inhibitor CPA resulted in a large cytosolic Ca^{2+} transient when extracellular Ca^{2+} was re-added to the medium [231]. Nevertheless, it is notable that the detailed characterization of CRACs and other SOCE molecules in mature or developing chondrocytes has not been performed previously to this work.

Although differentiating [231] and mature [233] chondrocytes have long been known to hold releasable ER Ca^{2+} stores, the detailed characterization of SOCE-generated transients was not available; **this work provides primal evidence of the functional expression of SOCE-mediating molecules in differentiating chondrocytes**. The mRNA expression levels of *Orai1*, *Stim1* and *Stim2* all turned out to be stable during the whole extent of culturing. Furthermore, we were also able to validate the expression of STIM1 at the protein level. Based on well-known characteristics of STIM2, – this molecule is switched on even by slight decreases in ER Ca^{2+} levels – it has been suggested to control basal cytosolic Ca^{2+} concentrations [293] and presumably has important functions in chondrogenic cells as well. As described in the results section, we likely have demonstrated the protein expression of the predicted isoform X1 of STIM2 in the western blots that were originally dedicated only to STIM1. We were not able to establish the presence of ORAI1 protein due to the lack of commercially available chicken-reactive antibodies. However, substantial amount of indirect evidence on the functional expression of the pore-forming subunit of CRACs is provided by our recordings of SOCE in cells of HDC during single cell fluorescent Ca^{2+} measurements. Over and above, in our experiments, ER Ca^{2+} store depletion by constant application of CPA in combination with **SOCE blockade caused the almost complete abolishment of *in vitro* cartilage formation**; this implies that SOCE, and more specifically, the interaction between STIM and ORAI subunits appear to play a critical role in the normal Ca^{2+} homeostasis of differentiating chondrocytes. Highly similar results were observed after targeting SOCE via an alternative mechanism, by inhibiting the reorganization of septin filaments, which is a recently described requirement of CRAC activation [2]. After Ca^{2+} homeostasis was disturbed as a consequence of deficient replenishment of ER Ca^{2+} stores, decreased cell division emerged as one of the likely factors behind abated chondrogenesis. Actually, the proliferation rate after ER Ca^{2+} store depletion or the inhibition of septin remodeling dropped to very low levels, while we have detected little to no effect on the mitochondrial metabolic activity of chondrogenic cells of HDC. These results provide further evidence for the **high degree of Ca^{2+} sensitivity of proliferation in differentiating chondrocytes**. Notably, this sensitivity was independent from the source of Ca^{2+}, as the perturbation of Ca^{2+} entry across the plasma membrane or Ca^{2+} release from internal stores both resulted in the abatement of proliferation. As reviewed earlier [288], the connection between ER Ca^{2+} and the regulation of the cell cycle is still disputed and appears to be a characteristic of the given cell type; however, in our case there appears to be a clear juncture. It is also noteworthy that PouV expression responds in a differentiation stage-dependent manner to treatments blocking the reorganization of septin filaments and thus disturbing SOCE, which suggests that the effects of perturbing Ca^{2+} homeostasis reach beyond diminishing proliferation rate. Also, the highly elevated mRNA expression of *Orai1* after FCF treatment during the period of differentiation (day 2) proposes a compensatory mechanism and an important role played by functional CRACs in the process of differentiation, not only proliferation.

5.2.2. Ca^{2+} Oscillations in Chondrogenic Cells of Chicken HDC

Information encrypted by the frequency of Ca^{2+} oscillations is able to regulate a diverse set of cellular functions, such as gene expression and cell division. Above all, according to the prevailing consensus of the field, both the efficiency and specificity of signaling pathways is increased by periodic Ca^{2+} oscillations at low levels of stimulation when compared with sustained rises in basal Ca^{2+} levels [226]. Consequently, Ca^{2+} oscillations are more adequate for non-excitable cells with low levels of stimulation; naturally, many non-excitable cells, such as MSCs and chondrocytes, have been observed to share these periodic changes of basal cytosolic Ca^{2+} concentration. The "spatially restricted pulsatile activity" of articular chondrocytes has been discussed as early as 1995 [233], which is perceived as the inception of the concept of rhythmic Ca^{2+} oscillations of these cells. The following years saw the expansion of this idea and spontaneous Ca^{2+} oscillations were also reported from sliced cartilage and chondrocytes; in addition, a paracrine purinergic pathway has been proposed to regulate mechanically induced Ca^{2+} waves [294]. Notably, an **ATP autocrine/paracrine circuit** was uncovered in hMSCs to control Ca^{2+} oscillations and the ensuing activation of NFAT that in turn regulates their proliferation and differentiation [295]. However, in ATDC5 cells Ca^{2+} oscillations intriguingly appear to generate ATP oscillations, which serves a pivotal role in their prechondrogenic condensation and secretion of ECM components [296]. Moreover, these Ca^{2+} induced ATP oscillations have been proposed to be triggered by the ionotropic purinergic receptor **P2X4** [297], which is the same receptor that **was denoted by our laboratory as a key element in mediating Ca^{2+} influx in chondrogenic cells of chicken HDC** [75]. Yet, we may infer a reciprocal regulatory loop between ATP and Ca^{2+} oscillations as a driving force behind the differentiation and proliferation of MSCs and chondrocytes.

Non-excitable cells demonstrate extensive variations regarding the temporal aspects of their Ca^{2+} oscillations. In hMSCs, cyclic Ca^{2+} transients took place every 5.7±3.0 min [197] on average while demonstrating a considerable individual variability. Cells of human osteoblast primary cultures were reported to display spontaneous oscillations with a comparable frequency of 0.25-0.6 min^{-1} [298]. Chondrocytes, on the other hand, exhibit higher variability. In chondrocytes of mature rabbit articular cartilage, spontaneous Ca^{2+} transients lasted as long as 30 seconds within a 120-sec-long observation time frame [294]. While ATP levels and cytosolic Ca^{2+} in the chondrogenic ATDC5 cell line displayed oscillations once in approx. every 6 hours [296]. On the other end of the spectrum, we have observed considerably **more frequent Ca^{2+} oscillations in differentiating chicken HDC**. Depending on the day of culturing, the ratio of oscillatory cells was dynamic (45 of 240 cells (19%) and in 175 of 317 cells (55%) on culturing days 1 and 2, respectively), plus these Fluo-4-loaded cells of HDC displayed transients at a rate of 0.08±0.01 Hz on day 1, which decreased to 0.06±0.003 Hz by culturing day 2. A study published

in 2012 reported a level of oscillatory frequency, which corresponds well with our results, in Fluo-4 loaded bovine articular chondrocytes; moreover, like in our case, these actions were conditional upon both extracellular and intracellular Ca^{2+} sources and the function of voltage-dependent and voltage-independent Ca^{2+} channels [299]. However, it has to be noted that the oscillations described in this study were generated by microcrystalline stress and had deleterious effects via proteoglycan degradation, which is in sharp contrast with our observations, where **spontaneous Ca^{2+} transients appeared to be a natural characteristic of limb bud-derived HDC**.

5.2.3. Release and Entry of Ca^{2+} in Ca^{2+} Oscillations

Only a few minutes after the replacement of the medium to a Ca^{2+} free one, Ca^{2+} oscillations were abolished by the absence of Ca^{2+} in the bath solution. This suggests the reliance of the phenomenon on Ca^{2+} entry across the plasma membrane, furthermore, it also conveys that internal stores alone can sustain oscillations for a limited period, likely due to their low amount of stored Ca^{2+}. Similarly, a study in relation to Ca^{2+} signaling pathways of hMSCs came to the same conclusion that Ca^{2+} entry was necessary to maintain Ca^{2+} oscillations [197]. Differentiating human osteoblast-like cells displayed similar characteristics to the above results [298]. Next, we examined the involvement of VDCCs that were key regulators of sustained Ca^{2+} transport through the plasma membrane, in this mechanism. Application of nifedipine, the L-type VDCC blocker, caused a slight reduction in the ratio of oscillatory cells and also the amplitude and frequency of their Ca^{2+} oscillations in fluorescent Ca^{2+} imaging experiments. This outcome suggests only a diminished role for influx via VDCCs in supporting Ca^{2+} oscillations of limb bud HDC, which is somewhat in accordance with the finding that nifedipine application had no effect on the Ca^{2+} oscillations of osteoblasts [298].

Subsequently, we have shifted our focus on SOCE. Application of $LaCl_3$ and YM-58483 – blockers that inhibit all forms of Ca^{2+} entry channels including CRAC – caused a severe disturbance in cytosolic Ca^{2+} and led to slight fluctuations instead of the usual periodic Ca^{2+} transients. The same blockers with the co-application of the SERCA-blocker CPA resulted in the complete disappearance of cytosolic Ca^{2+} level changes, regardless of the presence of extracellular Ca^{2+}. In summary, **these oscillations appear to be driven by the cycling of Ca^{2+} between the Ca^{2+} store and the cytosol**, as the spontaneous Ca^{2+} transients were perfectly abolished by the blockade of SOCE when combined with store depletion. These results resonate well with those of Tsai and coworkers who demonstrated that Ca^{2+} oscillations of human osteoblasts-like cells are blocked by thapsigargin-induced store depletion [298]. Similarly, the dependence of spontaneous Ca^{2+} oscillations on internal Ca^{2+} pools of hMSCs has been described as well [197], which, combined with the above results, suggests that Ca^{2+} oscillations are commonly

sustained by ER Ca^{2+} stores and their replenishment in mesenchymal cells and their differentiating derivatives.

The gradual elimination of Ca^{2+} oscillations after changing the medium to its Ca^{2+} free version suggests that cytoplasmic Ca^{2+} transients are not exclusively eliminated by SERCA pumps, which is responsible the gradual depletion of stores. This also supports the assumption that ER stores play a vital role in the maintenance of cytoplasmic Ca^{2+} oscillations. Information is scarcely available regarding the function of Ca^{2+} elimination pathways in chondrogenic cells. The functional expression of PMCA and NCX has been proven in hMSCs and mESCs [200, 227]. More relevantly, NCX has also been found to be present in a functional form in bovine mature articular chondrocytes [248]. According to our group's unpublished data (data not shown) mRNAs of NCX1 and -3 and PMCA1, -2 and -4 are all expressed in cells of chicken limb bud-derived micromass cultres, suggesting their likely relevance in the calcium homeostasis of chondrogenic cells.

5.2.4. Downstream Interpretation of Ca^{2+} Oscillations

The prevailing view is that the main **downstream targets of Ca^{2+} include Ca^{2+}-dependent protein kinases (classic PKCs, such as PKCalpha) and phosphoprotein phosphatases (calcineurin)**; these can subsequently activate various transcription factors (e.g. NFAT, NF-κB, JNK1, MEF2 and CREB) by changing their phosphorylation status. The frequency and amplitude of the transients are determinant with regards to which transcription factor becomes activated. Calcineurin was reported to be responsible for the calcineurin-dependent dephosphorylation and nuclear translocation of NFAT in lymphocytes, as well as in MSCs [295, 300]. The calcineurin-NFAT4 pathway has also been verified to be of significance during chondrogenesis [54, 142], thus the available information can be summarized by concluding that high-frequency Ca^{2+} oscillations are likely to play important roles in the proliferation and differentiation of chondrogenic cells via the activation of NFAT4.

Cyclic spontaneous Ca^{2+} transients may also result in the activation of Ca^{2+}-calmodulin dependent protein kinase II (CaMKII). This enzyme has been demonstrated to be able to decode the frequency of Ca^{2+} spikes into distinct amounts of kinase activity, as it is modulated by several factors [301]. Numerous cellular structures and functions, including ion channels, cytoskeleton, gene transcription and proliferation, can be modulated by CaMKII in diverse cell and tissue types, as a response to the rise of cytoplasmic Ca^{2+}. The activation of CaMKII is responsive to Ca^{2+} transients with a temporal pattern in the range of 0.1-10 s [302], which makes it particularly applicable to decode high-frequency Ca^{2+} oscillations. As the Ca^{2+} oscillations displayed by differentiating chondrogenic cells of the chicken limb bud HDC are precisely within this range, this molecule can be hypothesized to connect

the Ca^{2+} transients and the activation of transcription factors that can stimulate chondrogenic differentiation and matrix synthesis. Accordingly, mRNA and protein expression of various CaMKII isoforms has been reported in human articular chondrocytes [303]; moreover, **we were able to detect altering expression patterns of different CaMKII isoforms (alpha, beta, gamma and delta) in our limb bud micromass cultures (data not shown)**. Regardless, functional studies are necessary to verify the currently hypothetical role of CaMKII as a molecular decoder of Ca^{2+} oscillations in differentiating chondrocytes.

5.3. Combined Scheme of Ca^{2+} Oscillations and Related Mechanisms in Differentiating Cells of HDC

The following model in *Fig. 5.1.* aims to describe how spontaneous Ca^{2+} oscillations of chondrogenic cells are generated and maintained. It was established combining data presented here and in previous works of our research group with publications of other contributors of the field. Since these oscillations were sensitive to both Ca^{2+} deprivation from the extracellular medium and internal store depletion, the **transients apparently require Ca^{2+} to enter via the plasma membrane and also to be released from internal stores**. Accordingly, the Ca^{2+} oscillations can be classified to spawn from a minimum of three separate mechanisms.

Firstly, our group previously described an autocrine-paracrine purinergic regulatory loop that drives chondrogenesis of limb bud HDC [75]. This finding corresponds with observations made on rabbit mature articular chondrocytes [294] or hMSCs [295]. Multiple sources, including our group, reported that ATP is secreted by differentiating chondrocytes [75] at least partially via connexin hemichannels [304]. The released extracellular nucleotides can then act on two large subclasses of P2 purinergic receptors: the P2X receptor ion channels and the G protein-coupled metabotropic P2Y receptors. Expression of manifold **P2X and P2Y receptor types** has been verified in both differentiating and mature chondrocytes [75, 305]. The activation of P2 receptors by ATP acts via different pathways accordingly to their subclass; P2X receptors are ligand-gated ion channels that will enable Ca^{2+} influx, while metabotropic P2Y receptors release Ca^{2+} from ER stores through the PLC-InsP3 pathway *(Fig. 5.1.)*. Data previously published by our group established a particularly important role for P2X4 receptors in chicken chondrogenic cultures [75]. In either case, a transient elevation of cytosolic Ca^{2+} concentration takes place, which is then eliminated by exchangers and active Ca^{2+} pumps that remove cytoplasmic Ca^{2+} to subcellular compartments and the extracellular space *(Fig. 5.1.)*.

Secondly, being non-selective for cations is another important characteristic of **P2X receptors**, which means they enable Na^{+} influx, K^{+} efflux and also Ca^{2+} influx to some extent. As a consequence, **their activation induces depolarization of the plasma membrane** [306], which **results in the opening**

of VDCCs and additional Ca^{2+} entry via the cell membrane *(Fig. 5.1.)*. As noted before, VDCCs are significant contributors of Ca^{2+} oscillations, which is corroborated by our observations that their blockade by nifedipine modifies the frequency of the transients. Consecutively, Ca^{2+} activated K^+ channels may become activated by increased cytoplasmic Ca^{2+} levels [307, 308], which, in turn, leads to membrane repolarization and stimulation of other ion channels, such as voltage-dependent potassium channels (K_V). Our group previously verified the expression of K_V channels in chondrogenic cells at the mRNA and protein level. Furthermore, we have found that a switch between $K_V1.1$ and $K_V1.3$ isoforms in the plasma membrane fraction is imperative for *in vitro* cartilage development of chicken limb bud HDC [195]. The fluctuations in membrane potential induced by the above (and possibly further) processes are likely to activate different subsets of VDCCs, which also contributes to the periodicity of Ca^{2+} oscillations. Nevertheless, there are other Ca^{2+} channels (such as ARCs, NMDA receptors, members of the TRP family, etc.) involved in Ca^{2+} entry via the cell membrane *(Fig. 5.1.)*, but analyzing their role in Ca^{2+} oscillations of chondrogenic cells was not part of this effort.

Thirdly, numerous signaling pathways, including those that involve the metabotropic P2Y receptors, focalize on Ca^{2+} release from internal stores by activating the PLC-InsP3 cascade. The resulting depletion of the ER Ca^{2+} store causes activation of CRACs via binding of STIM-ORAI activating regions (SOAR) of STIM1 and STIM2 to ORAI (or possibly other) CRAC proteins [309] *(Fig. 5.1.)*. Oscillations disappeared in cells with depleted stores, which highlights the importance of internal Ca^{2+} stores and SOCE in their maintenance. It should be noted that both of these factors are necessary and Ca^{2+} release from internal stores cannot maintain oscillations on the long term in a Ca^{2+}-free medium, where Ca^{2+} entry was prevented. Thus, we may conclude that **SOCE is an essential process in differentiating chondrocytes for Ca^{2+} influx and store replenishment**.

As noted above, decoding of the information content of Ca^{2+} oscillations, which at least partially depends on CaMKII enzyme subtypes and the calcineurin-NFAT cascade, leads to the differentiation of chondrogenic mesenchymal cells *(Fig. 5.1.)*. Remarkably, although in a different experimental setting, Ca^{2+}-dependent calmodulin binding drives nuclear translocation of SOX9, which again, is a key chondrogenic transcription factor [310]; this raises the possibility of this pathway also being involved in decoding oscillations in limb bud HDC. Nevertheless, the characterization of the precise role of the mechanisms listed above is yet to be performed in a chondrogenic model.

Finally, it is also noteworthy that the release and entry processes of Ca^{2+} are inseparably linked and operate as part of an integral system, thus it is not possible to canvass their function in Ca^{2+} oscillations separately. Consequently, the global hypothesis of our model is that most likely all of the above-mentioned processes play a role in a harmonized manner to maintain the normal Ca^{2+}

homeostasis of chondrogenic cells, similarly to what Kawano and colleagues proposed in the case of human MSCs [295]. Where the balance between different components is set is most likely the function of the stage of development.

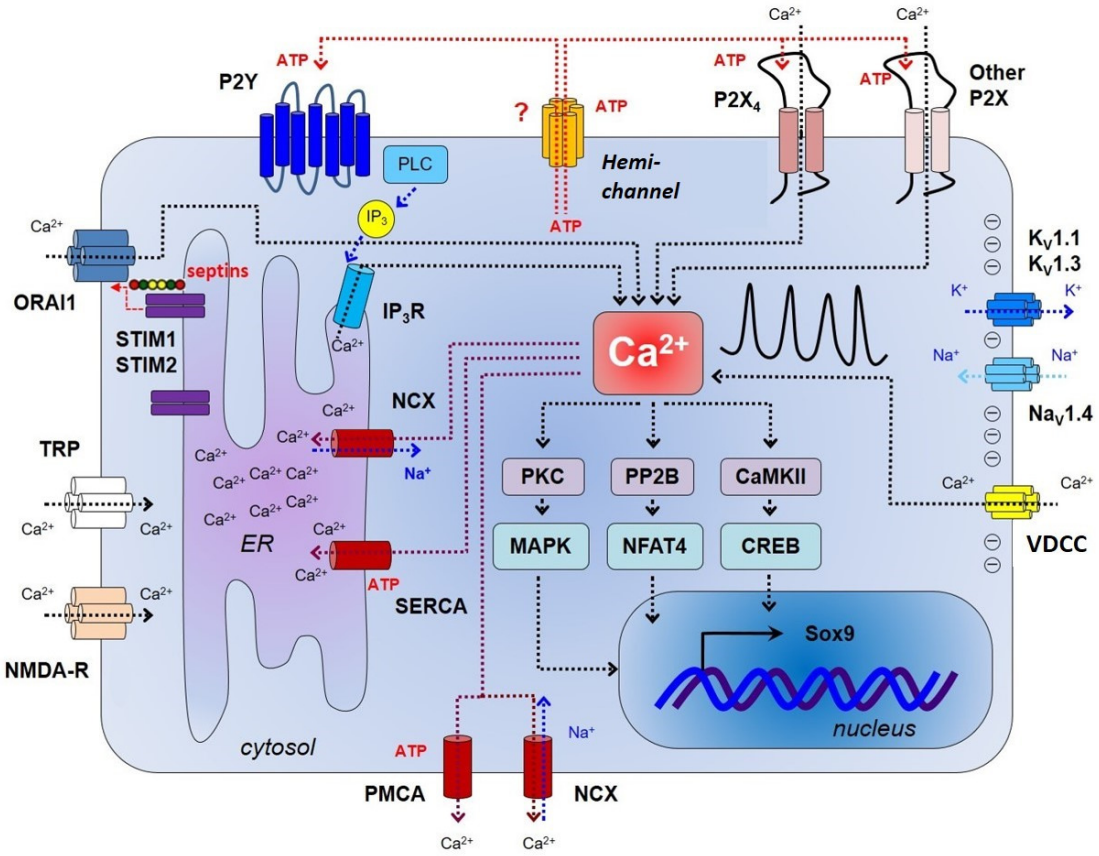

Fig. 5.1. Combined scheme of established components of Ca^{2+} homeostasis and signalling pathways that fine-tune Ca^{2+} oscillations in chondrogenic cells. Ca^{2+} entry is made possible by VDCCs, P2X purinergic receptors (P2X4 in particular), NMDA receptors or TRP channels. It may be hypothesized that connexin 43 hemichannels secrete ATP to the extracellular space. Voltage-gated K^+ channels convey alterations of resting membrane potential. A proven trigger of Ca^{2+}-release from the ER via the PLC-InsP3 cascade is the activation of Gq-coupled P2Y purinergic receptors. In turn, when Ca^{2+} stores are depleted, stromal interaction molecules (STIM1/STIM2) aggregate and trigger the opening of CRACs for which septin remodelling is also necessary. Ca^{2+} is taken back to the ER by SERCA and NCX. The concept of this figure is an adaptation from the work of Feske and coworkers [224].

5.4. Concluding Remarks

It has to be stated that not by a long shot can we consider the results and conclusions that are presented hereinbefore comprehensive. Although we are still quite a distance away from completely understanding Ca^{2+} signaling processes, let alone all regulatory mechanisms of chondrogenic cells of differentiating embryonic limb bud HDC, the present work should take us one step further in the desired direction.

As noted above, creating a human chondrogenic mesenchymal stem cell line that is capable of forming functional articular cartilage both *in vitro* and *in vivo* (and preferably without the external

addition of morphogens) is still among the number one challenges of our field. Regardless, our data obtained by the detailed comparison of differentiation potentials of some of the most common chondrogenic models can provide very useful guidance to make a choice for basic research purposes. We also provide instrumental perspectives that should be deliberated according to the purpose of the research. Notably, in addition to providing an analysis that applies a standardized temporal pattern to consider a unique and rich array of factors, which are only partially available from the literature, there are other groundbreaking aspects of our work: the assessment of Snorc, which is a novel marker for chondrogenic tissues and articular cartilage [263]; likewise, the monitoring of pluripotency markers in these chondrogenic micromass cultures has not been performed before and is also very scantily available for other models [311].

On the other hand, we have demonstrated that cells of the chicken primary micromass cultures display rapid transient elevations in their cytosolic Ca^{2+} concentration prior to and throughout differentiation (culturing days 1-2). These Ca^{2+} oscillations were characterized as spontaneous and albeit the molecular decoders of these cytosolic events are not well described, this work proposes some important mechanisms that are likely to play a critical role. Since oscillations eventually disappeared as chondroprogenitor cells turned into chondroblasts and chondrocytes, the phenomenon is presumably a characteristic of a particular stage of differentiation. There is accumulating evidence that suggests Ca^{2+} oscillations are implicated in the differentiation of numerous non-excitable cell types, including MSCs and articular chondrocytes. Furthermore, this work proposes the involvement of numerous pathways even if the nature and extent of their connection to rapid Ca^{2+} oscillations in chondrogenic cells is currently ambiguous; we have also noted cyclic changes in secreted ATP levels as a directly interacting partner of Ca^{2+} levels.

Even though our results are not directly translatable to the clinical practice, datasets such as this one can possibly lead to the identification of therapeutic targets for effective cures in the near future. The ultimate goal why we conduct research on the molecular processes of *in vitro* chondrogenesis is no less than to have an input in the shared effort that will eventually overcome articular chondropathies that hamper the life of millions of people. The findings above have the potential to be beneficial to future investigations that aim to employ the regeneration capacity of chondroprogenitor cells of both normal [312] and unhealthy articular cartilage [25].

6. Summary

This work summarizes the results of our research regarding the differentiation of the C3H10T1/2 cell line and primary limb bud-derived micromass cultures towards selected mesenchymal lineages, as well as the Ca^{2+} homeostasis of embryonic chicken chondrogenic limb bud HDC. **The most important results and conclusions of this PhD thesis are as follows**:

- Our comparative study demonstrated a largely punctual correlation between morphological and molecular investigations. Based on our analysis, **limb bud cultures are apparently a more suitable alternative to model osteochondral differentiation** *in vitro* than the examined cell line.
- Morphological signs of **adipogenesis were mainly found in c- and b-C3H10T1/2 micromass cultures**, while the BMP-2 overexpressing cells also demonstrated the **upregulation of *Pparγ2***.
- Although mRNA levels of the pluripotency markers display a relatively ambiguous pattern, the orderly **decreasing tendency in the expression of the avian homolog of *Oct4*, *PouV*** clearly suggests the proper advancement of differentiation.
- We were able to observe **rapid Ca^{2+} transients** displayed by cells of differentiating chicken HDC on days 1 and 2 of culturing and we have noted that the percentage of oscillatory cells demonstrated significant modifications concurrently with the progress of chondrogenesis.
- In addition to previously described contributing factors, **we have detected the expression of essential components of the molecular machinery needed to generate and maintain oscillations**: mRNAs of α_1 subunit of VDCCs (L-, R-, and T-type) and SOCE orchestrators (*Stim1*/*Stim2* and *Orai1*); protein level expression of the Ca^{2+} selective pore-forming α_1 subunit of VDCCs and STIM1/STIM2.
- We have shown that SOCE blockers impair the parameters of **SOCE** induced by store depletion during fluorescent single cell Ca^{2+} measurements of chicken limb bud HDC.
- It appears that Ca^{2+} entry blockers are able to cause serious disturbances in the Ca^{2+} homeostasis of cells of chick micromass cultures, while the previous treatment combined with store depletion had even more severe effects, suggesting the **importance of both the stores and the extracellular milieu in the maintenance of Ca^{2+} oscillations**; blockade of **L-type Ca^{2+} channels only appeared to influence the frequency of Ca^{2+} transients.**

7. Összefoglalás

A doktori értekezésben bemutatottak hivatottak összegezni a C3H10T1/2 sejtvonalból és az embrionális végtagtelepekből létrehozott high density kultúrák különböző mesenchymalis irányokban történő differenciálódását vizsgáló összehasonlító elemzésünk, valamint az embrionális csirke eredetű primer micromass kultúrák Ca^{2+} homeosztázisát célzó kísérleteink eredményeit. **A disszertáció legfontosabb eredményei és következtetései a következők**:

- Az összehasonlító tanulmányunk egyik jelentős tanulsága, hogy a morphologiai és molekuláris vizsgálataink túlnyomó részben jó korrelációban állnak. Analízisünk szerint **a végtagtelep eredetű sejtkultúrák előnyösebb alternatívát képeznek az osteochondralis differenciálódás *in vitro* modellezésére**, mint a vizsgált sejtvonal.
- **Az adipogenesis morphologiai jeleit elsősorban a c- és a b-C3H10T1/2 nagy sejtsűrűségű (HD – high density) kultúrák mutatják**, valamint ezzel párhuzamosan a BMP-2-t overexpresszáló sejtekben a *Pparγ2* felülszabályozása is megfigyelhető.
- Habár a pluripotencia markereinek mRNS szintjei meglehetősen zavaros mintázatot rajzolnak ki, **az *Oct4* csirke homológjának, azaz a *PouV*-nek, szabályos csökkenő tendenciát mutató kifejeződése egyértelműen a differenciálódás előrehaladását jelzi**.
- Sikeresen megfigyeltük a differenciálódó csirke HD kultúrák sejtjeire a tenyésztés első és második napján jellemző **gyors lefutású Ca^{2+} tranzienseket**, amik ráadásul a porcfejlődés előrehaladtával jelentősen változó számú és arányú sejtben jelennek meg.
- A laboratóriumunk által korábban leírt komponenseken túl **az oszcillációk képzéséhez és fenntartásához szükséges molekuláris gépezet számos nélkülözhetetlen elemét kimutattuk**: mRNS szinten a feszültségfüggő Ca^{2+} csatornák (L-, R- és T-típusú VDCC) α_1 alegységeit és a SOCE folyamatáért közvetlenül felelős molekulákat (*Stim1*/*Stim2* és *Orai1*) írtuk le. Egyúttal fehérje szinten pedig a feszültségfüggő Ca^{2+} csatornák kalciumszelektív pórus doménjét alkotó α_1 alegységek, valamint a STIM1/STIM2 fehérjék jelenlétét igazoltuk.
- Csirke végtagtelep HD kultúrákon végzett egysejtes Ca^{2+} mérések során kimutattuk, hogy az alkalmazott SOCE gátlás jelentősen lerontja a raktárürítést követő Ca^{2+} influx, azaz a **SOCE** paramétereit.
- Úgy tűnik, a Ca^{2+} belépését gátló kezelőanyagok önmagukban is képesek komoly zavarokat okozni a porcosodó csirke sejtkultúrák Ca^{2+} homeosztázisában, míg ezt a kezelést a belső raktárak ürítésével kombinálva még súlyosabb hatást tapasztaltunk, aminek ténye egyaránt **kiemeli a raktárak és az extracelluláris közeg szerepét is a Ca^{2+} oszcillációk fenntartásában**. Az **L-típusú feszültségfüggő Ca^{2+} csatornák gátlása megfigyeléseink szerint csak a Ca^{2+} tranziensek frekvenciáját befolyásolta**.

8. Bibliography

8.1. References

1. Yeung, M.Y., et al., *iCartiGD: the Integrated Cartilage Gene Database.* BMC Genet, 2007. **8**: p. 4.
2. Sharma, S., et al., *An siRNA screen for NFAT activation identifies septins as coordinators of store-operated Ca2+ entry.* Nature, 2013. **499**(7457): p. 238-42.
3. Shum, L. and G. Nuckolls, *The life cycle of chondrocytes in the developing skeleton.* Arthritis Res, 2002. **4**(2): p. 94-106.
4. Sadler, T.W., *Langman's Medical Embryology, 13th ed.* 2015: Wolters Kluwer Health.
5. LifeMap Sciences, I. *Human Cartilage Distribution/Embryonic Development Ontology Tree*. 2012 [cited 2017.
6. Pearle, A.D., R.F. Warren, and S.A. Rodeo, *Basic science of articular cartilage and osteoarthritis.* Clin Sports Med, 2005. **24**(1): p. 1-12.
7. Ross, M.H.P., W., *Histology: A Text and Atlas With Correlated Cell and Molecular Biology, 6th ed.* 2010: Lippincott Williams & Wilkins.
8. Eyre, D., *Collagen of articular cartilage.* Arthritis Res, 2002. **4**(1): p. 30-5.
9. Eyre, D.R., D.M. Brickley-Parsons, and M.J. Glimcher, *Predominance of type I collagen at the surface of avian articular cartilage.* FEBS Lett, 1978. **85**(2): p. 259-63.
10. Hagiwara, H., C. Schroter-Kermani, and H.J. Merker, *Localization of collagen type VI in articular cartilage of young and adult mice.* Cell Tissue Res, 1993. **272**(1): p. 155-60.
11. Poole, C.A., S. Ayad, and J.R. Schofield, *Chondrons from articular cartilage: I. Immunolocalization of type VI collagen in the pericellular capsule of isolated canine tibial chondrons.* J Cell Sci, 1988. **90 (Pt 4)**: p. 635-43.
12. Oldberg, A., et al., *Structure and function of extracellular matrix proteoglycans.* Biochem Soc Trans, 1990. **18**(5): p. 789-92.
13. Muir, I., *Biochemistry In Adult Articular Cartilage, 2nd ed.* 1979: Pitman Medical, Tunbridge Wells, England.
14. Kou, I. and S. Ikegawa, *SOX9-dependent and -independent transcriptional regulation of human cartilage link protein.* J Biol Chem, 2004. **279**(49): p. 50942-8.
15. Firner, S., et al., *Extracellular Distribution of Collagen II and Perifibrillar Adapter Proteins in Healthy and Osteoarthritic Human Knee Joint Cartilage.* J Histochem Cytochem, 2017. **65**(10): p. 593-606.
16. Poole, C.A., *Articular cartilage chondrons: form, function and failure.* J Anat, 1997. **191 (Pt 1)**: p. 1-13.
17. Wilusz, R.E., L.E. Defrate, and F. Guilak, *A biomechanical role for perlecan in the pericellular matrix of articular cartilage.* Matrix Biol, 2012. **31**(6): p. 320-7.
18. Poole, C.A., M.H. Flint, and B.W. Beaumont, *Morphological and functional interrelationships of articular cartilage matrices.* J Anat, 1984. **138 (Pt 1)**: p. 113-38.
19. Simkin, P.A., *A biography of the chondrocyte.* Ann Rheum Dis, 2008. **67**(8): p. 1064-8.
20. Linn, F.C. and L. Sokoloff, *Movement and Composition of Interstitial Fluid of Cartilage.* Arthritis Rheum, 1965. **8**: p. 481-94.
21. Mankin, H.J. and A.Z. Thrasher, *Water content and binding in normal and osteoarthritic human cartilage.* J Bone Joint Surg Am, 1975. **57**(1): p. 76-80.
22. Buckwalter, J.A., *Articular cartilage.* Instr Course Lect, 1983. **32**: p. 349-70.
23. Juhasz, T., et al., *Mechanical loading stimulates chondrogenesis via the PKA/CREB-Sox9 and PP2A pathways in chicken micromass cultures.* Cell Signal, 2014. **26**(3): p. 468-82.
24. Fellows, C.R., et al., *Adipose, Bone Marrow and Synovial Joint-Derived Mesenchymal Stem Cells for Cartilage Repair.* Front Genet, 2016. **7**: p. 213.
25. Koelling, S., et al., *Migratory chondrogenic progenitor cells from repair tissue during the later stages of human osteoarthritis.* Cell Stem Cell, 2009. **4**(4): p. 324-35.
26. Oussedik, S., K. Tsitskaris, and D. Parker, *Treatment of articular cartilage lesions of the knee by microfracture or autologous chondrocyte implantation: a systematic review.* Arthroscopy, 2015. **31**(4): p. 732-44.
27. Cancedda, R., et al., *Developmental control of chondrogenesis and osteogenesis.* Int J Dev Biol, 2000. **44**(6): p. 707-14.
28. Curl, W.W., et al., *Cartilage injuries: a review of 31,516 knee arthroscopies.* Arthroscopy, 1997. **13**(4): p. 456-60.
29. Widuchowski, W., J. Widuchowski, and T. Trzaska, *Articular cartilage defects: study of 25,124 knee arthroscopies.* Knee, 2007. **14**(3): p. 177-82.
30. Buckwalter, J.A. and T.D. Brown, *Joint injury, repair, and remodeling: roles in post-traumatic osteoarthritis.* Clin Orthop Relat Res, 2004(423): p. 7-16.
31. Mankin, H.J., *The response of articular cartilage to mechanical injury.* J Bone Joint Surg Am, 1982. **64**(3): p. 460-6.
32. Ochi, M., et al., *Transplantation of cartilage-like tissue made by tissue engineering in the treatment of cartilage defects of the knee.* J Bone Joint Surg Br, 2002. **84**(4): p. 571-8.
33. Dold, A.P., et al., *Platelet-rich plasma in the management of articular cartilage pathology: a systematic review.* Clin J Sport Med, 2014. **24**(1): p. 31-43.
34. Buckwalter, J.A. and H.J. Mankin, *Articular cartilage: tissue design and chondrocyte-matrix interactions.* Instr Course Lect, 1998. **47**: p. 477-86.
35. Furukawa, T., et al., *Biochemical studies on repair cartilage resurfacing experimental defects in the rabbit knee.* J Bone Joint Surg Am, 1980. **62**(1): p. 79-89.
36. Smith, G.D., G. Knutsen, and J.B. Richardson, *A clinical review of cartilage repair techniques.* J Bone Joint Surg Br, 2005. **87**(4): p. 445-9.
37. Holyoak, D.T., et al., *Osteoarthritis: Pathology, Mouse Models, and Nanoparticle Injectable Systems for Targeted Treatment.* Ann Biomed Eng, 2016. **44**(6): p. 2062-75.
38. Grodzinsky, A.J., et al., *Cartilage tissue remodeling in response to mechanical forces.* Annu Rev Biomed Eng, 2000. **2**: p. 691-713.
39. Mow, V.C. and X.E. Guo, *Mechano-electrochemical properties of articular cartilage: their inhomogeneities and anisotropies.* Annu Rev Biomed Eng, 2002. **4**: p. 175-209.
40. Nelson, F., et al., *Early post-traumatic osteoarthritis-like changes in human articular cartilage following rupture of the anterior cruciate ligament.* Osteoarthritis Cartilage, 2006. **14**(2): p. 114-9.
41. Williamson, A.K., A.C. Chen, and R.L. Sah, *Compressive properties and function-composition relationships of developing bovine articular cartilage.* J Orthop Res, 2001. **19**(6): p. 1113-21.
42. Hootman, J.M. and C.G. Helmick, *Projections of US prevalence of arthritis and associated activity limitations.* Arthritis Rheum, 2006. **54**(1): p. 226-9.
43. Hunter, D.J. and D.T. Felson, *Osteoarthritis.* BMJ, 2006. **332**(7542): p. 639-42.
44. Bank, R.A., et al., *The increased swelling and instantaneous deformation of osteoarthritic cartilage is highly correlated with collagen degradation.* Arthritis Rheum, 2000. **43**(10): p. 2202-10.

45. Maroudas, A.I., *Balance between swelling pressure and collagen tension in normal and degenerate cartilage.* Nature, 1976. **260**(5554): p. 808-9.
46. Khan, I.M., R. Williams, and C.W. Archer, *One flew over the progenitor's nest: migratory cells find a home in osteoarthritic cartilage.* Cell Stem Cell, 2009. **4**(4): p. 282-4.
47. Li, J. and S. Dong, *The Signaling Pathways Involved in Chondrocyte Differentiation and Hypertrophic Differentiation.* Stem Cells Int, 2016. **2016**: p. 2470351.
48. Matta, C., et al., *Purinergic signalling-evoked intracellular Ca(2+) concentration changes in the regulation of chondrogenesis and skeletal muscle formation.* Cell Calcium, 2016. **59**(2-3): p. 108-16.
49. Nakashima, K., et al., *The novel zinc finger-containing transcription factor osterix is required for osteoblast differentiation and bone formation.* Cell, 2002. **108**(1): p. 17-29.
50. Ahrens, P.B., M. Solursh, and R.S. Reiter, *Stage-related capacity for limb chondrogenesis in cell culture.* Dev Biol, 1977. **60**(1): p. 69-82.
51. Archer, C.W., et al., *Myogenic potential of chick limb bud mesenchyme in micromass culture.* Anat Embryol (Berl), 1992. **185**(3): p. 299-306.
52. Hamburger, V. and H.L. Hamilton, *A series of normal stages in the development of the chick embryo.* J Morphol, 1951. **88**(1): p. 49-92.
53. Oh, C.D., et al., *Opposing role of mitogen-activated protein kinase subtypes, erk-1/2 and p38, in the regulation of chondrogenesis of mesenchymes.* J Biol Chem, 2000. **275**(8): p. 5613-9.
54. Zakany, R., et al., *Hydrogen peroxide inhibits formation of cartilage in chicken micromass cultures and decreases the activity of calcineurin: implication of ERK1/2 and Sox9 pathways.* Exp Cell Res, 2005. **305**(1): p. 190-9.
55. Murakami, S., et al., *Up-regulation of the chondrogenic Sox9 gene by fibroblast growth factors is mediated by the mitogen-activated protein kinase pathway.* Proc Natl Acad Sci U S A, 2000. **97**(3): p. 1113-8.
56. Seghatoleslami, M.R., et al., *Progression of chondrogenesis in C3H10T1/2 cells is associated with prolonged and tight regulation of ERK1/2.* J Cell Biochem, 2003. **88**(6): p. 1129-44.
57. Somogyi, C.S., et al., *Polymodal Transient Receptor Potential Vanilloid (TRPV) Ion Channels in Chondrogenic Cells.* Int J Mol Sci, 2015. **16**(8): p. 18412-38.
58. Daumer, K.M., A.C. Tufan, and R.S. Tuan, *Long-term in vitro analysis of limb cartilage development: involvement of Wnt signaling.* J Cell Biochem, 2004. **93**(3): p. 526-41.
59. Hosseini-Farahabadi, S., et al., *Dual functions for WNT5A during cartilage development and in disease.* Matrix Biol, 2013. **32**(5): p. 252-64.
60. Lee, Y.S. and C.M. Chuong, *Activation of protein kinase A is a pivotal step involved in both BMP-2- and cyclic AMP-induced chondrogenesis.* J Cell Physiol, 1997. **170**(2): p. 153-65.
61. Solursh, M., et al., *Increase in levels of cyclic AMP during avian limb chondrogenesis in vitro.* Differentiation, 1979. **15**(3): p. 183-6.
62. Widelitz, R.B., et al., *Adhesion molecules in skeletogenesis: II. Neural cell adhesion molecules mediate precartilaginous mesenchymal condensations and enhance chondrogenesis.* J Cell Physiol, 1993. **156**(2): p. 399-411.
63. Zakany, R., et al., *Okadaic acid-induced inhibition of protein phosphatase 2A enhances chondrogenesis in chicken limb bud micromass cell cultures.* Anat Embryol (Berl), 2001. **203**(1): p. 23-34.
64. Matta, C. and R. Zakany, *Calcium signalling in chondrogenesis: implications for cartilage repair.* Front Biosci (Schol Ed), 2013. **5**: p. 305-24.
65. Cash, D.E., et al., *Retinoic acid receptor alpha function in vertebrate limb skeletogenesis: a modulator of chondrogenesis.* J Cell Biol, 1997. **136**(2): p. 445-57.
66. Bobick, B.E., P.G. Alexander, and R.S. Tuan, *High efficiency transfection of embryonic limb mesenchyme with plasmid DNA using square wave pulse electroporation and sucrose buffer.* Biotechniques, 2014. **56**(2): p. 85-9.
67. Benya, P.D. and J.D. Shaffer, *Dedifferentiated chondrocytes reexpress the differentiated collagen phenotype when cultured in agarose gels.* Cell, 1982. **30**(1): p. 215-24.
68. Schulze-Tanzil, G., et al., *Loss of chondrogenic potential in dedifferentiated chondrocytes correlates with deficient Shc-Erk interaction and apoptosis.* Osteoarthritis Cartilage, 2004. **12**(6): p. 448-58.
69. Atsumi, T., et al., *A chondrogenic cell line derived from a differentiating culture of AT805 teratocarcinoma cells.* Cell Differ Dev, 1990. **30**(2): p. 109-16.
70. Grigoriadis, A.E., J.N. Heersche, and J.E. Aubin, *Differentiation of muscle, fat, cartilage, and bone from progenitor cells present in a bone-derived clonal cell population: effect of dexamethasone.* J Cell Biol, 1988. **106**(6): p. 2139-51.
71. Denker, A.E., et al., *Chondrogenic differentiation of murine C3H10T1/2 multipotential mesenchymal cells: I. Stimulation by bone morphogenetic protein-2 in high-density micromass cultures.* Differentiation, 1999. **64**(2): p. 67-76.
72. Roy, R., et al., *Differentiation and mineralization of murine mesenchymal C3H10T1/2 cells in micromass culture.* Differentiation, 2010. **79**(4-5): p. 211-7.
73. Ahrens, M., et al., *Expression of human bone morphogenetic proteins-2 or -4 in murine mesenchymal progenitor C3H10T1/2 cells induces differentiation into distinct mesenchymal cell lineages.* DNA Cell Biol, 1993. **12**(10): p. 871-80.
74. Matta, C., et al., *Purinergic signalling is required for calcium oscillations in migratory chondrogenic progenitor cells.* Pflugers Arch, 2015. **467**(2): p. 429-42.
75. Fodor, J., et al., *Ionotropic purinergic receptor P2X4 is involved in the regulation of chondrogenesis in chicken micromass cell cultures.* Cell Calcium, 2009. **45**(5): p. 421-30.
76. Alsalameh, S., et al., *Identification of mesenchymal progenitor cells in normal and osteoarthritic human articular cartilage.* Arthritis Rheum, 2004. **50**(5): p. 1522-32.
77. Dowthwaite, G.P., et al., *The surface of articular cartilage contains a progenitor cell population.* J Cell Sci, 2004. **117**(Pt 6): p. 889-97.
78. de Sousa, E.B., et al., *Synovial fluid and synovial membrane mesenchymal stem cells: latest discoveries and therapeutic perspectives.* Stem Cell Res Ther, 2014. **5**(5): p. 112.
79. Nagura, I., et al., *Characterization of progenitor cells derived from torn human rotator cuff tendons by gene expression patterns of chondrogenesis, osteogenesis, and adipogenesis.* J Orthop Surg Res, 2016. **11**: p. 40.
80. Dragoo, J.L., et al., *Tissue-engineered cartilage and bone using stem cells from human infrapatellar fat pads.* J Bone Joint Surg Br, 2003. **85**(5): p. 740-7.
81. Wakitani, S., et al., *Human autologous culture expanded bone marrow mesenchymal cell transplantation for repair of cartilage defects in osteoarthritic knees.* Osteoarthritis Cartilage, 2002. **10**(3): p. 199-206.
82. Noth, U., et al., *Multilineage mesenchymal differentiation potential of human trabecular bone-derived cells.* J Orthop Res, 2002. **20**(5): p. 1060-9.
83. Jackson, W.M., L.J. Nesti, and R.S. Tuan, *Potential therapeutic applications of muscle-derived mesenchymal stem and progenitor cells.* Expert Opin Biol Ther, 2010. **10**(4): p. 505-17.
84. Tremolada, C., et al., *Mesenchymal Stem Cells in Lipogems, a Reverse Story: from Clinical Practice to Basic Science.* Methods Mol Biol, 2016. **1416**: p. 109-22.
85. Zuk, P.A., et al., *Multilineage cells from human adipose tissue: implications for cell-based therapies.* Tissue Eng, 2001. **7**(2): p. 211-28.

86. Fong, C.Y., et al., *Derivation efficiency, cell proliferation, freeze-thaw survival, stem-cell properties and differentiation of human Wharton's jelly stem cells.* Reprod Biomed Online, 2010. **21**(3): p. 391-401.
87. Heinonen, J., et al., *Defects in chondrocyte maturation and secondary ossification in mouse knee joint epiphyses due to Snorc deficiency.* Osteoarthritis Cartilage, 2017. **25**(7): p. 1132-1142.
88. Cleary, M.A., et al., *FGF, TGFbeta and Wnt crosstalk: embryonic to in vitro cartilage development from mesenchymal stem cells.* J Tissue Eng Regen Med, 2015. **9**(4): p. 332-42.
89. Waller, K.A., et al., *Intra-articular Recombinant Human Proteoglycan 4 Mitigates Cartilage Damage After Destabilization of the Medial Meniscus in the Yucatan Minipig.* Am J Sports Med, 2017. **45**(7): p. 1512-1521.
90. Shen, G., *The role of type X collagen in facilitating and regulating endochondral ossification of articular cartilage.* Orthod Craniofac Res, 2005. **8**(1): p. 11-7.
91. Ye, X., et al., *Inhibition of Runx2 signaling by TNF-alpha in ST2 murine bone marrow stromal cells undergoing osteogenic differentiation.* In Vitro Cell Dev Biol Anim, 2016. **52**(10): p. 1026-1033.
92. Rashid, H., et al., *Sp7 and Runx2 molecular complex synergistically regulate expression of target genes.* Connect Tissue Res, 2014. **55 Suppl 1**: p. 83-7.
93. Zaitseva, O.V., S.G. Shandrenko, and M.M. Veliky, *Biochemical markers of bone collagen type I metabolism.* Ukr Biochem J, 2015. **87**(1): p. 21-32.
94. Zhou, S., et al., *Effects of Hypergravity on Osteopontin Expression in Osteoblasts.* PLoS One, 2015. **10**(6): p. e0128846.
95. Seibel, M.J., *Biochemical markers of bone turnover: part I: biochemistry and variability.* Clin Biochem Rev, 2005. **26**(4): p. 97-122.
96. Yamamoto, T., et al., *Transcriptome and Metabolome Analyses in Exogenous FABP4- and FABP5-Treated Adipose-Derived Stem Cells.* PLoS One, 2016. **11**(12): p. e0167825.
97. Xu, A., et al., *Adipocyte fatty acid-binding protein is a plasma biomarker closely associated with obesity and metabolic syndrome.* Clin Chem, 2006. **52**(3): p. 405-13.
98. Otto, T.C. and M.D. Lane, *Adipose development: from stem cell to adipocyte.* Crit Rev Biochem Mol Biol, 2005. **40**(4): p. 229-42.
99. Choi, J., et al., *Maturation of Adipocytes is Suppressed by Fluid Shear Stress.* Cell Biochem Biophys, 2017. **75**(1): p. 87-94.
100. Ding, J., et al., *Oct4 links multiple epigenetic pathways to the pluripotency network.* Cell Res, 2012. **22**(1): p. 155-67.
101. Rosner, M.H., et al., *A POU-domain transcription factor in early stem cells and germ cells of the mammalian embryo.* Nature, 1990. **345**(6277): p. 686-92.
102. Kehler, J., et al., *Oct4 is required for primordial germ cell survival.* EMBO Rep, 2004. **5**(11): p. 1078-83.
103. Lavial, F., et al., *The Oct4 homologue PouV and Nanog regulate pluripotency in chicken embryonic stem cells.* Development, 2007. **134**(19): p. 3549-63.
104. Chambers, I., et al., *Functional expression cloning of Nanog, a pluripotency sustaining factor in embryonic stem cells.* Cell, 2003. **113**(5): p. 643-55.
105. Liu, K., et al., *The multiple roles for Sox2 in stem cell maintenance and tumorigenesis.* Cell Signal, 2013. **25**(5): p. 1264-71.
106. Bieberich, E.W., G., *Molecular Mechanisms Underlying Pluripotency*, in *Pluripotent Stem Cells*, D.N.L. Bhartiya, N., Editor. 2013, IntechOpen: London, United Kingdom.
107. Cancedda, R., F. Descalzi Cancedda, and P. Castagnola, *Chondrocyte differentiation.* Int Rev Cytol, 1995. **159**: p. 265-358.
108. Oberlender, S.A. and R.S. Tuan, *Expression and functional involvement of N-cadherin in embryonic limb chondrogenesis.* Development, 1994. **120**(1): p. 177-87.
109. Yodmuang, S., et al., *Synergistic effects of hypoxia and morphogenetic factors on early chondrogenic commitment of human embryonic stem cells in embryoid body culture.* Stem Cell Rev Rep, 2015. **11**(2): p. 228-41.
110. Ornitz, D.M. and P.J. Marie, *FGF signaling pathways in endochondral and intramembranous bone development and human genetic disease.* Genes Dev, 2002. **16**(12): p. 1446-65.
111. Tavella, S., et al., *N-CAM and N-cadherin expression during in vitro chondrogenesis.* Exp Cell Res, 1994. **215**(2): p. 354-62.
112. Zhang, W., C. Green, and N.S. Stott, *Bone morphogenetic protein-2 modulation of chondrogenic differentiation in vitro involves gap junction-mediated intercellular communication.* J Cell Physiol, 2002. **193**(2): p. 233-43.
113. Makarenkova, H. and K. Patel, *Gap junction signalling mediated through connexin-43 is required for chick limb development.* Dev Biol, 1999. **207**(2): p. 380-92.
114. Wezeman, F.H., *Morphological foundations of precartilage development in mesenchyme.* Microsc Res Tech, 1998. **43**(2): p. 91-101.
115. Ichinose, S., et al., *Comparative sequential morphological analyses during in vitro chondrogenesis and osteogenesis of mesenchymal stem cells embedded in collagen gels.* Med Mol Morphol, 2013. **46**(1): p. 24-33.
116. Kim, M., et al., *Staurosporine and cytochalasin D induce chondrogenesis by regulation of actin dynamics in different way.* Exp Mol Med, 2012. **44**(9): p. 521-8.
117. Carballo, C.B., et al., *Basic Science of Articular Cartilage.* Clin Sports Med, 2017. **36**(3): p. 413-425.
118. Gelsleichter, J. and J.A. Musick, *Effects of insulin-like growth factor-I, corticosterone, and 3,3', 5-tri-iodo-L-thyronine on glycosaminoglycan synthesis in vertebral cartilage of the clearnose skate, Raja eglanteria.* J Exp Zool, 1999. **284**(5): p. 549-56.
119. Jakob, M., et al., *Chondrogenesis of expanded adult human articular chondrocytes is enhanced by specific prostaglandins.* Rheumatology (Oxford), 2004. **43**(7): p. 852-7.
120. Bertolo, A., et al., *Physiological testosterone levels enhance chondrogenic extracellular matrix synthesis by male intervertebral disc cells in vitro, but not by mesenchymal stem cells.* Spine J, 2014. **14**(3): p. 455-68.
121. Koelling, S. and N. Miosge, *Sex differences of chondrogenic progenitor cells in late stages of osteoarthritis.* Arthritis Rheum, 2010. **62**(4): p. 1077-87.
122. Jiang, H., et al., *Modulation of limb bud chondrogenesis by retinoic acid and retinoic acid receptors.* Int J Dev Biol, 1995. **39**(4): p. 617-27.
123. Tavella, S., et al., *Regulated expression of fibronectin, laminin and related integrin receptors during the early chondrocyte differentiation.* J Cell Sci, 1997. **110 (Pt 18)**: p. 2261-70.
124. Mackie, E.J. and L.I. Murphy, *The role of tenascin-C and related glycoproteins in early chondrogenesis.* Microsc Res Tech, 1998. **43**(2): p. 102-10.
125. Tien, J.Y. and A.P. Spicer, *Three vertebrate hyaluronan synthases are expressed during mouse development in distinct spatial and temporal patterns.* Dev Dyn, 2005. **233**(1): p. 130-41.
126. Li, Y., et al., *Hyaluronan in limb morphogenesis.* Dev Biol, 2007. **305**(2): p. 411-20.
127. Nicoll, S.B., et al., *Hyaluronidases and CD44 undergo differential modulation during chondrogenesis.* Biochem Biophys Res Commun, 2002. **292**(4): p. 819-25.
128. von der Mark, K., *Biochemical processes in cartilage and bone formation: Effect of collagen on the chondrogenic differentiation of somite and limb bud mesenchyme. In FEBS Federation of European Biochemical Societies 11th Meeting Copenhagen 1977*, ed. K.W.N. Kastrup, J. H. Vol. vol. 48, colloquium B3. 1978: Pergamon Press, Oxford, New York.
129. Dessau, W., et al., *Changes in the patterns of collagens and fibronectin during limb-bud chondrogenesis.* J Embryol Exp Morphol, 1980. **57**: p. 51-60.

130. Lui, V.C., et al., *Tissue-specific and differential expression of alternatively spliced alpha 1(II) collagen mRNAs in early human embryos.* Dev Dyn, 1995. **203**(2): p. 198-211.
131. Takacs, R., et al., *Comparative analysis of osteogenic/chondrogenic differentiation potential in primary limb bud-derived and C3H10T1/2 cell line-based mouse micromass cultures.* Int J Mol Sci, 2013. **14**(8): p. 16141-67.
132. Minegishi, Y., K. Hosokawa, and N. Tsumaki, *Time-lapse observation of the dedifferentiation process in mouse chondrocytes using chondrocyte-specific reporters.* Osteoarthritis Cartilage, 2013. **21**(12): p. 1968-75.
133. Kawakami, Y., J. Rodriguez-Leon, and J.C. Izpisua Belmonte, *The role of TGFbetas and Sox9 during limb chondrogenesis.* Curr Opin Cell Biol, 2006. **18**(6): p. 723-9.
134. Quintana, L., N.I. zur Nieden, and C.E. Semino, *Morphogenetic and regulatory mechanisms during developmental chondrogenesis: new paradigms for cartilage tissue engineering.* Tissue Eng Part B Rev, 2009. **15**(1): p. 29-41.
135. Lefebvre, V., P. Li, and B. de Crombrugghe, *A new long form of Sox5 (L-Sox5), Sox6 and Sox9 are coexpressed in chondrogenesis and cooperatively activate the type II collagen gene.* EMBO J, 1998. **17**(19): p. 5718-33.
136. Matta, C., et al., *Ser/Thr-phosphoprotein phosphatases in chondrogenesis: neglected components of a two-player game.* Cell Signal, 2014. **26**(10): p. 2175-85.
137. Kosher, R.A., M.P. Savage, and S.C. Chan, *Cyclic AMP derivatives stimulate the chondrogenic differentiation of the mesoderm subjacent to the apical ectodermal ridge of the chick limb bud.* J Exp Zool, 1979. **209**(2): p. 221-7.
138. Matta, C. and A. Mobasheri, *Regulation of chondrogenesis by protein kinase C: Emerging new roles in calcium signalling.* Cell Signal, 2014. **26**(5): p. 979-1000.
139. Piera-Velazquez, S., et al., *Regulation of the human SOX9 promoter by Sp1 and CREB.* Exp Cell Res, 2007. **313**(6): p. 1069-79.
140. Huang, W., et al., *Phosphorylation of SOX9 by cyclic AMP-dependent protein kinase A enhances SOX9's ability to transactivate a Col2a1 chondrocyte-specific enhancer.* Mol Cell Biol, 2000. **20**(11): p. 4149-58.
141. Zakany, R., et al., *Protein phosphatase 2A is involved in the regulation of protein kinase A signaling pathway during in vitro chondrogenesis.* Exp Cell Res, 2002. **275**(1): p. 1-8.
142. Tomita, M., et al., *Calcineurin and NFAT4 induce chondrogenesis.* J Biol Chem, 2002. **277**(44): p. 42214-8.
143. Crabtree, G.R. and E.N. Olson, *NFAT signaling: choreographing the social lives of cells.* Cell, 2002. **109 Suppl**: p. S67-79.
144. Crabtree, G.R., *Calcium, calcineurin, and the control of transcription.* J Biol Chem, 2001. **276**(4): p. 2313-6.
145. Yaykasli, K.O., et al., *ADAMTS9 activation by interleukin 1 beta via NFATc1 in OUMS-27 chondrosarcoma cells and in human chondrocytes.* Mol Cell Biochem, 2009. **323**(1-2): p. 69-79.
146. Green, J.D., et al., *Multifaceted signaling regulators of chondrogenesis: Implications in cartilage regeneration and tissue engineering.* Genes Dis, 2015. **2**(4): p. 307-327.
147. Karamboulas, K., H.J. Dranse, and T.M. Underhill, *Regulation of BMP-dependent chondrogenesis in early limb mesenchyme by TGFbeta signals.* J Cell Sci, 2010. **123**(Pt 12): p. 2068-76.
148. Yoon, B.S., et al., *Bmpr1a and Bmpr1b have overlapping functions and are essential for chondrogenesis in vivo.* Proc Natl Acad Sci U S A, 2005. **102**(14): p. 5062-7.
149. Madry, H., et al., *Transforming growth factor Beta-releasing scaffolds for cartilage tissue engineering.* Tissue Eng Part B Rev, 2014. **20**(2): p. 106-25.
150. Coleman, C.M. and R.S. Tuan, *Growth/differentiation factor 5 enhances chondrocyte maturation.* Dev Dyn, 2003. **228**(2): p. 208-16.
151. Francis-West, P.H., et al., *BMP/GDF-signalling interactions during synovial joint development.* Cell Tissue Res, 1999. **296**(1): p. 111-9.
152. Massague, J., J. Seoane, and D. Wotton, *Smad transcription factors.* Genes Dev, 2005. **19**(23): p. 2783-810.
153. Iwai, T., et al., *Smad7 Inhibits chondrocyte differentiation at multiple steps during endochondral bone formation and down-regulates p38 MAPK pathways.* J Biol Chem, 2008. **283**(40): p. 27154-64.
154. Zhang, Y.E., *Non-Smad pathways in TGF-beta signaling.* Cell Res, 2009. **19**(1): p. 128-39.
155. Pizette, S. and L. Niswander, *BMPs are required at two steps of limb chondrogenesis: formation of prechondrogenic condensations and their differentiation into chondrocytes.* Dev Biol, 2000. **219**(2): p. 237-49.
156. Merino, R., et al., *The BMP antagonist Gremlin regulates outgrowth, chondrogenesis and programmed cell death in the developing limb.* Development, 1999. **126**(23): p. 5515-22.
157. Niswander, L., et al., *FGF-4 replaces the apical ectodermal ridge and directs outgrowth and patterning of the limb.* Cell, 1993. **75**(3): p. 579-87.
158. Ito, T., et al., *FGF-2 suppresses cellular senescence of human mesenchymal stem cells by down-regulation of TGF-beta2.* Biochem Biophys Res Commun, 2007. **359**(1): p. 108-14.
159. Sawada, R., T. Ito, and T. Tsuchiya, *Changes in expression of genes related to cell proliferation in human mesenchymal stem cells during in vitro culture in comparison with cancer cells.* J Artif Organs, 2006. **9**(3): p. 179-84.
160. Retting, K.N., et al., *BMP canonical Smad signaling through Smad1 and Smad5 is required for endochondral bone formation.* Development, 2009. **136**(7): p. 1093-104.
161. Chubinskaya, S. and K.E. Kuettner, *Regulation of osteogenic proteins by chondrocytes.* Int J Biochem Cell Biol, 2003. **35**(9): p. 1323-40.
162. Grunder, T., et al., *Bone morphogenetic protein (BMP)-2 enhances the expression of type II collagen and aggrecan in chondrocytes embedded in alginate beads.* Osteoarthritis Cartilage, 2004. **12**(7): p. 559-67.
163. Hellingman, C.A., et al., *Smad signaling determines chondrogenic differentiation of bone-marrow-derived mesenchymal stem cells: inhibition of Smad1/5/8P prevents terminal differentiation and calcification.* Tissue Eng Part A, 2011. **17**(7-8): p. 1157-67.
164. Hata, K., et al., *Differential roles of Smad1 and p38 kinase in regulation of peroxisome proliferator-activating receptor gamma during bone morphogenetic protein 2-induced adipogenesis.* Mol Biol Cell, 2003. **14**(2): p. 545-55.
165. Mellor, H. and P.J. Parker, *The extended protein kinase C superfamily.* Biochem J, 1998. **332 (Pt 2)**: p. 281-92.
166. Choi, B., et al., *Expression of protein kinase C isozymes that are required for chondrogenesis of chick limb bud mesenchymal cells.* Biochem Biophys Res Commun, 1995. **216**(3): p. 1034-40.
167. Oancea, E. and T. Meyer, *Protein kinase C as a molecular machine for decoding calcium and diacylglycerol signals.* Cell, 1998. **95**(3): p. 307-18.
168. Yu, J.C. and A.I. Gotlieb, *Disruption of endothelial actin microfilaments by protein kinase C inhibitors.* Microvasc Res, 1992. **43**(1): p. 100-11.
169. Scherle, P.A., et al., *The effects of IL-1 on mitogen-activated protein kinases in rabbit articular chondrocytes.* Biochem Biophys Res Commun, 1997. **230**(3): p. 573-7.
170. Matta, C., et al., *PKCdelta is a positive regulator of chondrogenesis in chicken high density micromass cell cultures.* Biochimie, 2011. **93**(2): p. 149-59.
171. Chang, S.H., et al., *Protein kinase C regulates chondrogenesis of mesenchymes via mitogen-activated protein kinase signaling.* J Biol Chem, 1998. **273**(30): p. 19213-9.
172. Yoon, Y.M., et al., *Protein kinase A regulates chondrogenesis of mesenchymal cells at the post-precartilage condensation stage via protein kinase C-alpha signaling.* J Bone Miner Res, 2000. **15**(11): p. 2197-205.

173. Martin, F., et al., *Protein kinase C phosphorylates the cAMP response element binding protein in the hypothalamic paraventricular nucleus during morphine withdrawal.* Br J Pharmacol, 2011. **163**(4): p. 857-75.
174. Kawasaki, T., et al., *Protein kinase C-induced phosphorylation of Orai1 regulates the intracellular Ca2+ level via the store-operated Ca2+ channel.* J Biol Chem, 2010. **285**(33): p. 25720-30.
175. Ma, R., et al., *Protein kinase C activates store-operated Ca(2+) channels in human glomerular mesangial cells.* J Biol Chem, 2001. **276**(28): p. 25759-65.
176. Schubert, R., T. Noack, and V.N. Serebryakov, *Protein kinase C reduces the KCa current of rat tail artery smooth muscle cells.* Am J Physiol, 1999. **276**(3): p. C648-58.
177. Nagahama, T., et al., *Role of protein kinase C in angiotensin II-induced constriction of renal microvessels.* Kidney Int, 2000. **57**(1): p. 215-23.
178. Pearson, G., et al., *Mitogen-activated protein (MAP) kinase pathways: regulation and physiological functions.* Endocr Rev, 2001. **22**(2): p. 153-83.
179. Nakamura, K., et al., *p38 mitogen-activated protein kinase functionally contributes to chondrogenesis induced by growth/differentiation factor-5 in ATDC5 cells.* Exp Cell Res, 1999. **250**(2): p. 351-63.
180. Hwang, S.G., et al., *Wnt-3a regulates chondrocyte differentiation via c-Jun/AP-1 pathway.* FEBS Lett, 2005. **579**(21): p. 4837-42.
181. Stanton, L.A., T.M. Underhill, and F. Beier, *MAP kinases in chondrocyte differentiation.* Dev Biol, 2003. **263**(2): p. 165-75.
182. Mobasheri, A., et al., *Integrins and stretch activated ion channels; putative components of functional cell surface mechanoreceptors in articular chondrocytes.* Cell Biol Int, 2002. **26**(1): p. 1-18.
183. Endo, M., *Calcium ion as a second messenger with special reference to excitation-contraction coupling.* J Pharmacol Sci, 2006. **100**(5): p. 519-24.
184. Contreras, L., et al., *Mitochondria: the calcium connection.* Biochim Biophys Acta, 2010. **1797**(6-7): p. 607-18.
185. Pinton, P., T. Pozzan, and R. Rizzuto, *The Golgi apparatus is an inositol 1,4,5-trisphosphate-sensitive Ca2+ store, with functional properties distinct from those of the endoplasmic reticulum.* EMBO J, 1998. **17**(18): p. 5298-308.
186. Mitchell, K.J., et al., *Dense core secretory vesicles revealed as a dynamic Ca(2+) store in neuroendocrine cells with a vesicle-associated membrane protein aequorin chimaera.* J Cell Biol, 2001. **155**(1): p. 41-51.
187. Drago, I., et al., *Calcium dynamics in the peroxisomal lumen of living cells.* J Biol Chem, 2008. **283**(21): p. 14384-90.
188. Gerasimenko, J.V., et al., *Calcium uptake via endocytosis with rapid release from acidifying endosomes.* Curr Biol, 1998. **8**(24): p. 1335-8.
189. Rodriguez, A., et al., *Lysosomes behave as Ca2+-regulated exocytic vesicles in fibroblasts and epithelial cells.* J Cell Biol, 1997. **137**(1): p. 93-104.
190. Machaca, K., *Ca(2+) signaling, genes and the cell cycle.* Cell Calcium, 2011. **49**(5): p. 323-30.
191. Delling, M., et al., *Primary cilia are specialized calcium signalling organelles.* Nature, 2013. **504**(7479): p. 311-4.
192. Gehlert, S., W. Bloch, and F. Suhr, *Ca2+-dependent regulations and signaling in skeletal muscle: from electro-mechanical coupling to adaptation.* Int J Mol Sci, 2015. **16**(1): p. 1066-95.
193. Berridge, M.J., M.D. Bootman, and H.L. Roderick, *Calcium signalling: dynamics, homeostasis and remodelling.* Nat Rev Mol Cell Biol, 2003. **4**(7): p. 517-29.
194. Apati, A., T. Berecz, and B. Sarkadi, *Calcium signaling in human pluripotent stem cells.* Cell Calcium, 2016. **59**(2-3): p. 117-23.
195. Varga, Z., et al., *Switch of voltage-gated K+ channel expression in the plasma membrane of chondrogenic cells affects cytosolic Ca2+-oscillations and cartilage formation.* PLoS One, 2011. **6**(11): p. e27957.
196. Smyth, J.T., et al., *Activation and regulation of store-operated calcium entry.* J Cell Mol Med, 2010. **14**(10): p. 2337-49.
197. Kawano, S., et al., *Characterization of Ca(2+) signaling pathways in human mesenchymal stem cells.* Cell Calcium, 2002. **32**(4): p. 165-74.
198. Elliott, A.C., *Recent developments in non-excitable cell calcium entry.* Cell Calcium, 2001. **30**(2): p. 73-93.
199. Forostyak, O., et al., *Physiology of Ca(2+) signalling in stem cells of different origins and differentiation stages.* Cell Calcium, 2016. **59**(2-3): p. 57-66.
200. Yanagida, E., et al., *Functional expression of Ca2+ signaling pathways in mouse embryonic stem cells.* Cell Calcium, 2004. **36**(2): p. 135-46.
201. Bai, X., et al., *Electrophysiological properties of human adipose tissue-derived stem cells.* Am J Physiol Cell Physiol, 2007. **293**(5): p. C1539-50.
202. Wang, K., et al., *Electrophysiological properties of pluripotent human and mouse embryonic stem cells.* Stem Cells, 2005. **23**(10): p. 1526-34.
203. Li, G.R., et al., *Ion channels in mesenchymal stem cells from rat bone marrow.* Stem Cells, 2006. **24**(6): p. 1519-28.
204. Zahanich, I., et al., *Molecular and functional expression of voltage-operated calcium channels during osteogenic differentiation of human mesenchymal stem cells.* J Bone Miner Res, 2005. **20**(9): p. 1637-46.
205. Rodriguez-Gomez, J.A., K.L. Levitsky, and J. Lopez-Barneo, *T-type Ca2+ channels in mouse embryonic stem cells: modulation during cell cycle and contribution to self-renewal.* Am J Physiol Cell Physiol, 2012. **302**(3): p. C494-504.
206. Shakibaei, M. and A. Mobasheri, *Beta1-integrins co-localize with Na, K-ATPase, epithelial sodium channels (ENaC) and voltage activated calcium channels (VACC) in mechanoreceptor complexes of mouse limb-bud chondrocytes.* Histol Histopathol, 2003. **18**(2): p. 343-51.
207. Shao, Y., M. Alicknavitch, and M.C. Farach-Carson, *Expression of voltage sensitive calcium channel (VSCC) L-type Cav1.2 (alpha1C) and T-type Cav3.2 (alpha1H) subunits during mouse bone development.* Dev Dyn, 2005. **234**(1): p. 54-62.
208. Poiraudeau, S., et al., *Different mechanisms are involved in intracellular calcium increase by insulin-like growth factors 1 and 2 in articular chondrocytes: voltage-gated calcium channels, and/or phospholipase C coupled to a pertussis-sensitive G-protein.* J Cell Biochem, 1997. **64**(3): p. 414-22.
209. Putney, J.W., Jr., *A model for receptor-regulated calcium entry.* Cell Calcium, 1986. **7**(1): p. 1-12.
210. Lopez, J.J., et al., *Molecular modulators of store-operated calcium entry.* Biochim Biophys Acta, 2016. **1863**(8): p. 2037-43.
211. Albarran, L., et al., *STIM1 regulates TRPC6 heteromultimerization and subcellular location.* Biochem J, 2014. **463**(3): p. 373-81.
212. Tiruppathi, C., et al., *Ca2+ signaling, TRP channels, and endothelial permeability.* Microcirculation, 2006. **13**(8): p. 693-708.
213. Zhang, S.L., et al., *STIM1 is a Ca2+ sensor that activates CRAC channels and migrates from the Ca2+ store to the plasma membrane.* Nature, 2005. **437**(7060): p. 902-5.
214. Roos, J., et al., *STIM1, an essential and conserved component of store-operated Ca2+ channel function.* J Cell Biol, 2005. **169**(3): p. 435-45.
215. Prakriya, M., et al., *Orai1 is an essential pore subunit of the CRAC channel.* Nature, 2006. **443**(7108): p. 230-3.
216. Soboloff, J., et al., *Orai1 and STIM reconstitute store-operated calcium channel function.* J Biol Chem, 2006. **281**(30): p. 20661-5.
217. Liou, J., et al., *STIM is a Ca2+ sensor essential for Ca2+-store-depletion-triggered Ca2+ influx.* Curr Biol, 2005. **15**(13): p. 1235-41.
218. Baba, Y., et al., *Coupling of STIM1 to store-operated Ca2+ entry through its constitutive and inducible movement in the endoplasmic reticulum.* Proc Natl Acad Sci U S A, 2006. **103**(45): p. 16704-9.
219. Mignen, O., J.L. Thompson, and T.J. Shuttleworth, *STIM1 regulates Ca2+ entry via arachidonate-regulated Ca2+-selective (ARC) channels without store depletion or translocation to the plasma membrane.* J Physiol, 2007. **579**(Pt 3): p. 703-15.
220. Darbellay, B., et al., *STIM1L is a new actin-binding splice variant involved in fast repetitive Ca2+ release.* J Cell Biol, 2011. **194**(2): p. 335-46.

221. Desai, P.N., et al., *Multiple types of calcium channels arising from alternative translation initiation of the Orai1 message.* Sci Signal, 2015. **8**(387): p. ra74.
222. Ong, H.L., et al., *Dynamic assembly of TRPC1-STIM1-Orai1 ternary complex is involved in store-operated calcium influx. Evidence for similarities in store-operated and calcium release-activated calcium channel components.* J Biol Chem, 2007. **282**(12): p. 9105-16.
223. Frischauf, I., et al., *The STIM/Orai coupling machinery.* Channels (Austin), 2008. **2**(4): p. 261-8.
224. Feske, S., E.Y. Skolnik, and M. Prakriya, *Ion channels and transporters in lymphocyte function and immunity.* Nat Rev Immunol, 2012. **12**(7): p. 532-47.
225. Zhang, X., et al., *Complex role of STIM1 in the activation of store-independent Orai1/3 channels.* J Gen Physiol, 2014. **143**(3): p. 345-59.
226. Shuttleworth, T.J., J.L. Thompson, and O. Mignen, *ARC channels: a novel pathway for receptor-activated calcium entry.* Physiology (Bethesda), 2004. **19**: p. 355-61.
227. Kawano, S., et al., *Ca(2+) oscillations regulated by Na(+)-Ca(2+) exchanger and plasma membrane Ca(2+) pump induce fluctuations of membrane currents and potentials in human mesenchymal stem cells.* Cell Calcium, 2003. **34**(2): p. 145-56.
228. Chepenik, K.P., et al., *Arachidonate metabolism during chondrogenesis in vitro.* Calcif Tissue Int, 1984. **36**(2): p. 175-81.
229. Sanchez, J.C., T.A. Danks, and R.J. Wilkins, *Mechanisms involved in the increase in intracellular calcium following hypotonic shock in bovine articular chondrocytes.* Gen Physiol Biophys, 2003. **22**(4): p. 487-500.
230. Huser, C.A. and M.E. Davies, *Calcium signaling leads to mitochondrial depolarization in impact-induced chondrocyte death in equine articular cartilage explants.* Arthritis Rheum, 2007. **56**(7): p. 2322-34.
231. Matta, C., et al., *Cytosolic free Ca2+ concentration exhibits a characteristic temporal pattern during in vitro cartilage differentiation: a possible regulatory role of calcineurin in Ca-signalling of chondrogenic cells.* Cell Calcium, 2008. **44**(3): p. 310-23.
232. Shuttleworth, T.J., *Arachidonic acid, ARC channels, and Orai proteins.* Cell Calcium, 2009. **45**(6): p. 602-10.
233. D'Andrea, P. and F. Vittur, *Spatial and temporal Ca2+ signalling in articular chondrocytes.* Biochem Biophys Res Commun, 1995. **215**(1): p. 129-35.
234. Lee, S.H., et al., *Orai1 mediates osteogenic differentiation via BMP signaling pathway in bone marrow mesenchymal stem cells.* Biochem Biophys Res Commun, 2016. **473**(4): p. 1309-1314.
235. Leipe, D.D., et al., *Classification and evolution of P-loop GTPases and related ATPases.* J Mol Biol, 2002. **317**(1): p. 41-72.
236. Mostowy, S. and P. Cossart, *Septins: the fourth component of the cytoskeleton.* Nat Rev Mol Cell Biol, 2012. **13**(3): p. 183-94.
237. Hartwell, L.H., *Genetic control of the cell division cycle in yeast. IV. Genes controlling bud emergence and cytokinesis.* Exp Cell Res, 1971. **69**(2): p. 265-76.
238. Nishihama, R., M. Onishi, and J.R. Pringle, *New insights into the phylogenetic distribution and evolutionary origins of the septins.* Biol Chem, 2011. **392**(8-9): p. 681-7.
239. Russell, S.E. and P.A. Hall, *Septin genomics: a road less travelled.* Biol Chem, 2011. **392**(8-9): p. 763-7.
240. Weirich, C.S., J.P. Erzberger, and Y. Barral, *The septin family of GTPases: architecture and dynamics.* Nat Rev Mol Cell Biol, 2008. **9**(6): p. 478-89.
241. Sirajuddin, M., et al., *Structural insight into filament formation by mammalian septins.* Nature, 2007. **449**(7160): p. 311-5.
242. Sirajuddin, M., et al., *GTP-induced conformational changes in septins and implications for function.* Proc Natl Acad Sci U S A, 2009. **106**(39): p. 16592-7.
243. Wittinghofer, A. and I.R. Vetter, *Structure-function relationships of the G domain, a canonical switch motif.* Annu Rev Biochem, 2011. **80**: p. 943-71.
244. Hu, Q., W.J. Nelson, and E.T. Spiliotis, *Forchlorfenuron alters mammalian septin assembly, organization, and dynamics.* J Biol Chem, 2008. **283**(43): p. 29563-71.
245. Deb, B.K., T. Pathak, and G. Hasan, *Store-independent modulation of Ca(2+) entry through Orai by Septin 7.* Nat Commun, 2016. **7**: p. 11751.
246. Rasola, A. and P. Bernardi, *The mitochondrial permeability transition pore and its involvement in cell death and in disease pathogenesis.* Apoptosis, 2007. **12**(5): p. 815-33.
247. Kroemer, G., L. Galluzzi, and C. Brenner, *Mitochondrial membrane permeabilization in cell death.* Physiol Rev, 2007. **87**(1): p. 99-163.
248. Sanchez, J.C., et al., *Electrophysiological demonstration of Na+/Ca2+ exchange in bovine articular chondrocytes.* Biorheology, 2006. **43**(1): p. 83-94.
249. Hegedus, L., et al., *The plasma membrane Ca(2+) pump PMCA4b inhibits the migratory and metastatic activity of BRAF mutant melanoma cells.* Int J Cancer, 2017. **140**(12): p. 2758-2770.
250. Harper, M.T. and A.W. Poole, *Store-operated calcium entry and non-capacitative calcium entry have distinct roles in thrombin-induced calcium signalling in human platelets.* Cell Calcium, 2011. **50**(4): p. 351-8.
251. Grynkiewicz, G., M. Poenie, and R.Y. Tsien, *A new generation of Ca2+ indicators with greatly improved fluorescence properties.* J Biol Chem, 1985. **260**(6): p. 3440-50.
252. Gould, R.P., A. Day, and L. Wolpert, *Mesenchymal condensation and cell contact in early morphogenesis of the chick limb.* Exp Cell Res, 1972. **72**(1): p. 325-36.
253. Beederman, M., et al., *BMP signaling in mesenchymal stem cell differentiation and bone formation.* J Biomed Sci Eng, 2013. **6**(8A): p. 32-52.
254. Kostovic-Knezevic, L., Z. Bradamante, and A. Svajger, *Ultrastructure of elastic cartilage in the rat external ear.* Cell Tissue Res, 1981. **218**(1): p. 149-60.
255. Feske, S., *CRAC channelopathies.* Pflugers Arch, 2010. **460**(2): p. 417-35.
256. Inayama, M., et al., *Orai1-Orai2 complex is involved in store-operated calcium entry in chondrocyte cell lines.* Cell Calcium, 2015. **57**(5-6): p. 337-47.
257. Edwall-Arvidsson, C. and J. Wroblewski, *Characterization of chondrogenesis in cells isolated from limb buds in mouse.* Anat Embryol (Berl), 1996. **193**(5): p. 453-61.
258. Zhang, X., et al., *Primary murine limb bud mesenchymal cells in long-term culture complete chondrocyte differentiation: TGF-beta delays hypertrophy and PGE2 inhibits terminal differentiation.* Bone, 2004. **34**(5): p. 809-17.
259. Duprez, D.M., et al., *Bone morphogenetic protein-2 (BMP-2) inhibits muscle development and promotes cartilage formation in chick limb bud cultures.* Dev Biol, 1996. **174**(2): p. 448-52.
260. Hogan, B.L., *Bone morphogenetic proteins: multifunctional regulators of vertebrate development.* Genes Dev, 1996. **10**(13): p. 1580-94.
261. Delise, A.M. and R.S. Tuan, *Analysis of N-cadherin function in limb mesenchymal chondrogenesis in vitro.* Dev Dyn, 2002. **225**(2): p. 195-204.
262. Haas, A.R. and R.S. Tuan, *Chondrogenic differentiation of murine C3H10T1/2 multipotential mesenchymal cells: II. Stimulation by bone morphogenetic protein-2 requires modulation of N-cadherin expression and function.* Differentiation, 1999. **64**(2): p. 77-89.
263. Heinonen, J., et al., *Snorc is a novel cartilage specific small membrane proteoglycan expressed in differentiating and articular chondrocytes.* Osteoarthritis Cartilage, 2011. **19**(8): p. 1026-35.
264. Jay, G.D. and K.A. Waller, *The biology of lubricin: near frictionless joint motion.* Matrix Biol, 2014. **39**: p. 17-24.

265. Eerola, I., et al., *Type X collagen, a natural component of mouse articular cartilage: association with growth, aging, and osteoarthritis.* Arthritis Rheum, 1998. **41**(7): p. 1287-95.
266. O'Keefe, R.J., et al., *Analysis of type II and type X collagen synthesis in cultured growth plate chondrocytes by in situ hybridization: rapid induction of type X collagen in culture.* J Bone Miner Res, 1994. **9**(11): p. 1713-22.
267. Komori, T., *Regulation of osteoblast differentiation by transcription factors.* J Cell Biochem, 2006. **99**(5): p. 1233-9.
268. Stanton, L.A. and F. Beier, *Inhibition of p38 MAPK signaling in chondrocyte cultures results in enhanced osteogenic differentiation of perichondral cells.* Exp Cell Res, 2007. **313**(1): p. 146-55.
269. Teixeira, C.C., et al., *Changes in matrix protein gene expression associated with mineralization in the differentiating chick limb-bud micromass culture system.* J Cell Biochem, 2011. **112**(2): p. 607-13.
270. Matsubara, T., et al., *BMP2 regulates Osterix through Msx2 and Runx2 during osteoblast differentiation.* J Biol Chem, 2008. **283**(43): p. 29119-25.
271. Peng, Y., et al., *Characterization of Osterix protein stability and physiological role in osteoblast differentiation.* PLoS One, 2013. **8**(2): p. e56451.
272. Shea, C.M., et al., *BMP treatment of C3H10T1/2 mesenchymal stem cells induces both chondrogenesis and osteogenesis.* J Cell Biochem, 2003. **90**(6): p. 1112-27.
273. Boskey, A.L., et al., *Modulation of extracellular matrix protein phosphorylation alters mineralization in differentiating chick limb-bud mesenchymal cell micromass cultures.* Bone, 2008. **42**(6): p. 1061-71.
274. Shan, T., W. Liu, and S. Kuang, *Fatty acid binding protein 4 expression marks a population of adipocyte progenitors in white and brown adipose tissues.* FASEB J, 2013. **27**(1): p. 277-87.
275. Tontonoz, P., E. Hu, and B.M. Spiegelman, *Stimulation of adipogenesis in fibroblasts by PPAR gamma 2, a lipid-activated transcription factor.* Cell, 1994. **79**(7): p. 1147-56.
276. Pringle, S., et al., *Mesenchymal differentiation propensity of a human embryonic stem cell line.* Cell Prolif, 2011. **44**(2): p. 120-7.
277. Muhammad, H., B. Schminke, and N. Miosge, *Current concepts in stem cell therapy for articular cartilage repair.* Expert Opin Biol Ther, 2013. **13**(4): p. 541-8.
278. Shi, H., et al., *Role of intracellular calcium in human adipocyte differentiation.* Physiol Genomics, 2000. **3**(2): p. 75-82.
279. San Antonio, J.D. and R.S. Tuan, *Chondrogenesis of limb bud mesenchyme in vitro: stimulation by cations.* Dev Biol, 1986. **115**(2): p. 313-24.
280. Jacenko, O. and R.S. Tuan, *Chondrogenic potential of chick embryonic calvaria: I. Low calcium permits cartilage differentiation.* Dev Dyn, 1995. **202**(1): p. 13-26.
281. Zimmermann, B., et al., *Inhibition of chondrogenesis and endochondral mineralization in vitro by different calcium channel blockers.* Eur J Cell Biol, 1994. **63**(1): p. 114-21.
282. Phan, M.N., et al., *Functional characterization of TRPV4 as an osmotically sensitive ion channel in porcine articular chondrocytes.* Arthritis Rheum, 2009. **60**(10): p. 3028-37.
283. Singh, P., et al., *N-methyl-D-aspartate receptor mechanosensitivity is governed by C terminus of NR2B subunit.* J Biol Chem, 2012. **287**(6): p. 4348-59.
284. Matta, C., R. Zakany, and A. Mobasheri, *Voltage-dependent calcium channels in chondrocytes: roles in health and disease.* Curr Rheumatol Rep, 2015. **17**(7): p. 43.
285. Raizman, I., et al., *Calcium regulates cyclic compression-induced early changes in chondrocytes during in vitro cartilage tissue formation.* Cell Calcium, 2010. **48**(4): p. 232-42.
286. Atsuta, Y., et al., *L-type voltage-gated Ca(2+) channel CaV1.2 regulates chondrogenesis during limb development.* Proc Natl Acad Sci U S A, 2019. **116**(43): p. 21592-21601.
287. Ramsdell, J.S., *Voltage-dependent calcium channels regulate GH4 pituitary cell proliferation at two stages of the cell cycle.* J Cell Physiol, 1991. **146**(2): p. 197-206.
288. Capiod, T., *Cell proliferation, calcium influx and calcium channels.* Biochimie, 2011. **93**(12): p. 2075-9.
289. Rosemblit, N., et al., *Intracellular calcium release channel expression during embryogenesis.* Dev Biol, 1999. **206**(2): p. 163-77.
290. Yellowley, C.E., C.R. Jacobs, and H.J. Donahue, *Mechanisms contributing to fluid-flow-induced Ca2+ mobilization in articular chondrocytes.* J Cell Physiol, 1999. **180**(3): p. 402-8.
291. Funabashi, K., et al., *Accelerated Ca2+ entry by membrane hyperpolarization due to Ca2+-activated K+ channel activation in response to histamine in chondrocytes.* Am J Physiol Cell Physiol, 2010. **298**(4): p. C786-97.
292. Evans, J.F., et al., *Adrenocorticotropin evokes transient elevations in intracellular free calcium ([Ca2+]i) and increases basal [Ca2+]i in resting chondrocytes through a phospholipase C-dependent mechanism.* Endocrinology, 2005. **146**(7): p. 3123-32.
293. Brandman, O., et al., *STIM2 is a feedback regulator that stabilizes basal cytosolic and endoplasmic reticulum Ca2+ levels.* Cell, 2007. **131**(7): p. 1327-39.
294. Kono, T., et al., *Spontaneous oscillation and mechanically induced calcium waves in chondrocytes.* Cell Biochem Funct, 2006. **24**(2): p. 103-11.
295. Kawano, S., et al., *ATP autocrine/paracrine signaling induces calcium oscillations and NFAT activation in human mesenchymal stem cells.* Cell Calcium, 2006. **39**(4): p. 313-24.
296. Kwon, H.J., et al., *Synchronized ATP oscillations have a critical role in prechondrogenic condensation during chondrogenesis.* Cell Death Dis, 2012. **3**: p. e278.
297. Kwon, H.J., *Extracellular ATP signaling via P2X(4) receptor and cAMP/PKA signaling mediate ATP oscillations essential for prechondrogenic condensation.* J Endocrinol, 2012. **214**(3): p. 337-48.
298. Tsai, J.A., O. Larsson, and H. Kindmark, *Spontaneous and stimulated transients in cytoplasmic free Ca(2+) in normal human osteoblast-like cells: aspects of their regulation.* Biochem Biophys Res Commun, 1999. **263**(1): p. 206-12.
299. Nguyen, C., et al., *Intracellular calcium oscillations in articular chondrocytes induced by basic calcium phosphate crystals lead to cartilage degradation.* Osteoarthritis Cartilage, 2012. **20**(11): p. 1399-408.
300. Rao, A., *Signaling to gene expression: calcium, calcineurin and NFAT.* Nat Immunol, 2009. **10**(1): p. 3-5.
301. De Koninck, P. and H. Schulman, *Sensitivity of CaM kinase II to the frequency of Ca2+ oscillations.* Science, 1998. **279**(5348): p. 227-30.
302. Dupont, G. and A. Goldbeter, *CaM kinase II as frequency decoder of Ca2+ oscillations.* Bioessays, 1998. **20**(8): p. 607-10.
303. Shimazaki, A., et al., *Calcium/calmodulin-dependent protein kinase II in human articular chondrocytes.* Biorheology, 2006. **43**(3,4): p. 223-33.
304. Schrobback, K., T.J. Klein, and T.B. Woodfield, *The importance of connexin hemichannels during chondroprogenitor cell differentiation in hydrogel versus microtissue culture models.* Tissue Eng Part A, 2015. **21**(11-12): p. 1785-94.
305. Knight, M.M., et al., *Articular chondrocytes express connexin 43 hemichannels and P2 receptors - a putative mechanoreceptor complex involving the primary cilium?* J Anat, 2009. **214**(2): p. 275-83.
306. Erb, L., et al., *P2 receptors: intracellular signaling.* Pflugers Arch, 2006. **452**(5): p. 552-62.

307. Clark, R.B., et al., *Two-pore domain K(+) channels regulate membrane potential of isolated human articular chondrocytes.* J Physiol, 2011. **589**(Pt 21): p. 5071-89.
308. Mobasheri, A., et al., *Characterization of a stretch-activated potassium channel in chondrocytes.* J Cell Physiol, 2010. **223**(2): p. 511-8.
309. Prakriya, M., *Store-operated Orai channels: structure and function.* Curr Top Membr, 2013. **71**: p. 1-32.
310. Argentaro, A., et al., *A SOX9 defect of calmodulin-dependent nuclear import in campomelic dysplasia/autosomal sex reversal.* J Biol Chem, 2003. **278**(36): p. 33839-47.
311. Joergensen, N.L., et al., *Gradient Fractionated Separation of Chondrogenically Committed Cells Derived from Human Embryonic Stem Cells.* Biores Open Access, 2015. **4**(1): p. 109-14.
312. Williams, R., et al., *Identification and clonal characterisation of a progenitor cell sub-population in normal human articular cartilage.* PLoS One, 2010. **5**(10): p. e13246.

8.2. List of Publications

UNIVERSITY of DEBRECEN

UNIVERSITY AND NATIONAL LIBRARY
UNIVERSITY OF DEBRECEN
H-4002 Egyetem tér 1, Debrecen
Phone: +3652/410-443, email: publikaciok@lib.unideb.hu

Registry number: DEENK/66/2020.PL
Subject: PhD Publikációs Lista

Candidate: Roland Ádám Takács
Neptun ID: U1K98N
Doctoral School: Doctoral School of Molecular Medicine

List of publications related to the dissertation

1. **Takács, R. Á.**, Matta, C., Somogyi, C., Juhász, T., Zákány, R.: Comparative Analysis of Osteogenic/Chondrogenic Differentiation Potential in Primary Limb Bud-Derived and C3H10T1/2 Cell Line-Based Mouse Micromass Cultures.
   Int. J. Mol. Sci. 14 (8), 16141-16167, 2013.
   DOI: http://dx.doi.org/10.3390/ijms140816141
   IF: 2.339

2. Fodor, J., Matta, C., Oláh, T., Juhász, T., **Takács, R. Á.**, Tóth, A., Dienes, B., Csernoch, L., Zákány, R.: Store-operated calcium entry and calcium influx via voltage-operated calcium channels regulate intracellular calcium oscillations in chondrogenic cells.
   Cell Calcium. 54, 1-16, 2013.
   DOI: http://dx.doi.org/10.1016/j.ceca.2013.03.003
   IF: 4.21

UNIVERSITY AND NATIONAL LIBRARY
UNIVERSITY OF DEBRECEN
H-4002 Egyetem tér 1, Debrecen
Phone: +3652/410-443, email: publikaciok@lib.unideb.hu

List of other publications

3. Alagha, M. A., Vágó, J., Katona, É., **Takács, R. Á.**, Veen, D. v. d., Zákány, R., Matta, C.: A Synchronized Circadian Clock Enhances Early Chondrogenesis.
Cartilage. [Epub ahead of print], 1-15, 2020.
DOI: http://dx.doi.org/10.1177/1947603520903425
IF: 2.961 (2018)

4. Matta, C., Juhász, T., Fodor, J., Hajdú, T., Mészár, K. É., Somogyi, C., **Takács, R. Á.**, Vágó, J., Oláh, T., Bartók, Á., Varga, Z., Panyi, G., Csernoch, L., Zákány, R.: N-methyl-D-aspartate (NMDA) receptor expression and function is required for early chondrogenesis.
Cell Commun Signal. 17 (1), 1-19, 2019.
DOI: http://dx.doi.org/10.1186/s12964-019-0487-3
IF: 5.111 (2018)

5. Juhász, T., Szentléleky, E., Somogyi, C., **Takács, R. Á.**, Dobrosi, N., Engler, M., Tamás, A., Reglődi, D., Zákány, R.: Pituitary Adenylate Cyclase Activating Polypeptide (PACAP) Pathway Is Induced by Mechanical Load and Reduces the Activity of Hedgehog Signaling in Chondrogenic Micromass Cell Cultures.
Int. J. Mol. Sci. 16 (8), 17344-17367, 2015.
DOI: http://dx.doi.org/10.3390/ijms160817344
IF: 3.257

6. Somogyi, C., Matta, C., Földvári, Z., Juhász, T., Mészár, K. É., **Takács, R. Á.**, Hajdú, T., Dobrosi, N., Gergely, P., Zákány, R.: Polymodal Transient Receptor Potential Vanilloid (TRPV) Ion Channels in Chondrogenic Cells.
Int. J. Mol. Sci. 16 (8), 18412-18438, 2015.
DOI: http://dx.doi.org/10.3390/ijms160818412
IF: 3.257

7. Matta, C., Fodor, J., Miosge, N., **Takács, R. Á.**, Juhász, T., Rybaltovszki, H., Tóth, A., Csernoch, L., Zákány, R.: Purinergic signalling is required for calcium oscillations in migratory chondrogenic progenitor cells.
Pflugers Arch. 467 (2), 429-442, 2015.
DOI: http://dx.doi.org/10.1007/s00424-014-1529-8
IF: 3.654

8. Juhász, T., Matta, C., Somogyi, C., Mészár, K. É., **Takács, R. Á.**, Soha, R. F., Szabó, I. A., Cserháti, C., Sződy, R., Karácsonyi, Z., Bakó, É., Gergely, P., Zákány, R.: Mechanical loading stimulates chondrogenesis via the PKA/CREB-Sox9 and PP2A pathways in chicken micromass cultures.
Cell. Signal. 26 (3), 468-482, 2014.
DOI: http://dx.doi.org/10.1016/j.cellsig.2013.12.001
IF: 4.315

UNIVERSITY AND NATIONAL LIBRARY
UNIVERSITY OF DEBRECEN
H-4002 Egyetem tér 1, Debrecen
Phone: +3652/410-443, email: publikaciok@lib.unideb.hu

9. Juhász, T., Matta, C., Mészár, K. É., Somogyi, C., **Takács, R. Á.**, Hajdú, T., Helgadottir, S. L., Fodor, J., Csernoch, L., Tóth, G., Bakó, É., Reglődi, D., Tamás, A., Zákány, R.: Pituitary Adenylate Cyclase-Activating Polypeptide (PACAP) Signalling Enhances Osteogenesis in UMR-106 Cell Line.
J. Mol. Neurosci. 54 (3), 555-573, 2014.
DOI: http://dx.doi.org/10.1007/s12031-014-0389-1
IF: 2.343

10. Juhász, T., Matta, C., Mészár, K. É., Somogyi, C., **Takács, R. Á.**, Gergely, P., Csernoch, L., Panyi, G., Tóth, G., Reglődi, D., Tamás, A., Zákány, R.: Pituitary adenylate cyclase activating polypeptide (PACAP) signalling exerts chondrogenesis promoting and protecting effects: implication of calcineurin as a downstream target.
PLoS One. 9 (3), [1-15], 2014.
DOI: http://dx.doi.org/10.1371/journal.pone.0091541
IF: 3.234

Total IF of journals (all publications): 34,681
Total IF of journals (publications related to the dissertation): 6,549

The Candidate's publication data submitted to the iDEa Tudóstér have been validated by DEENK on the basis of the Journal Citation Report (Impact Factor) database.

05 March, 2020

DEBRECENI EGYETEM
Egyetemi és Nemzeti Könyvtár

9. Key Words

in vitro chondrogenesis, C3H101/2 cell line, limb bud chondrogenic HDC, cytosolic [Ca^{2+}] measurements, SOCE, VDCCs, septins, chondro-, osteo- and adipogenic marker genes, pluripotency factors

10. Tárgyszavak

in vitro porcfejlődés, C3H101/2 sejtvonal, végtagtelep eredetű porcosodó HD kultúra, citoszólikus [Ca^{2+}] mérések, SOCE, VDCCk, septinek, chondro-, osteo- és adipogenikus markergének, pluripotencia faktorok

11. Acknowledgements

Firstly, I need to express an enormous amount of gratitude to my supervisor, Dr. Róza Zákány on numerous levels. She is a major inspiration with her experience and constant drive to explore new scientific grounds and in general, an exceptional human being, who has a kind heart and is always helpful and considerate beyond the expectable with anyone having personal issues, which is probably the most important pillar of making our research group feel like a family.

My colleague and friend, Dr. Csaba Matta needs to be mentioned among the firsts. He is a great person/scientist and a role model for any male in the research field with his incredible determination, sense and success in balancing between family and professional life. He is also someone whom I owe a special amount of tribute for his contribution to my progress, this current work and being where I am right now.

I am extremely grateful to our assistant, Krisztina Bíróné Barna who in addition to providing excellent technical support throughout many years also became a very trustworthy friend and a major emotional support to many of us.

The rest of our current and past colleagues at the Signal Transductioin Group – including undergraduates – are also worth every bit of praise for their dedicated work, helpfulness and for maintaining such an incredibly good morale.

The author also wishes to extend special thanks to all of our collaborators at the Department of Physiology, especially Dr. János Fodor for his work and insightful contribution and Prof. László Csernoch for his input and enabling this quite fruitful collaboration to flourish, which was essential for the production of this work.

I am highly appreciative of the head of our Department, Dr. Péter Szücs for enabling me to work at such a high-standard institution and generously providing for the needs of our research group.

All my family and friends have earned massive amounts of my gratitude for the countless times they have helped me through difficulties. Among these people, I am exceptionally thankful to my wife, Barbara for her love, tremendous amount of support and patience that she needed to provide to bear with me along this not always easy journey and my wonderful baby boy, Roland, who – even without being aware of it – provided me immense motivation and energy to become a better version of myself and also, to finally finish this work.

Finally, I would like to dedicate this work to the memory of my late grandmother, Elvira. She always had and will have a special place in my heart for countless reasons, but could not stay with us long enough to see this chapter of my life come to an end.

12. Appendix

The thesis is based on the following publications: